

**“Keratose” sponge fossils and microbialites: a geobiological contribution to
the understanding of metazoan origin**

Dissertation

zur Erlangung des mathematisch-naturwissenschaftlichen Doktorgrades

"Doctor rerum naturalium"

der Georg-August-Universität Göttingen

im Promotionsprogramm Geowissenschaften

der Georg-August University School of Science (GAUSS)

vorgelegt von

Cui Luo

aus Chongqing, V. R. China

Göttingen 2015

Betreuungsausschuss:

Prof. Dr. Joachim Reitner, Abteilung Geobiologie, Geowissenschaftliches Zentrum, Georg-August-Universität Göttingen

Prof. Dr. Volker Thiel, Abteilung Geobiologie, Geowissenschaftliches Zentrum, Georg-August-Universität Göttingen

Mitglieder der Prüfungskommission:**Referent:**

Prof. Dr. Joachim Reitner, Abteilung Geobiologie, Geowissenschaftliches Zentrum, Georg-August-Universität Göttingen

Korreferent:

Prof. Dr. Volker Thiel, Abteilung Geobiologie, Geowissenschaftliches Zentrum, Georg-August-Universität Göttingen

weitere Mitglieder der Prüfungskommission:

PD Dr. Michael Hoppert, Institut für Mikrobiologie und Genetik, Abteilung für Allgemeine Mikrobiologie, Universität Göttingen

PD Dr. Mike Reich, Bayerische Staatssammlung für Paläontologie und Geologie

Dr. Jan Peter Duda, Abteilung Geobiologie, Geowissenschaftliches Zentrum, Georg-August-Universität Göttingen

Dr. Klaus Simon, Abteilung Geochemie, Geowissenschaftliches Zentrum, Georg-August-Universität Göttingen

Tag der mündlichen Prüfung:

10.02.2015

生而不有 為而不恃 長而不宰 是謂玄德

It gives them birth and does not own them,

Acts (helps) and does not appropriate them,

Is superior, and does not control them.

- This is the Mystic Virtue.

Tao Te Ching , Ch 51

translated by Lin Yutang, 1948

Acknowledgements

Without many other prerequisites and supports, this PhD study cannot be accomplished and presented here. I regard myself as rather the major contributor of this work than the single creator of it.

My supervisor Prof. Dr. Joachim Reitner and my previous supervisor Prof. Dr. Maoyan Zhu provided me the chance to do PhD research at the University of Göttingen. The Chinese Scholarship Council (CSC) financially supported this program. My families kindly tolerated my absence from their life and constantly backed me up. My stay in this foreign country was helped and accompanied by a lot of colleagues and friends, like Dr. Jan Peter Duda, Dr. Filiz Afşar, Dorothea Hause-Reitner, Ms. Schmidt, Dr. Nadine Schäfer, Dr. Steffen Kiel, Dr. Frank Wiese, Axel Hackmann, Wolfgang Dröse, Dr. Lixia Li, Boyang Liu and Lianghao Dai. It will be another chapter of this dissertation if I list up all the names which come up to my mind right now. They all once aided my work and/or illuminated my life during the past 40 months.

This doctoral study is based on a large collection of fossils. The major part of them is from Prof. Dr. Joachim Reitner's collection while some are from other resources. For this reason, special appreciations are dedicated to the following researchers who kindly allowed me to study their fossil collections or allocated us part of their fossil materials. They are Prof. Dr. Maoyan Zhu from Nanjing Institute of Geology and Palaeontology, Chinese Academy of Sciences (carbonaceous fossils in chapter 1); Dr. Klaus Warnke (organ-pipe stromatolites in chapter 4); Prof. Dr. Gerhard Bachman from University of Halle (the stromatolitic crusts in *Placunopsis* reefs in chapter 4), Dr. Sylvain Richoz from University of Graz (the Permian-Triassic fossils in chapter 5); and Dr. Pierre Kruse from South Australian Museum (the Botomian and the Tommotian fossils in chapter 5).

Directly related to the writing of this dissertation, Liping Dong, Fei Wang, Yan Chen and Wenchi Jin are heartily appreciated for helping to improve the language of chapters 1, 5, 6 and 7. My Chinese colleague Lanyun Miao helped a lot in collecting important Chinese literature.

I am thankful for having so many great people around! I hope this dissertation, as a gift of thank, will make you all satisfied and delighted.

The following manuscripts are part of this dissertation (*corresponding author):

Luo C, Reitner J* (2014) First report of fossil "keratose" demosponges in Phanerozoic carbonates: preservation and 3-D reconstruction. *Naturwissenschaften* 101 (6):467-477

doi: 10.1007/s00114-014-1176-0 (Chapter 3)

Luo C*, Schäfer N, Duda J-P, Li L-X (2014) Preservation of organic matter in sponge fossils: a case study of 'round sponge fossils' from the Cambrian Chengjiang Biota with Raman spectroscopy. *Göttingen Contributions to Geosciences* 77: 29-38

<http://dx.doi.org/10.3249/webdoc-3914> (Chapter 2)

Luo C*, Reitner J (in review) "Stromatolites" built by sponges and microbes – a new type of Phanerozoic bioconstruction. *Lethaia* (submitted on Dec. 10, 2014). (Chapter 4)

Table of Contents

Chapter 1	Introduction	1
1.1	Biological perspectives on metazoan origin	1
1.1.1	What is a metazoan?	1
1.1.2	Models on animal origin	4
1.1.3	Tracing the ancestors: metazoan phylogeny and molecular clock	5
1.2	The geological background of metazoan origin	6
1.2.1	Paleoenvironmental conditions	7
1.2.2	Fossil record of early animals	9
1.3	Summary of this chapter and introduction to the doctoral work	11
	References	14
Chapter 2	Preservation of organic matter in sponge fossils: a case study of “round sponge fossils” from the Cambrian Chengjiang Biota with Raman spectroscopy	20
	Abstract	20
2.1	Introduction	21
2.2	Material and Methods	22
2.3	Results	24
2.3.1	Preservation of carbonaceous remains in studied fossils	24
2.3.2	Raman spectra	27
2.4	Discussion	29
2.5	Conclusions	34
	Acknowledgement	35
	References	36
Chapter 3	First report of fossil “keratose” demosponges in Phanerozoic carbonates: preservation and 3-D reconstruction	40
	Abstract	40
3.1	Introduction	41
3.2	Material and geological background	42
3.2.1	Middle Devonian bioherms from Boulonnais, northern France	42
3.2.2	Triassic microbialites from the Middle Muschelkalk, Poland	44
3.2.3	Dried skeletons of modern keratose demosponges	44
3.3	Methods	45
3.4	Results	49

3.5	Discussion	53
3.6	Conclusion	56
	Acknowledgements	57
	References	58
	Supplementary material	63
Chapter 4	“Stromatolites” built by sponges and microbes – a new type of Phanerozoic bioconstruction	64
	Abstract	64
4.1	Introduction	65
4.2	Material	68
4.3	Methods	69
	4.3.1 Microscope observation	69
	4.3.2 LA-ICP-MS	70
	4.3.3 Carbon and oxygen isotopes	70
4.4	Results	71
	4.4.1 Description of the Triassic material	71
	4.4.2 Description of the Carboniferous material	77
	4.4.3 LA-ICP-MS data	83
	4.4.4 Carbon and oxygen isotopes	84
4.5	Discussion	85
	4.5.1 Sponge origin of the micritic aggregations	85
	4.5.2 Construction of the columnar buildups	87
4.6	Conclusion and implications	90
	Acknowledgment	91
	References	92
	Supplementary material	97
Chapter 5	Secular occurrences of keratose sponge fossils	98
5.1	Introduction	98
5.2	Description	99
5.3	Summary	114
	References	116
Chapter 6	Implication of microstructures of the Precambrian carbonate microbialites	118
6.1	Introduction	118
6.2	Dendrolites, Leiolites and Thrombolites	119

6.3	Stromatolites—current understanding on the diversity and secular changes of their microstructures	122
6.4	Microstructures of Mesoproterozoic and Tonian stromatolites	127
6.5	Microbialites in Sturtian cap carbonates	130
6.5.1	Peloidal grainstone	130
6.5.2	Chambered structures	133
6.6	Conclusion	136
	References	138
Chapter 7	Summary	143
	References	149
	Curriculum vitae	150

- Chapter 1 -

Introduction

Among all the multicellular life forms, animal multicellularity is the only type which has given birth to intelligence, the ability that allows and impels us to reflect on ourselves and question our own origin. The topic “origin of animals” involves several different aspects and sub-questions, including “what is the fundamental difference between animals and other organisms”, “how was the first animal like”, “when did it appear”, “what was the trigger (s)”, etc. Answering these questions requires a long-term effort of researchers from many different disciplines. In this doctoral work, I tried to contribute to this topic by exploring the question “how can the earliest animals be identified in fossil record”. Particularly, I checked the preservation and morphological characters of non-spicular demosponges in Phanerozoic carbonates as well as some meso- and microstructures of Precambrian microbialites. In this chapter, I will first give a panoramic view on the background of this study (1.1–1.2), and then explain the concept of my own work and introduce the content and structure of the next chapters (1.3).

1.1 Biological perspectives on metazoan origin

1.1.1 What is a metazoan?

Historically, Kingdom Animalia Linnaeus, 1758 was set up for “natural objects that grow, live and sense” (in Nielsen 2012, p. 7). Later, Haeckel (1874) separated these “natural objects” into Metazoa and Protozoa, with the former characterized by tissues and organs. The development of molecular techniques and informatics has greatly changed our concept on the systematics of lives on the earth by enabling us to investigate their phylogenetic relationships using DNA, RNA and proteins—the molecular manipulators lying behind morphological, histological and developmental phenotypes. According to the new taxonomic scheme of eukaryotes, Metazoa Haeckel, 1874, which is defined as “Multicellular; cells typically held together by intercellular junctions; extracellular matrix with fibrous

proteins, typically collagens, between two dissimilar epithelia, except in *Trichoplax* or where secondarily lost; sexual with production of an egg cell that is fertilized by a smaller, often monociliated sperm cell; phagotrophic and osmotrophic; without cell wall” (Adl et al. 2012, p. 438), embraces sub-lineages of Porifera Grant, 1836 (Parazoa Sollas, 1884), *Trichoplax* Schulze, 1883 (Placozoa Grell, 1971) and Animalia Linnaeus, 1758, emend. Adl et al., 2005 (Eumetazoa, Bütschli 1910). However, outside of the taxonomic scientific community, or in relatively informal situations, the word “animal” is normally used in a sense equal to Metazoa. The position of Metazoa in the eukaryotic phylogenetic tree is shown in Fig. 1.1. More detailed phylogenetic structure inside of the metazoan lineage will be introduced in 1.1.3.

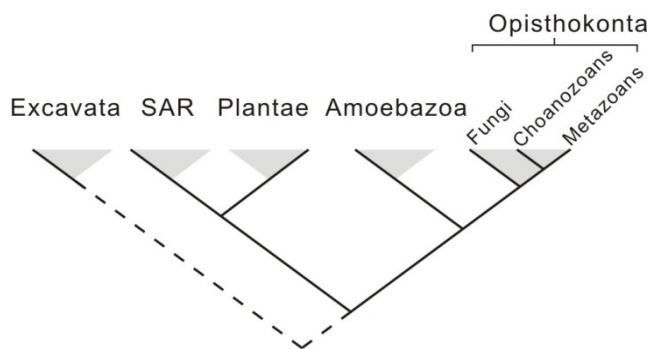


Fig. 1.1 Simplified phylogenetic tree of eukaryotes, after Adl et al. (2012) and Butterfield (2014).

This new phylogenetic and taxonomic scheme is concluded largely based on molecular phylogenetic studies; several taxonomic groups, such as Holozoa and Nucletmycea, are defined purely based on molecular data. Although the new tree perhaps demonstrates the phylogenetic relationship of organisms in a more correct way, it is the evolution of morphological, physiological and developmental characters that are ultimately cared by other scientists out of the molecular taxonomic community. As say the words of Raff et al. (1989), which were quoted in Nielsen (2012, p. 4): “after all, it is the history of morphological change we wish to explain”.

Multicellularity is a character which has long been used to differentiate metazoan from protozoan, and is also a part of the metazoan definition quoted above. However, modern biological studies have discovered that within the Opisthokonta group, many unicellular organisms show temporal multicellularity in their life cycles. Choanoflagellates are the known closest unicellular relatives of animals. Colony-forming choanoflagellates can form multicellular structures by keeping cell attachment after division with simple cell differentiation (e.g. Fairclough et al. 2010; Dayel et al.

2011). However, the resulted differentiated cells in these protozoans are not adequate to be called as tissue.

In animals, epithelium is the first tissue formed in embryogenesis, and is the basis of other complexities, because it shapes all the organs by separating the inner space from outer environment and enables the regulation of chemical exchange between the two sides (e.g. Tyler 2003; Bryant and Mostov 2008). Epithelium is defined as “tissues in which the component cells share an aligned polarity, are joined by belt-form junctions, and associate with extracellular matrix only on their basal and apical sides” (Tyler 2003, p. 55). In recent years, the social amoeba *Dictyostellium discoideum* was found able to produce epithelium-like structure in the tip of the fruiting body which is formed in the multicellular reproductive stage. This structure show polarized cells bound by adherens junctions (Dickinson et al. 2011, 2012). However, a metazoan adherens junction requires the protein set of cadherin, α -catenin and β -catenin, while in the amoeba adherens junction, cadherin is lacking and the Dd α -catenin and Aardvark (homologs of α - and β -catenins) seem to have been involved independently (Parfrey and Lahr 2013). Furthermore, most animal epithelia have a basement membrane, which is a very conservative and unique character specifically in Eumetazoa. Most sponges, perhaps except some homoscleromorphs, possess only part of the genomic and molecular bricks of basement membrane, i.e. fibrillar collagens and laminin subunits; while in choanoflagellates, none of the constructing proteins of the basement membrane is known encoded (Hynes 2012). Although the amoeba “epithelium” may well be a product of convergent evolution, it indicates that some multicellular structures in protists can be quite close to the metazoan analogues in appearance.

After comparing Metazoa with their unicellular relatives, Richter and King (2013) summarized a few animal-specific features, which are largely overlapped with the definition of Adl et al. (2012) cited above: 1) complex tissue morphogenesis (gastrulation or invagination during development); 2) epithelium; 3) stem cells and the Piwi regulation (Funayama 2010, Juliano et al. 2011); 4) producing sperm and eggs during reproduction. Based on these essential characters, they depicted the first animal as an organism appearing very similar to modern sponges, especially in that, this organism was probably bacterivore and its epithelial layer was at least partly composed of uniflagellate collar cells.

1.1.2 Models on animal origin

In the more than one hundred years history of questioning the origin of multicellular animals, many hypotheses and models have been proposed (reviewed in Mikhailov et al. 2009). The most representative ones are:

1) Haeckel's Gastraea theory, which assumes that the story started when a group of flagellates formed a hollow multicellular ball (Blastaea) by aggregation and then this ball approached to a real metazoan by developing invagination, just like the gastrulation process in the metazoan embryogenesis (Haeckel 1874). The recent emendation of this theory hypothesizes the metazoan ancestor as pelagic spheres consisting of choanocytes, which is called "choanoblastaea" (Nielsen 2008).

2) Bütschli's Placula theory, which hypothesizes the ancestral metazoan as a flat colony composed of differentiated feeding and locomotory protist cells (Bütschli 1884). This colony delaminated by the proliferation of these cells and a Placozoa-like structure was then produced. The latter could also subsequently undergo invagination.

3) Zakhvatkin's Synzoospore theory, which interpretes blastula (i.e. Haeckel's Blastaea) as attached zoospores (synzoospores), compared with the separated dispersal cells (unicellular spores) in protists. In light of the later discovery of complex life cycles and transient multicellular stages in protists, a advanced model based on this theory argues that the metazoan ancestor had a complex life cycle as well; part of the cycle was a sedentary and filter feeding form, while the other part was blastula-like larva, which became more complex and dominant in the later evolution (Mikhailov et al. 2009).

These theories listed above focus mainly on the intrinsic causes of animal origin. Recently, increasing researchers start to consider the role which the extrinsic factors, for example ambient prokaryotes, may have played in this evolutionary event. Growing amount of studies have revealed that nearly every aspect of animal life is strongly affected by bacteria, including origin and evolution (reviewed in

McFall-Ngai et al. 2013). The collar cells, which are found in both choanoflagellates and sponges, are thought to be related to bacteria preying (Nichols et al. 2009; McFall-Ngai et al. 2013). While another study shows that the presence of bacteria *Algoriphagus machipongonensis* is critical for the choanoflagellates *Salpingoeca rosetta* to form multicellular colonies (Alegado et al. 2012). As the known most primitive metazoan (see 1.1.3), sponges have close symbiosis with prokaryotes and can keep a bacterial population as much as 40% of its tissue volume. These prokaryotes participate the elemental metabolisms of the host, serve as food, protect the host from unfavorable environmental conditions (e.g. chemical defense, shelter from excessive light) and can be vertically passed down to descendants (Taylor 2007). The larvae settlement of sponges and many other sessile animals is strongly affected by chemical cues produced by prokaryotes (Hadfield 2011). Furthermore, prokaryotes also influence the evolution of animals by lateral gene transfer (e.g. Nakashima et al. 2004). It is perhaps difficult to evaluate to which extent or in which ways the animal evolutionary history has been impacted by the environmental factors, but a realistic view on the origin of Metazoa must take these environmental factors into consideration.

1.1.3 Tracing the ancestors: metazoan phylogeny and molecular clock

Phylogenetics is to resolve the affinity or the evolutionary relationship between organisms by analyzing homologous characters, while molecular clock provides a way to date the evolutionary divergence events. Thanks to the advent of genomics and the technological development of molecular sequencing and informatics, both disciplines have entered an era of studying large genomic dataset using complex mathematic algorithms (Kumar 2005; Edgecombe et al. 2011).

During the development of molecular phylogenetic method, different phylogenetic trees have been yielded based on different sampling ranges, tested genomic sequences and calculation methods. These results and controversies have been well reviewed in several studies like Edgecombe et al. (2011), Philippe et al. (2011) and Wörheide (2012). It seems that a consensus has almost been reached between different research groups that sponges represent the known most basic animal lineage (e.g. Peterson et al. 2008; Philippe et al. 2009, 2011; Sperling et al. 2009; Pick et al. 2010; Erwin et al. 2011;

Nielsen 2012), although some studies still claim the basic position of ctenophores (e.g. discussion in Dohrmann and Wörheide 2013; Moroz et al. 2014; Fig. 1.2a). Concerned with sponges, there is one more controversy: whether they are monophyletic or paraphyletic. One opinion is based on the most comprehensive phylogenomic dataset, grouping sponges into a monophyletic clade, with Hexactinellida + Demospongiae and Calcarea + Homoscleromorpha forming sister groups (Philippe et al. 2009, 2011; Pick et al. 2010; Fig. 1.2b); while the other widely supported suggestion is that sponge is paraphyletic, with Hexactinellida + Demospongiae forming sister groups with Calcarea + Homoscleromorpha + other animals (e.g. Erwin et al. 2011; Sperling et al. 2009; Fig. 1.2c). The most widely used molecular clock estimations by paleontologists adopt the “sponges basal and paraphyletic” trees (e.g. Peterson et al. 2008; Sperling et al. 2010; Erwin et al. 2011). All these clocks are calibrated with the animal fossil record known from the time, thus could provide an evaluation of the minimum age of the evolutionary events. It is predicted that metazoan diverged from protozoan during 800-750 Ma, before the Sturtian glaciation in the Cryogenian (Fig. 1.3).

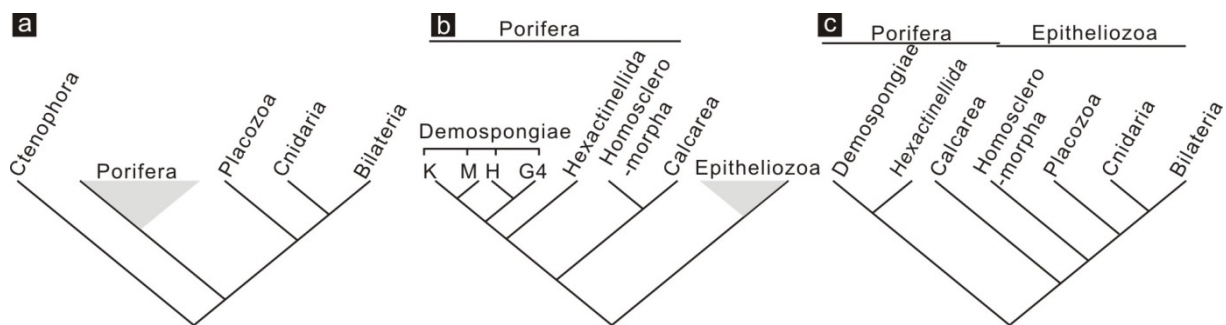


Fig. 1.2 Different hypothesized branching pattern of basal animals. **a** Ctenophora as the first branched animal, according to e.g. Moroz et al. (2014). **b-c** Porifera forms the most basal branch, either as a monophyletic group (**b**) or as a paraphyletic group (**c**). **b** is modified after Wörheide et al. (2012). **c** is modified after Sperling et al. (2009) and Erwin et al. (2011), in these studies, Ctenophora was not included in the original trees. Abbreviations: K, Keratosa; M, Myxospongiae; H, marine haplosclerids; G, “G4”.

1.2 The geological background of metazoan origin

Geobiology is a young discipline appeared at the turn of the 21st century based on the demand of understanding the planetary bio- and geo-mechanisms as a whole interweaving system (Olszewski 2001; Noffke 2005; Reitner and Thiel 2011). Its holistic view on the natural processes impels us to investigate the origin of metazoan in a more realistic scenario.

1.2.1 Paleoenvironmental conditions

It is still controversial whether the carbonaceous materials with very low $\delta^{13}\text{C}$ values in the Greenland rocks of 3.83–3.7 Ga age are remains of early life (e.g. Rosing 1999; Rosing et al. 2004; McCollom and Seewald 2006), but life originated at least before 3.49 Ga according to the record of stromatolites (e.g. Walter 1980), possible microscopic fossils (e.g. Ueno et al. 2001) and relevant geochemical signals in the Archean rocks in the Pilbara Craton (reviewed in Van Kranendonk 2006; Van Kranendonk et al. 2012). Many authors suggest that eukaryotic organisms may have appeared before the end of the Paleoproterozoic (e.g. reviews in Porter 2004; Van Kranendonk et al. 2012; Butterfield 2014; Knoll 2014), slowly diversified in Mesoproterozoic and achieved multicellularity in the late part of this eon (e.g. 1.2 Ga old *Bangiomorpha pubescens*, reported by Butterfield 2000), then greatly diversified and radiated since the Middle Neoproterozoic. The last event includes the appearance of vase shaped fossils, scaled microfossils, diversified acritarchs, unpreceded complex carbonaceous

compression fossils, etc. (reviewed in e.g. Porter 2004; Knoll 2014). The origin of animals can also be treated as a part of this event.

Most workers relate the evolution of eukaryotes with the increase of oxygen in atmosphere and ocean during the Precambrian. The Great Oxidation Event (GOE) in 2.4–2.0 Ga, during which molecular oxygen was released to the atmosphere and the

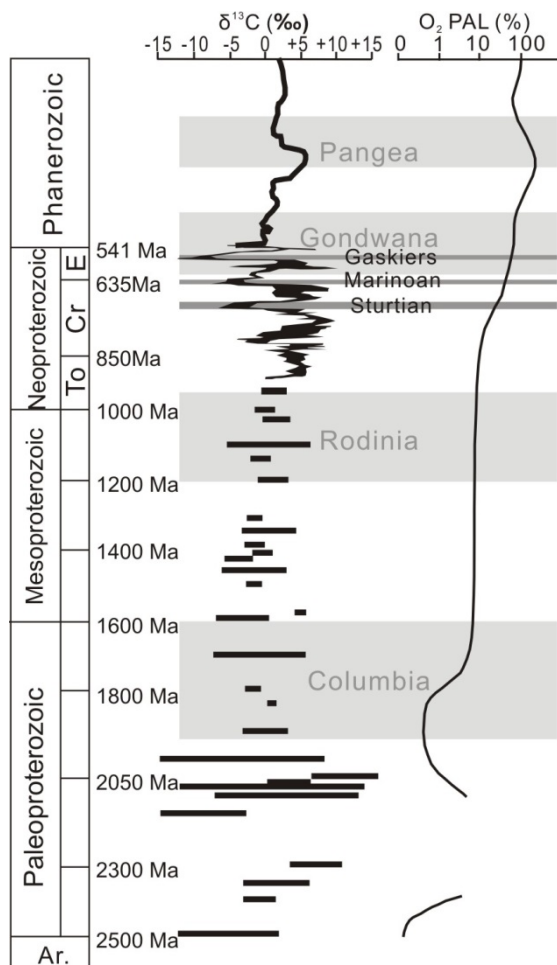


Fig. 1.3 Major environmental changes since the Paleoproterozoic. All the data are collected from literature. The chronological subdivision: the ICS scheme 2012 (in Van Kranendonk et al. 2012). The Precambrian carbon isotope variation and ages of glaciations (dark gray bars): Saltzman and Thomas (2012). The Phanerozoic carbon variation and the historical change of oxygen level: Shields-Zhou and Och (2011). Duration of supercontinents (light gray boxes): Nance et al. (2014).

surface of ocean, is regarded as either a cause (e.g. Gross and Bhattacharya 2010; Knoll 2014) or a consequence (cf. Butterfield 2014) of the eukaryote origin. In the subsequent one billion years (1.85–0.85 Ga), the ocean was stably stratified with oxygenated surface water and euxinic bottom water, and the latter was probably responsible for locking some bio-essential elements and caused the slow evolution of eukaryotes in the Late Paleoproterozoic and the Mesoproterozoic (Canfield 1998; Anbar and Knoll 2002).

This situation was terminated since about 850 Ma. A series of tectonic (disassembly of Rodinia) and climatic (global glaciations) events were accompanied by another oxidation event, the Neoproterozoic Oxidation Event (NOE) (Shields-Zhou and Och 2011; Och and Shield-Zhou 2012). The oxygen concentration finally reached a level close to the modern situation and sufficient to trigger the rise of metazoan. Although recent studies have found that some animals can survive in anerobic or oxygen-depleted environments (e.g. Hoffmann et al. 2005; Mills et al. 2014), animals do need molecule oxygen to produce some basic molecules, such as collagen, which is critical in cell binding and cell-cell signaling (Towe 1981; Saul 2009). The low oxygen level before the GOE was perhaps already sufficient to support the origin of animal life forms, but only when the oxygen concentration became high enough to support a bigger body-size, these organisms started to leave recognizable fossil records (e.g. Towe 1970; Mentel et al. 2014). On the other hand, the appearance of animals may have enhanced the co-evolution of life and environment. Now an increasing number of researchers start to hypothesize that primitive, sponge-grade animals may have been present before the NOE and have contributed to the ventilation of the ancient sea water by consuming organic particles by filter feeding (e.g. Erwin and Tweedt 2012; Lenton et al. 2014). Some authors even attribute the diversification of other eukaryotes in the Middle Neoproterozoic to the advent of ancestral metazoan, because a lot of large lorica and scale-bearing protists appeared at that time and scales and loricae are regarded as protective strategies against predation (Butterfield 2014).

Beside of oxygen, another important element related to these evolutionary events is calcium. Ca^{2+} is critical in modern multicellular organisms in cell-cell binding and signaling, but high Ca^{2+} concentration is proved toxic to cells. Grounded on the “soda ocean” hypothesis (Kempe and Degens

1985) and according to the realities that all cells share a Ca^{2+} concentration of 10^{-7} M while this concentration is 10^{-3} M and 10^{-2} M in body fluids and modern sea water, respectively, Kazmierczak et al. (2013) hypothesized that the concentration of calcium in sea water rose 4 orders of magnitude from Archean, when life originated, to Recent. Multicellularity, similar to the later innovated biomineralization, is probably a detoxification strategy for our unicellular ancestors against the rising level of oxygen and calcium (Simkiss 1977; Saul 2009). However, there are only sparse direct evidences for the historical increase of Ca^{2+} in sea water (e.g. Brennan et al. 2004).

1.2.2 Fossil record of early animals

Since the discovery of the Ediacara Biota (e.g. Murray 1868; Glaessner 1959), large amount of putative animal fossils has been subsequently described worldwide from Precambrian rocks. However, the affinity of these fossils to the Phanerozoic organisms was/is always associated with intensive contention.

The famous Ediacara Biota, present after the Gaskiers glaciation (c.a. 582 Ma), is composed of macroscopic fossils which are preserved mainly as impressions and molds in siliciclastic deposits and rarely in carbonates (Chen et al. 2014). These fossils are dominantly soft-bodied, except a few weakly calcified groups from the horizon close to the Precambrian-Cambrian boundary, like *Cloudina* and *Namacalathus* (e.g. Grotzinger et al. 2000). Many members of the Ediacara Biota are not comparable to the Phanerozoic life forms, but a few of them, such as *Dickinsonia* and *Kimberella*, were compared to metazoans (e.g. Fedonkin and Waggoner 1997; Zhang and Reitner 2006, Sperling and Vinther 2010). Development of analyzing techniques is also bringing new views on acquainted fossils. A restudy of the Late Ediacaran *Sabellidites* indicated that the microstructures of the preserved organic walls are similar to that of the modern siboglinids (Moczydłowska et al. 2014). However, the most robust evidences for the appearance of animals in the Ediacara Biota are probably the unequivocal animal trace fossils reported from this interval (e.g. Jensen et al. 2000, 2006; Chen et al. 2013).

An older record of possible Metazoa in the Ediacaran is some of the large acanthomorphic acritarchs preserved in the phosphates and chert nodules of older than 580 Ma which are interpreted as animal eggs and embryos (e.g. Xiao et al. 1998; Yin et al. 2007). By analyzing the embryo development patterns, it is even suggested that divergence of Porifera, Cnidaria and Bilateria already happened at the time the fossil organisms lived (e.g. Chen et al. 2009; Yin et al. 2013). However, because epithelium has not been observed from these fossils, other interpretations, such as metazoan stem group (Hagadorn et al. 2006) and non-metazoan holozoan (Hultgren et al. 2011), were also proposed for these fossils. The debate on this issue is still being continued.

Contemporaneous with or even older than these microscopic fossils, Lantian Biota is probably the oldest assemblage of macroscopic fossils in the Ediacaran Period (Yuan et al. 2011). These fossils are preserved as carbonaceous compressions in black shales. Though the majority of this biota may be algae, some of the fossils have been interpreted as of cnidarian origin (Van Iten et al. 2013).

All these researches together cast an impression that animals have already developed to some extent of complexity and diversity in the Ediacaran and should be rooted in deeper time. However, the fossils preceding the Ediacaran are even more contentious to be of animal origin.

Discoid fossils comprise part of the Ediacara Biota. Their analogues have been reported in pre-Ediacaran localities such as the Twitya Formation in Northwest Canada (Hofmann et al. 1990), the Stirling Group in Australia (Cruse and Harris 1994; Bengtson et al. 2007), the Upper Riphean in Kazakhstan (Meert et al. 2011) and the boundary between the Nanguanling and Changlingzi Formations in North China (e.g. Xing and Liu 1979). These fossils share the same taphonomy with the Ediacaran discs, although many of them are simpler in morphology, sparser in occurrence and lower in diversity than their Ediacaran analogues. Whereas, like the discoid fossils in the Ediacara Biota (MacGabhann 2007), these older discoid structures can be of multiple origins and have not been fully understood yet.

Other than that, a series of unusual structures have been described from old rocks and related with sponges. These reports include: polymud fabrics interpreted as possible products of sponge decomposition in the Tonian–Cryogenian bioherms (Neuweiler et al. 2009), bizarre fragments in 650-

Ma-old interglacial limestones of Canada (Maloof et al. 2010), sponge-like microfossils (Brain et al. 2012) from 548–760-Ma-old strata of Namibia and chambered fossils from Cryogenian reefs in Australia (Wallace et al. 2014). Yet none of these reports has been accepted as an unequivocal argument for early animal (e.g. Antcliffe 2014). This is partly because the poriferan group is morphologically simple and the early lineages have not developed the ability to build robust skeletons. Spicules and skeletal frames, the consentient indicators of sponge affinity in Phanerozoic fossil record, are not available in such old rocks.

Biomarker is another method to detect taphonomically labile organisms in rock record. 24-isopropylcholestane was previously regarded as a reliable sponge biomarker and has been discovered in Cryogenian or even older rocks (McCaffrey et al 1994, Love et al. 2009). However, this molecule can also diagenetically derive from 24-n-propylidenecholesterol, a product of pelagophytes (Love et al. 2009; Antcliffe 2013). Additionally, another research has discovered that the genes responsible for the production of 24-isopropyl steroids is encoded in poribacteria, the prokaryotic symbionts in demosponges (Siegl et al. 2011), and the symbiotic history of the two organisms is still obscure.

1.3 Summary of this chapter and introduction to the doctoral work

As discussed in 1.1.3, according to phylogenetic studies, sponges are probably the most primitive extant animal. Even if not, their physiological characters match best the theoretic models of the animal common ancestor (1.1.1–1.1.2; Mikhailov 2009; Richter and King 2013). Because of its evolutionary significance, many paleontologists have been devoted to looking for evidences of sponges in the Precambrian rocks. However, although molecular clock and the Ediacaran fossil record indicate that ancestral animals, including sponges, should have appeared in the Precambrian, reliable fossils of this lineage are still not known from rocks of that old (1.2.2). This is probably because spicules, the hallmark of sponges, did not appear until the Early Cambrian (Antcliffe et al. 2014); Precambrian sponges were probably similar to the other animals at that time in being unable to build mineral skeletons (Wood 2011). This requires us to learn other ways to recognize non-spicular sponges in fossil record.

On the other hand, ancestral animals rose from a world full of other prokaryotic and eukaryotic microbial lives (1.2.1). Today we are still at the beginning in evaluating the impact of bacteria on animal evolution (1.1.2), but it is already known that sponges have intensive symbiosis with microbes (Taylor et al. 2007; Siegl et al. 2011). It seems reasonable to assume that Precambrian sponges had intensive interactions with the microbial substrates as well. In this situation, it may be wise to check the Precambrian record of microbialites. The microbial-induced mineralization could also increase the chance of the ancient animals or their interactions with the microbial environments being recorded in rocks.

For these two reasons stated above, this doctoral work made its effort to contribute to our understanding of animal origin by exploring possible fossil record of non-spicular sponges and their ecological relationship with microbial mats, and then trying to apply this knowledge to the study of Precambrian fossils, especially microbialites. The second part is very difficult, because the earliest animals were probably very simple in structure (1.1.1–1.1.2) and their impact on the microbial substrates may be indistinguishable from the affects of other eukaryotic relatives which also have complex multicellular stage in their life cycles. But no matter in which situation, this direction is still worthy to explore.

Chapter 2 is my first attempt to study sponge fossils. The Cambrian “round sponge fossils” in Chengjiang Biota are preserved with unusually thick carbonaceous remains. This study shows that some soft tissue in sponges is more durable in diagenesis than previously expected. However, because of the diagenetic alteration, the sponge-derived carbonaceous remains are difficult to be differentiated from those from other sources. If these “round sponge fossils” occurred in Precambrian shales without the spicules impressions, they will certainly be assigned to algal remains. Therefore, before more powerful biogeochemical methods being invented, morphological features seem still to be the only practical tool in searching for Precambrian sponges.

Chapter 3 moves the study to focus on carbonate materials. Using grinding tomography and 3-D reconstruction, it is declared that, except the previously known single fossil taxon *Vauxia* from the Middle Cambrian shales, non-spicular sponges are also preserved in Phanerozoic carbonates. The

organic skeleton of keratose demosponges (*sensu* Minchin 1900, details see discussion in 3.1) are preserved in the same way as the siliceous spicules of other sponges, i.e. being moulded by rapidly precipitated automicrites derived from the decay of other soft tissues and then replaced by carbonate spars.

Subsequently, these structures related to keratose demosponges, along with some extent of microbial mats, are recognized as the main components in two Phanerozoic stromatolite-like bioconstructions (Chapter 4). These bioconstructions were previously regarded as stromatolites, and the keratose-sponge-related carbonate texture was once described as “vermiform microstructures” in some Middle Cambrian stromatolites in Australia. Interestingly, a recent study found similar sponges as the main constructor of the “maze-like microbialites” (previously regarded as thrombolites), although they diagnosed those fossils only as “demosponges” (Lee et al. 2014).

The fossilization potential of non-spicular sponges was previously largely underestimated. During the whole doctoral study, more occurrences of these fossils were encountered in literature and fossil collections. It seems that non-spicular sponges have been recorded actually all through the Phanerozoic. Chapter 5 is dedicated to summarize the known occurrences.

As indicated in chapter 4, the microbialites assigned to stromatolites or thrombolites according to mesostructures can be in fact constructed by sponges. The only way to figure out the real constructors of these buildups and their biological activities is to study the buildups in the microstructure scale. Chapter 6 is a literature survey on microstructures of Precambrian microbialites, especially those of stromatolites, accompanied with thin section study of a few examples which are interesting within the scope of this doctoral work. However, due to the limit in time, accessible rock material and financial foundation, the work presented in this chapter is rather a start than a conclusion of this topic.

References

- Adl SM, Simpson AGB, Farmer MA, Andersen RA, Anderson OR, Barta JR, Bowser SS, Brugerolle GUY, Fensome RA, Fredericq S, James TY, Karpov S, Kugrens P, Krug J, Lane CE, Lewis LA, Lodge J, Lynn DH, Mann DG, McCourt RM, Mendoza L, Moestrup Ø, Mozley-Stanridge SE, Nerad TA, Shearer CA, Smirnov AV, Spiegel FW, Taylor MFJR (2005) The new higher level classification of eukaryotes with emphasis on the taxonomy of protists. *Journal of Eukaryotic Microbiology* 52 (5):399–451
- Adl SM, Simpson AGB, Lane CE, Lukeš J, Bass D, Bowser SS, Brown MW, Burki F, Dunthorn M, Hampl V, Heiss A, Hoppenrath M, Lara E, le Gall L, Lynn DH, McManus H, Mitchell EAD, Mozley-Stanridge SE, Parfrey LW, Pawlowski J, Rueckert S, Shadwick L, Schoch CL, Smirnov A, Spiegel FW (2012) The revised classification of eukaryotes. *Journal of Eukaryotic Microbiology* 59 (5):429–514
- Alegado RA, Brown LW, Cao S, Dermenjian RK, Zuzow R, Fairclough SR, Clardy J, King N (2012) A bacterial sulfonolipid triggers multicellular development in the closest living relatives of animals. *eLife* 1:e00013
- Anbar AD, Knoll AH (2002) Proterozoic ocean chemistry and evolution: A bioinorganic bridge? *Science* 297 (5584):1137–1142
- Antcliffe JB (2013) Questioning the evidence of organic compounds called sponge biomarkers. *Palaeontology* 56 (5):917–925
- Antcliffe JB, Callow RHT, Brasier MD (2014) Giving the early fossil record of sponges a squeeze. *Biological Reviews* 89:972–1004
- Bengtson S, Rasmussen B, Krapež B (2007) The Paleoproterozoic megascopic Stirling Biota. *Paleobiology* 33 (3):351–381
- Brain CK, Prave AR, Hoffmann K-H, Fallick AE, Botha A, Herd DA, Sturrock C, Young I, Condon DJ, Allison SG (2012) The first animals: ca. 760-million-year-old sponge-like fossils from Namibia. *South Africa Journal of Sciences* 108 (1/2):658–665
- Brennan ST, Lowenstein TK, Horita J (2004) Seawater chemistry and the advent of biocalcification. *Geology* 32 (6):473–476
- Bryant DM, Mostov KE (2008) From cells to organs: Building polarized tissue. *Nature Reviews Molecular Cell Biology* 9 (11):887–901
- Bütschli O (1884) Bemerkungen zur Gastraea-Theorie. *Morphologisches Jahrbuch* 9:415–427
- Butterfield NJ (2000) *Bangiomorpha pubescens* n. gen., n. sp.: Implications for the evolution of sex, multicellularity, and the Mesoproterozoic/Neoproterozoic radiation of eukaryotes. *Paleobiology* 26 (3):386–404
- Butterfield NJ (2014) Early evolution of the Eukaryota. *Palaeontology* (online version) doi:10.1111/pala.12139
- Canfield DE (1998) A new model for Proterozoic ocean chemistry. *Nature* 396 (6710):450–453
- Chen J-Y, Bottjer DJ, Davidson EH, Li G, Gao F, Cameron RA, Hadfield MG, Xian D-C, Tafforeau P, Jia Q-J, Sugiyama H, Tang R (2009) Phase contrast synchrotron X-ray microtomography of Ediacaran (Doushantuo) metazoan microfossils: Phylogenetic diversity and evolutionary implications. *Precambrian Research* 173 (1–4):191–200
- Chen Z, Zhou C, Meyer M, Xiang K, Schiffbauer JD, Yuan X, Xiao S (2013) Trace fossil evidence for Ediacaran bilaterian animals with complex behaviors. *Precambrian Research* 224 (0):690–701
- Chen Z, Zhou C, Xiao S, Wang W, Guan C, Hua H, Yuan X (2014) New Ediacara fossils preserved in marine limestone and their ecological implications. *Scientific Reports* 4: 4180. doi:10.1038/srep04180
- Cruse T, Harris LB (1994) Ediacaran fossils from the Stirling Range Formation, Western Australia. *Precambrian Research* 67:1–10

- Dayel MJ, Alegado RA, Fairclough SR, Levin TC, Nichols SA, McDonald K, King N (2011) Cell differentiation and morphogenesis in the colony-forming choanoflagellate *Salpingoeca rosetta*. *Developmental biology* 357 (1):73–82
- Dickinson, DJ, Nelson, WJ, and Weis, WI (2011) A polarized epithelium organized by β - and α -catenin predates cadherin and metazoan origins. *Science* 331(6022):1336–1339.
- Dickinson DJ, Nelson WJ, Weis WI (2012) An epithelial tissue in *Dictyostelium* challenges the traditional origin of metazoan multicellularity. *BioEssays* 34 (10):833–840
- Dohrmann M, Wörheide G (2013) Novel scenarios of early animal evolution—Is it time to rewrite textbooks? *Integrative and Comparative Biology* 53 (3):503–511
- Edgecombe GD, Giribet G, Dunn CW, Hejnol A, Kristensen RM, Neves RC, Rouse GW, Worsaae K, Sorensen MV (2011) Higher-level metazoan relationships: recent progress and remaining questions. *Organisms Diversity & Evolution* 11 (2):151–172
- Erwin D, Tweedt S (2012) Ecological drivers of the Ediacaran-Cambrian diversification of Metazoa. *Evolutionary Ecology* 26 (2):417–433
- Erwin DH, Laflamme M, Tweedt SM, Sperling EA, Pisani D, Peterson KJ (2011) The Cambrian Conundrum: Early divergence and later ecological success in the early history of animals. *Science* 334 (6059):1091–1097
- Fairclough SR, Dayel MJ, King N (2010) Multicellular development in a choanoflagellate. *Current Biology* 20 (20):R875–R876
- Fedonkin MA, Waggoner BM (1997) The Late Precambrian fossil *Kimberella* is a mollusc-like bilaterian organism. *Nature* 388 (6645):868–871
- Funayama N (2010) The stem cell system in demosponges: Insights into the origin of somatic stem cells. *Development, Growth & Differentiation* 52 (1):1–14
- Glaessner MF (1959) The oldest fossil faunas of South Australia. *Geologische Rundschau* 47 (2):522–531
- Gross J, Bhattacharya D (2010) Uniting sex and eukaryote origins in an emerging oxygenic world. *Biology Direct* 5 (1):53. doi:10.1186/1745-6150-5-53
- Grotzinger JP, Watters WA, Knoll AH (2000) Calcified metazoans in thrombolite-stromatolite reefs of the terminal Proterozoic Nama Group, Namibia. *Paleobiology* 26 (3):334–359
- Hadfield MG (2011) Biofilms and marine invertebrate larvae: What bacteria produce that larvae use to choose settlement sites. *Annual Review of Marine Science* 3 (1):453–470
- Haeckel E (1874) Die Gastraea-Theorie, die phylogenetische Classification des Thierreichs, und die Homologie der Keimblätter. *Jenaische Zeitschrift für Naturwissenschaft* 8:1–55
- Hagadorn JW, Xiao S, Donoghue PCJ, Bengtson S, Gostling NJ, Pawlowska M, Raff EC, Raff RA, Turner FR, Chongyu Y, Zhou C, Yuan X, McFeely MB, Stampanoni M, Neilson KH (2006) Cellular and subcellular structure of Neoproterozoic animal embryos. *Science* 314 (5797):291–294
- Hoffmann F, Larsen O, Thiel V, Rapp HT, Pape T, Michaelis W, Reitner J (2005) An anaerobic world in sponges. *Geomicrobiology Journal* 22 (1-2):1–10
- Hofmann HJ, Narbonne GM, Aitken JD (1990) Ediacaran remains from intertillite beds in northwestern Canada. *Geology* 18 (12):1199–1202
- Hultgren T, Cunningham JA, Yin C, Stampanoni M, Marone F, Donoghue PCJ, Bengtson S (2011) Fossilized nuclei and germination structures identify Ediacaran “animal embryos” as encysting protists. *Science* 334 (6063):1696–1699
- Hynes RO (2012) The evolution of metazoan extracellular matrix. *The Journal of Cell Biology* 196 (6):671–679
- Jensen S, Droser ML, Gehling JG (2006) A critical look at the Ediacaran trace fossil record. In: Xiao S,

- Kaufman AJ (eds) Neoproterozoic Geobiology and Paleobiology. pp 115–157
- Jensen S, Saylor BZ, Gehling JG, Germs GJB (2000) Complex trace fossils from the terminal Proterozoic of Namibia. *Geology* 28 (2):143–146
- Juliano C, Wang J, Lin H (2011) Uniting germline and stem cells: The function of Piwi Proteins and the piRNA pathway in diverse organisms. *Annual Review of Genetics* 45. doi:10.1146/annurev-genet-110410-132541
- Kazmierczak J, Kempe S, Kremer B (2013) Calcium in the early evolution of living systems: A biohistorical approach. *Current Organic Chemistry* 17 (16):1738–1750
- Kempe S, Degens ET (1985) An early soda ocean? *Chemical Geology* 53 (1–2):95–108
- Knoll AH (2014) Paleobiological perspectives on early eukaryotic evolution. *Cold Spring Harbor Perspectives in Biology* 6 (1):a016121. doi:10.1101/cshperspect.a016121
- Kumar S (2005) Molecular clocks: four decades of evolution. *Nature Reviews Genetics* 6 (8):654–662
- Lee J-H, Chen J-T, Choh S-J, Lee D-J, Han Z-Z, Chough SK (2014) Furongian (Late Cambrian) sponge–microbial maze-like reefs in the North China Platform. *Palaios* 29:27–37
- Lenton TM, Boyle RA, Poulton SW, Shields-Zhou GA, Butterfield NJ (2014) Co-evolution of eukaryotes and ocean oxygenation in the Neoproterozoic era. *Nature Geoscience* 7 (4):257–265
- Linnaeus C (1758) *Systema Naturæ*. 10 edn. Laurentius Salvius, Stockholm
- Love GD, Grosjean E, Stalvies C, Fike DA, Grotzinger JP, Bradley AS, Kelly AE, Bhatia M, Meredith W, Snape CE, Bowring SA, Condon DJ, Summons RE (2009) Fossil steroids record the appearance of Demospongiae during the Cryogenian period. *Nature* 457 (7230):718–721
- MacGabhann BA (2007) Discoidal fossils of the Ediacaran biota: a review of current understanding. In: Vinckers-Rich P, Komarower P (eds) *The Rise and Fall of the Ediacaran Biota*. Geological Society, London, Special Publications, London, pp 297–313
- Maloof AC, Rose CV, Beach R, Samuels B, Calmet CC, Erwin DH, Poirier GR, Yao N, Simons FJ (2010) Possible animal-body fossils in pre-Marinoan limestones from South Australia. *Nature Geoscience* 3:653–659
- McCaffrey MA, Michael Moldowan J, Lipton PA, Summons RE, Peters KE, Jeganathan A, Watt DS (1994) Paleoenvironmental implications of novel C30 steranes in Precambrian to Cenozoic Age petroleum and bitumen. *Geochimica et Cosmochimica Acta* 58 (1):529–532
- McCullom TM, Seewald JS (2006) Carbon isotope composition of organic compounds produced by abiotic synthesis under hydrothermal conditions. *Earth and Planetary Science Letters* 243 (1–2):74–84
- McFall-Ngai M, Hadfield MG, Bosch TCG, Carey HV, Domazet-Lošo T, Douglas AE, Dubilier N, Eberl G, Fukami T, Gilbert SF, Hentschel U, King N, Kjelleberg S, Knoll AH, Kremer N, Mazmanian SK, Metcalf JL, Nealson K, Pierce NE, Rawls JF, Reid A, Ruby EG, Rumpho M, Sanders JG, Tautz D, Wernegreen JJ (2013) Animals in a bacterial world, a new imperative for the life sciences. *Proceedings of the National Academy of Sciences* 110 (9):3229–3236
- Meert JG, Gibsher AS, Levashova NM, Grice WC, Kamenov GD, Ryabinin AB (2011) Glaciation and ~ 770 Ma Ediacara (?) fossils from the Lesser Karatau Microcontinent, Kazakhstan. *Gondwana Research* 19 (4):867–880
- Mentel M, Röttger M, Leys S, Tielens AGM, Martin WF (2014) Of early animals, anaerobic mitochondria, and a modern sponge. *BioEssays* 36 (10):924–932
- Mikhailov KV, Konstantinova AV, Nikitin MA, Troshin PV, Rusin LY, Lyubetsky VA, Panchin YV, Mylnikov AP, Moroz LL, Kumar S, Aleoshin VV (2009) The origin of Metazoa: A transition from temporal to spatial cell differentiation. *BioEssays* 31 (7):758–768
- Mills DB, Ward LM, Jones C, Sweeten B, Forth M, Treusch AH, Canfield DE (2014) Oxygen requirements of

- the earliest animals. *Proceedings of the National Academy of Sciences* 111 (11):4168–4172
- Minchin EA (1900) Chapter III. Sponges. In: Lankester ER (ed) *A treatise on zoology. Part II. The Porifera and Coelenterata*. Adam & Charles Black, London, pp 1–178
- Moczyłowska M, Westall F, Foucher F (2014) Microstructure and biogeochemistry of the organically preserved Ediacaran metazoan *Sabellidites*. *Journal of Paleontology* 88 (2):224–239
- Moroz LL, Kocot KM, Citarella MR, Dosung S, Norekian TP, Povolotskaya IS, Grigorenko AP, Dailey C, Berezikov E, Buckley KM, Ptitsyn A, Reshetov D, Mukherjee K, Moroz TP, Bobkova Y, Yu F, Kapitonov VV, Jurka J, Bobkov YV, Swore JJ, Girardo DO, Fodor A, Gusev F, Sanford R, Bruders R, Kittler E, Mills CE, Rast JP, Derelle R, Solovyev VV, Kondrashov FA, Swalla BJ, Sweedler JV, Rogaev EI, Halanych KM, Kohn AB (2014) The ctenophore genome and the evolutionary origins of neural systems. *Nature* 510 (7503):109–114
- Muller WEG (2001) Review: How was metazoan threshold crossed? The hypothetical Urmetazoa. *Comparative Biochemistry and Physiology Part A* 129 (2-3):433–460
- Murray A (1868) Report upon the Geological Survey of Newfoundland for the year 1868. St. John's, Robert Winton, 65 pp
- Nakashima K, Yamada L, Satou Y, Azuma J-i, Satoh N (2004) The evolutionary origin of animal cellulose synthase. *Development Genes and Evolution* 214 (2):81–88
- Nance RD, Murphy JB, Santosh M (2014) The supercontinent cycle: A retrospective essay. *Gondwana Research* 25 (1):4–29
- Neuweiler F, Turner EC, Burdige DJ (2009) Early Neoproterozoic origin of the metazoan clade recorded in carbonate rock texture. *Geology* 37 (5):475–478
- Nichols SA, Dayel MJ, King N (2009) Genomic, phylogenetic, and cell biological insights into metazoan origins. In: Telford MJ, Littlewood DTJ (eds) *Animal Evolution Genomes, Fossils, and Trees*. Oxford University Press, New York, pp 24–32
- Nielsen C (2008) Six major steps in animal evolution: are we derived sponge larvae? *Evolution & Development* 10 (2):241–257
- Nielsen C (2012) *Animal evolution: interrelationships of the living phyla*. 3 edn. Oxford University Press, New York, 402 pp
- Noffke N (2005) Geobiology—a holistic scientific discipline. *Palaeogeography, Palaeoclimatology, Palaeoecology* 219 (1–2):1–3
- Nosenko T, Schreiber F, Adamska M, Adamski M, Eitel M, Hammel J, Maldonado M, Müller WEG, Nickel M, Schierwater B, Vacelet J, Wiens M, Wörheide G (2013) Deep metazoan phylogeny: When different genes tell different stories. *Molecular Phylogenetics and Evolution* 67 (1):223–233
- Och LM, Shields-Zhou GA (2012) The Neoproterozoic oxygenation event: Environmental perturbations and biogeochemical cycling. *Earth-Science Reviews* 110 (1–4):26–57
- Olszewski TD (2001) Geobiology: A Golden Opportunity and a Call to Action. *Palaios* 16 (6):533–534
- Osigus H-J, Eitel M, Bernt M, Donath A, Schierwater B (2013) Mitogenomics at the base of Metazoa. *Molecular Phylogenetics and Evolution* 69 (2):339–351
- Parfrey LW, Lahr DJG (2013) Multicellularity arose several times in the evolution of eukaryotes (Response to DOI 10.1002/bies.201100187). *BioEssays* 35 (4):339–347
- Peterson KJ, Cotton JA, Gehling JG, Pisani D (2008) The Ediacaran emergence of bilaterians: congruence between the genetic and the geological fossil records. *Phil Trans R Soc B* 363:1435–1443
- Peterson KJ, Dietrich MR, McPeck MA (2009) MicroRNAs and metazoan macroevolution: insights into canalization, complexity, and the Cambrian explosion. *BioEssays* 31 (7):736–747

- Peterson KJ, Lyons JB, Nowak KS, Takacs CM, Wargo MJ, McPeck MA (2004) Estimating metazoan divergence times with a molecular clock. *PNAS* 101 (17):6536–6541
- Philippe H, Brinkmann H, Lavrov DV, Littlewood DTJ, Manuel M, Wörheide G, Baurain D (2011) Resolving Difficult Phylogenetic Questions: Why More Sequences Are Not Enough. *PLoS Biol* 9 (3):e1000602
- Philippe H, Derelle R, Lopez P, Pick K, Borchellini C, Boury-Esnault N, Vacelet J, Renard E, Houliston E, Quéinnec E, Da Silva C, Wincker P, Le Guyader H, Leys S, Jackson DJ, Schreiber F, Erpenbeck D, Morgenstern B, Wörheide G, Manuel M (2009) Phylogenomics Revives Traditional Views on Deep Animal Relationships. *Current Biology* 19 (8):706–712
- Pick KS, Philippe H, Schreiber F, Erpenbeck D, Jackson DJ, Wrede P, Wiens M, Alié A, Morgenstern B, Manuel M, Wörheide G (2010) Improved phylogenomic taxon sampling noticeably affects nonbilaterian relationships. *Molecular Biology and Evolution* 27 (9):1983–1987
- Porter SM (2004) The fossil record of early eukaryotic diversification. *Paleontological Society Papers* 10:35–50
- Raff RA, Field KG, Olsen GJ, al. e (1989) Metazoan phylogeny based on analysis of 18S ribosomal RNA. In: Fernholm B, Bremer K, Jörnvall H (eds) *The Hierarchy of Life: Molecules and Morphology in Phylogenetic Analysis*. Excerpta Medica/Elsevier, Amsterdam, pp 247–260
- Reitner J, Thiel V (eds) (2011) *Encyclopedia of Geobiology*. Springer, Dordrecht, Netherlands, 927 pp
- Richter DJ, King N (2013) The genomic and cellular foundations of animal origins. *Annual Review of Genetics* 47 (1):509–537
- Rosing MT (1999) ^{13}C -Depleted Carbon Microparticles in >3700-Ma Sea-Floor Sedimentary Rocks from West Greenland. *Science* 283 (5402):674–676
- Rosing MT, Frei R (2004) U-rich Archaean sea-floor sediments from Greenland – indications of > 3700 Ma oxygenic photosynthesis. *Earth and Planetary Science Letters* 217 (3–4):237–244
- Saltzman MR, Thomas E (2012) Chapter 11 - Carbon isotope stratigraphy. In: Gradstein FM, Ogg JG, Schmitz MD, Ogg GM (eds) *The Geologic Time Scale*. Elsevier, Boston, 207–232
- Saul JM (2009) Did detoxification processes cause complex life to emerge? *Lethaia* 42 (2):179–184
- Shields-Zhou G, Och L (2011) The case for a Neoproterozoic oxygenation event: Geochemical evidence and biological consequences. *GSA Today* 21 (3):4–11
- Siegl A, Kamke J, Hochmuth T, Piel J, Richter M, Liang C, Dandekar T, Hentschel U (2011) Single-cell genomics reveals the lifestyle of Poribacteria, a candidate phylum symbiotically associated with marine sponges. *ISME Journal* 5 (1):61–70
- Simkiss K (1977) Biomineralization and detoxification. *Calc Tis Res* 24 (1):199–200
- Sperling EA, Peterson KJ, Pisani D (2009) Phylogenetic-signal dissection of nuclear housekeeping genes supports the paraphyly of sponges and the monophyly of eumetazoa. *Molecular Biology and Evolution* 26 (10):2261–2274
- Sperling EA, Robinson JM, Pisani D, Peterson KJ (2010) Where's the glass? Biomarkers, molecular clocks, and microRNAs suggest a 200-Myr missing Precambrian fossil record of siliceous sponge spicules. *Geobiology* 8 (1):24–36
- Sperling EA, Vinther J (2010) A placozoan affinity for *Dickinsonia* and the evolution of late Proterozoic metazoan feeding modes. *Evolution & Development* 12 (2):201–209
- Taylor MW, Radax R, Steger D, Wagner M (2007) Sponge-associated microorganisms: evolution, ecology, and biotechnological potential. *Microbiology and Molecular Biology Reviews* 71 (2):295–347
- Towe KM (1970) Oxygen-Collagen Priority and the Early Metazoan Fossil Record. *Proceedings of the National Academy of Sciences of the United States of America* 65 (4):781–788
- Towe KM (1981) Biochemical keys to the emergence of complex life. In: Billingham J (ed) *Life in the Universe*.

MIT Press, Cambridge, MA, pp 297–305

- Tyler S (2003) Epithelium—The primary building block for metazoan complexity. *Integrative and Comparative Biology* 43 (1):55–63
- Ueno Y, Isozaki Y, Yurimoto H, Maruyama S (2001) Carbon isotopic signatures of individual Archean microfossils(?) from Western Australia. *International Geology Review* 43 (3):196–212
- Van Iten H, Leme JDM, Marques AC, Simões MG (2013) Alternative interpretations of some earliest Ediacaran fossils from China. *Acta Palaeontologica Polonica* 58 (1):111–113
- Van Kranendonk MJ (2006) Volcanic degassing, hydrothermal circulation and the flourishing of early life on Earth: A review of the evidence from c. 3490–3240 Ma rocks of the Pilbara Supergroup, Pilbara Craton, Western Australia. *Earth-Science Reviews* 74 (3–4):197–240
- Van Kranendonk MJ, Contributors, Altermann W, Beard BL, Hoffman PF, Johnson CM, Kasting JF, Melezhik VA, Nutman AP, Papineau D, Pirajno F (2012) Chapter 16 - A chronostratigraphic division of the Precambrian: Possibilities and challenges. In: Gradstein FM, Ogg JG, Schmitz MD, Ogg GM (eds) *The Geologic Time Scale*. Elsevier, Boston, pp 299–392
- Wallace MW, Hood AvS, Woon EMS, Hoffmann K-H, Reed CP (2014) Enigmatic chambered structures in Cryogenian reefs: The oldest sponge-grade organisms? *Precambrian Research* 255, Part 1 (0):109–123
- Walter MR, Buick R, Dunlop JSR (1980) Stromatolites 3,400–3,500 Myr old from the North Pole area, Western Australia. *Nature* 284 (5755):443–445
- Wood RA (2011) Paleoecology of the earliest skeletal metazoan communities: Implications for early biomineralization. *Earth-Science Reviews* 106 (1–2):184–190
- Wörheide G, Dohrmann M, Erpenbeck D, Larroux C, Maldonado M, Voigt O, Borchellini C, Lavrov DV (2012) Chapter one - Deep phylogeny and evolution of sponges (Phylum Porifera). In: Becerro MA, Uriz MJ, Maldonado M, Xavier T (eds) *Advances in Marine Biology*, Volume 61. Academic Press, pp 1–78
- Xiao S, Zhang Y, Knoll AH (1998) Three-dimensional preservation of algae and animal embryos in a Neoproterozoic phosphorite. *Nature* 391 (6667):553–558
- Xing Y, Liu G (1979) Coelenterate fossils from the Sinian System of Southern Liaoning and its stratigraphical significance. *Acta Geologica Sinica* (3):168–172
- Yin L, Zhu M, Knoll AH, Yuan X, Zhang J, Hu J (2007) Doushantuo embryos preserved inside diapause egg cysts. *Nature* 446 (7136):661–663
- Yin Z, Zhu M, Tafforeau P, Chen J, Liu P, Li G (2013) Early embryogenesis of potential bilaterian animals with polar lobe formation from the Ediacaran Weng'an Biota, South China. *Precambrian Research* 225:44–57
- Zakhvatkin AA (1949) The comparative embryology of the low invertebrates. Sources and method of the origin of metazoan development. Soviet Science, Moscow, 395 pp
- Zhang X, Reitner J (2006) A fresh look at *Dickinsonia*: Removing it from Vendobionta. *Acta Geologica Sinica - English Edition* 80 (5):636–642

- Chapter 2 -

Preservation of organic matter in sponge fossils: a case study of “round sponge fossils” from the Cambrian Chengjiang Biota with Raman spectroscopy

(Göttingen Contributions to Geosciences (2014), 77: 29–38, <http://dx.doi.org/10.3249/webdoc-3914>)

Cui Luo, Nadine Schäfer, Jan-Peter Duda, Li-Xia Li

Abstract

Understanding the taphonomy of organic matter of sponges will be helpful in reconstructing a more exhaustive picture of the evolutionary history of these organisms from fossil records. The so-called “round sponge fossils” (RSF) from the Burgess Shale-type (BST) Chengjiang Lagerstätte predominantly yield explicit organic remains, which seem more durable than the carbonaceous components of other fossils in the same Lagerstätte. In order to characterize these carbonaceous remains with Raman spectroscopy, a quick and non-destructive technique with the ability of analyzing the molecular composition and crystal structure in high resolution, 5 RSF specimens were examined in this study. Another Cambrian sponge fossil from the Xiaoyanxi Formation and a few algal remains from the Ediacaran Wenghui Biota were also measured for comparison.

The resulting Raman spectra of the macroscopic fossils confirmed previous observations on microfossils by Bower et al. (2013) that carbonaceous material with compositionally complex precursor material and low diagenetic thermal affection will plot in a certain region in a Γ_D over R1 diagram. The results also successfully differentiated the sponge material from the algal material, as well as the fossil-derived signal from the background. However, it is still uncertain whether the different clustering of the RSF data and the algal data reflects the variance of precursor material or only the diagenetic and geological history. The variance within the RSF data appears to be larger than that within the algal data. Considering the similar diagenetic history of the RSF, this is possibly reflecting the difference in precursor material. Nonetheless, further measurements on other fossil algal and poriferan material must be involved in the future, in order to improve and testify the current interpretation.

Despite the properties revealed by Raman spectroscopy, the taphonomy of carbonaceous material in RSF has not been investigated. According to our observation, as well as the phenomenon described in previous studies, the preservation of the carbonaceous material in RSF does not show obvious taxonomical preferences. Because the RSF are polyphylogenetic and currently lack evidence to indicate that they represent any special development stage of sponges, we infer that this unusual carbonaceous preservation is due to diagenetic bias relating to their specific morphology, which in turn is possibly controlled by similar living environments. Again, to test these inferences, more detailed taxonomical and paleoecological studies are necessary.

Keywords

Porifera, Cambrian, Burgess Shale-type preservation, Raman spectroscopy, China

2.1 Introduction

Porifera is the known most primitive lineage of Metazoa (e.g. Philippe et al. 2009; Sperling et al. 2009) and is now suspected having originated as early as Cryogenian (Peterson et al. 2008; Sperling et al. 2010). However, the commonly acknowledged fossil record of this lineage is not older than the Early Cambrian, although a group of unusual structures from Precambrian rocks have been proposed as candidates of early sponges (e.g. Maloof et al. 2010; Brain et al. 2012). This is partly because spicules, the traditionally adopted criteria for setting up a poriferan affinity, may have not been evolved in Precambrian, or the taphonomical windows at that time were not favorable for the spicular material (Sperling et al. 2010). Therefore, a revaluation of the taphonomical potential of sponges may lead to a new understanding on the early evolutionary history of Porifera.

One aspect of this question is the preservation of the sponge-derived organic matter. It was generally believed that the soft part is of low potential to be fossilized as macroscopic fossils, and the poriferan fossil record has therefore a strong bias toward mineral skeletons (Pisera 2006). However, at least the Burgess Shale-type (BST) Lagerstätten yield exceptions. From the Middle Cambrian Burgess Shale (Rigby and Collins 2004), *Vauxia* has been identified as the earliest fossil of ceractinomorph demosponges due to the preservation of carbon remains in the coring fibers of these fossils. Li et al. (1998) also mentioned an observation of a single specimen of keratose sponge in their collection from Chengjiang fauna.

The so-called “round sponge fossils” (RSF) from the Chengjiang Biota are another example. They are always circular to sub-circular in shape, small in size (3–40 mm in diameter, mostly <10 mm) and exhibiting an intensive or even continuous carbonaceous cover on the surface. Because of these morphological similarities, they were loosely mentioned as a group under the name RSF by Wu (2004), although they seem polyphyletic and the affinity is still unresolved. Compared to most other fossils from the same locality, which are strongly weathered and exhibit very few organic remains (e.g. Zhu et al. 2005), the dense carbonaceous cover of RSF appears quite unique.

Raman spectroscopy is a valuable tool for almost non-destructive high resolution analysis of the molecular composition and crystal structure of samples. It does not need extensive sample preparation

and can give comparatively quick information. However, when applying this method in fossil studies, the interpretation of the data is not always clear and often critically discussed (e.g. in case of putative microfossils in Archean rocks; Kudryavtsev et al. 2001; Brasier et al. 2002; Pasteris and Wopenka 2002; Schopf et al. 2002; Schopf et al. 2005). Already Marshall et al. (2012) made an approach for investigating BST type preservation on a fossil from the Cambrian Spence Shale with Raman spectroscopy. They focused on mineral replacement on different parts of the fossil and the associated thermal history. Only recently Bower et al. (2013) published comprehensive results concerning the interpretation of carbon signals from microfossils, in regard of tracing the differences in the putative precursor material. The most promising parameters turned out to be the full width at half height of the D-band (Γ_D) and the intensity ratio of the D- and the G-band (R1). As in our case the biogenicity of the sponge fossils is not questionable, the application of Raman spectroscopy serves the purpose of revealing the nature of the carbon cover of the RSF and at the same time extending the results to macroscopic fossils following the work of Bower et al. (2013).

In this study, a few specimens of RSF were examined with a short description and discussion on their taphonomy and taxonomical affinity. The Raman spectra of their carbonaceous cover were illustrated and analyzed. In order to identify the characters of these RSF-derived spectra, a sponge fossil from Cambrian Xiaoyanxi Formation and several algal remains from the Ediacaran Wenghui Biota were also examined for comparison.

2.2 Material and Methods

All the specimens studied in this paper are from the collection of Prof. Dr. Mao-Yan Zhu's group in the Nanjing Institute of Geology and Palaeontology, Chinese Academy of Sciences, including five RSF from the Cambrian Chengjiang Biota (inventory numbers no. 41047, no. 42436, no. 42446, no. 42952 and no. 42982; Fig. 2.2), one sponge fossil from the Cambrian Xiaoyanxi Formation (inventory name XYX) and several algal fossils from the Wenghui Biota (inventory name WH). These fossils were observed with a ZEISS Stemi 2000-C microscope and photographed with a CANON EOS 500D. For Raman spectroscopic analysis a confocal Horiba Jobin-Yvon LabRam-HR 800 UV Raman

spectrometer attached to an Olympus BX41 microscope was used. The excitation wavelength for the Raman spectra was the 488 nm line of an Argon Ion Laser (Melles Griot IMA 106020B0S) with a laser power of 20 mW. A detailed description of the spectrometer is given in Beimforde et al. (2011). All spectra were recorded and processed using LabSpec™ version 5.19.17 (Horiba Jobin-Yvon, Villeneuve d'Ascq, France). Mineral identification was performed on the basis of the Horiba Jobin-Yvon database for minerals.

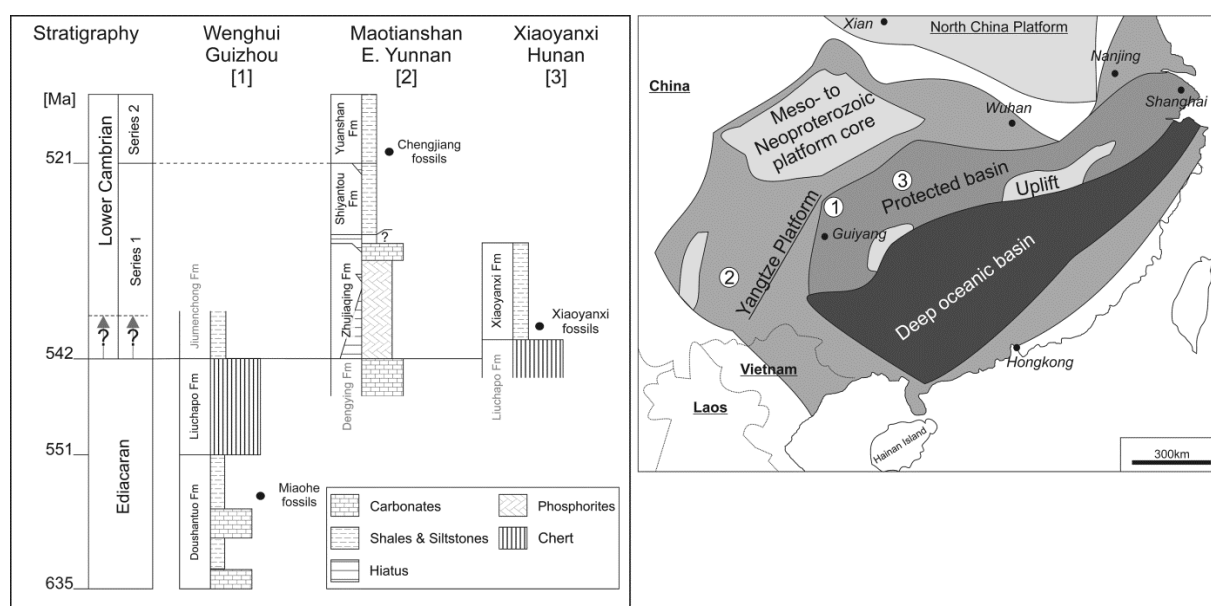


Fig. 2.1 Stratigraphy, locality and depositional environments of the sampled sections. Numbers of sections refer to the marked positions on the map [stratigraphy based on Steiner et al. (2001, 2005); Condon et al. (2005); Guo et al. (2007); Zhu et al. (2007); map based on Steiner et al. (2001)].

The RSF were collected from fossil sites near Chengjiang County, mainly from Maotianshan and Xiaolantian (Wu 2004). They are preserved in the yellowish-green shale from the Maotianshan Shale Member of the Yu'an-shan Formation (Fig. 2.1). The age of the fossiliferous layer has been estimated as ca. 520 Ma (Hu 2005). Previous research distinguished two types of sediments from the Maotianshan Shale: the slowly deposited background beds and the rapidly deposited event beds which probably represent storm-induced distal tempestites (Hu 2005). Because the collection of these RSF is contributed by several workers over a long period, it is now impossible to know the exact type of sediments in which each RSF was collected. However, it has been confirmed by quantitative analysis that the fossils in the two taphonomical facies originated from a single local community, because the

two types of beds exhibit similar recurrent and abundant species, as well as similar temporal trends in evenness and richness (Zhao et al. 2009).

The sponge fossil from the carbonaceous black shale of Xiaoyanxi Formation in Yuanling, Hunan Province has not yet been taxonomically described (Fig. 2.1; Fig. 2.3a). Similar to other Lower Cambrian sequences in South China, the fossiliferous black shale is successively underlain by a layer of Ni-Mo ore, a phosphorite layer and then the Precambrian sedimentary rocks. The absolute age of the fossil horizon was evaluated as younger than 532 Ma (Jiang et al. 2012).

The algal remains are of Ediacaran age and were collected from the Wenghui Biota in Guizhou Province (Zhao et al. 2004; Wang et al. 2007). This fossil assemblage is composed of dominantly algal organisms preserved in the black shale of the upper Doushantuo Formation (Fig. 2.1; Fig. 2.3b–d). These algae appear to be benthic and buried *in situ*, therefore considering the paleogeography of the Doushantuo Formation, the sedimentary environment of these rocks was believed as on the slope, below the storm wave base but still within the photic zone (Jiang et al. 2011; Zhu et al. 2012).

2.3 Results

2.3.1 *Preservation of carbonaceous remains in studied fossils*

Except one incomplete specimen (no. 41047), the other four RSF studied in this paper have an elliptical outline and a diameter of 0.6–0.8 cm. no.42952 maintains the thickest carbonaceous remains. Polygonal cracks are developed on the upper surface of the carbonaceous cover while traces of spicules are absent (Fig. 2.2a–c). However, the carbonaceous cover on this fossil can be removed quite easily, and where the cover is absent, impression of a hexactinellid skeleton similar to that of *Triticispongia diagonata* turns out to be quite clear (Fig. 2.2b). By comparison, no.42436 (Fig. 2.2d–f) and no.42446 (Fig. 2.2g–i) show a thinner but also continuous carbonaceous cover, which is more tightly compacted to the siliciclastic matrix and not easy to remove. Some small and faint marks, resembling moulds of hexactinellid spicules, are distributed on parts of the fossil surface (Fig. 2.2e, h–i). The carbonaceous cover of no. 41047 (Fig. 2.2j) is not continuous as those of the aforementioned

three specimens, although it looks also intensive. The siliceous skeleton of this specimen is distinctly preserved as mould and shows characters of a hexactinellid, whose skeletons seem denser and better interconnected than *T. diagonata*. No.42982 exhibits a reddish surface with weakly preserved moulds of spicules and only scattered carbonaceous remains (Fig. 2.2k–l), generally resembling the surface of no. 42952 after removal of the carbonaceous cover. In the research of Wu (2004) on ca. 270 RSF specimens, it has been described that in these fossils the conspicuousness of the spicules decreases with increasing density of the carbonaceous cover. However, our observations indicate there may not be any definite relationship between the preservational qualities of the carbonaceous remains and the spicules.

In contrast to the RSF, the sponge specimen from Xiaoyanxi Formation does not have an obvious carbonaceous cover. Though the fossil region appears generally darker than the background, the boundary between them can be quite obscure in many places (Fig. 2.3a).

The Ediacaran algal specimens show high morphological diversity within only square-decimeter scale. Although the thickness of carbonaceous remains of these fossils varies between different morphological taxa (Fig. 2.3b–d) and between different parts of a single individual (Fig. 2.3e), the boundary between fossil and background is mostly distinct.

In some individuals, the carbonaceous remains are extremely thick and form polygonal fractures on the surface like those in RSF no.42952 (Fig. 2.3d, f).

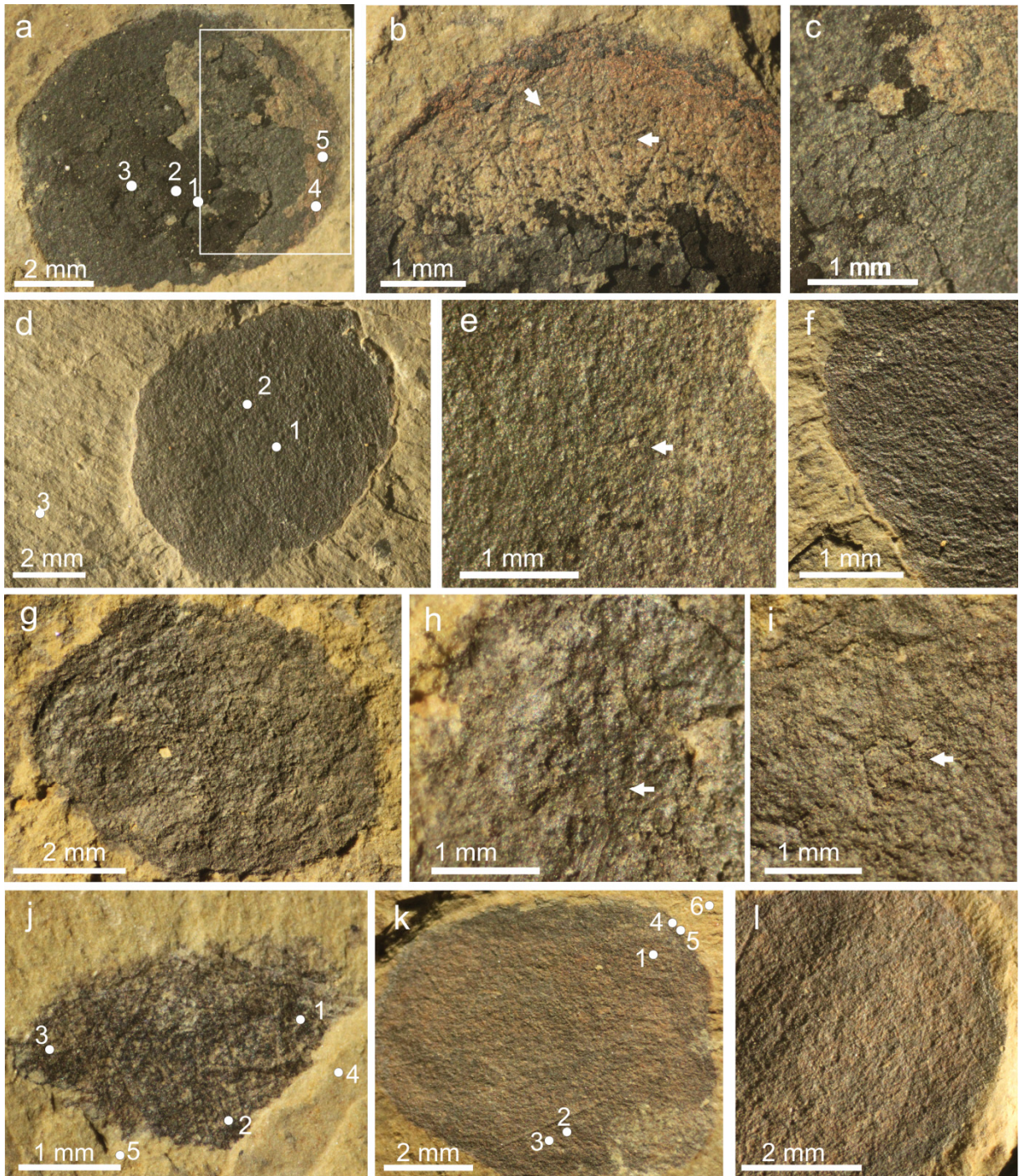


Fig. 2.2 “Round sponge fossils” (RSF) from the Chengjiang Biota. **a–c**, specimen no. 42952; **b–c**, details of **a**, note cracks on the surface of the carbonaceous film. The white arrows in **b** point to marks of spicules. **d–f**, specimen no.42436; **e–f** show details of **d**, the white arrow in **e** points to a possible mark of spicule. **g–i**, specimen no.42446; **h–i**, details of **g**, white arrows pointing to possible mineral skeleton marks. **j**, specimen no. 41047. **k–l**, specimen no. 42982; **l**, detail of **k**, note apparent spicular structures. Number marks in **a**, **d**, **j** and **k** show the Raman spectra sample spots.

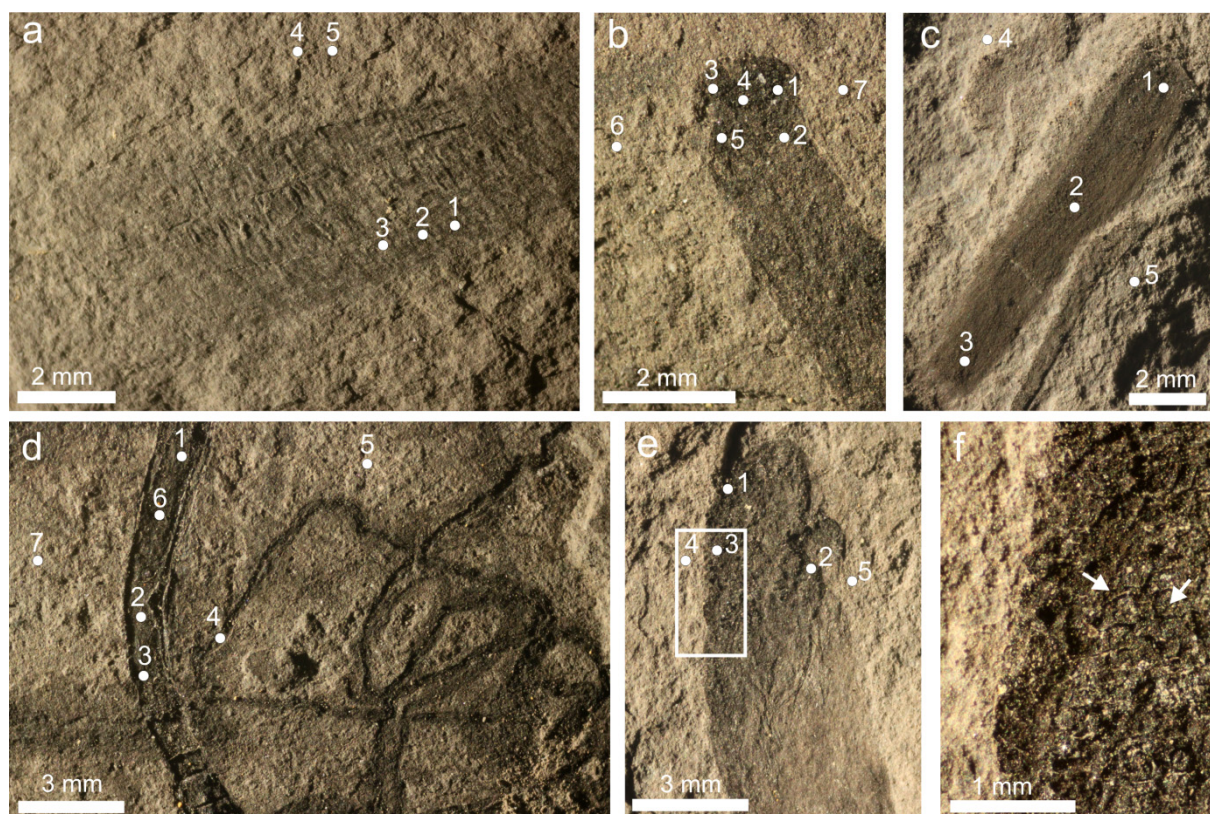
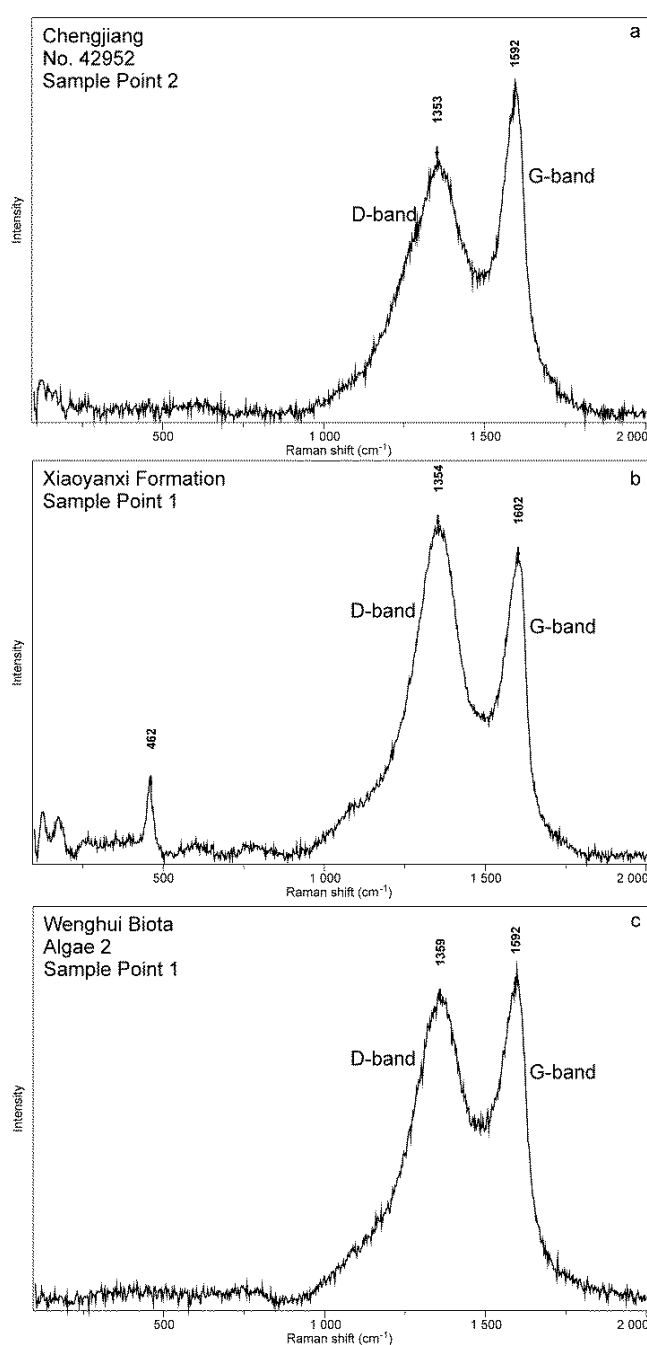


Fig. 2.3 **a**, the sponge fossil from the Early Cambrian Xiaoyanxi Formation. **b–e**, algal fossils from the Ediacaran Wenghui Biota; **b** corresponds to algae 2, **c** corresponds to algae 4, **d** corresponds to algae 1 and **e** corresponds to algae 3 in Fig. 2.5. **f**, detail of **e**, white arrows pointing to polygonal cracks in the densely preserved carbon film. Number marks in **a–e** represent the location of Raman spectra sample spots.

2.3.2 Raman spectra

Totally 46 Raman spectra have been obtained from four of the Chengjiang fossils, the sponge fossil from the Xiaoyanxi Formation and a few algal remains from Wenghui Biota (Fig. 2.4). The most prominent signals from all the samples are typical for amorphous carbon, characterized by two prominent bands in the lower wavenumber region around 1600 cm^{-1} (G-band; graphite-band) and around 1350 cm^{-1} (D-band; disorder-band) (cf. Tuinstra and Koenig 1970; Wopenka and Pasteris 1993; Quirico et al. 2009). Sometimes additional bands for minerals also occur, which are a good sign for influence of the background material. Furthermore, especially the background shale material exhibits a high fluorescence, which can be caused by the extremely fine grained clay minerals, resulting in a reduction of the Raman signal (Wang and Valentine 2002). Since this study is focused on the analysis of the carbon signal, the mineral- and fluorescence-influenced spectra are not shown in this paper.

On first sight, the results for all samples look quite similar, with the exception of XYX (Fig. 2.4), in which the D-band is always higher than the G-band. The differences between the fossil and background material are also difficult to recognize. However, it is well known that peak intensities of the two bands can vary in a small range due to several independent factors, e.g., thermal alteration, the original carbonaceous material, and crystallinity of the carbon (Robertson 1986; Pasteris and Wopenka 2003; Busemann et al. 2007; Marshall et al. 2010). Therefore, geologically valuable information was extracted by calculating the relative intensity ratio between the D- and the G-band (R_1) and the full width at half height of the D-band (Γ_D). Both parameters seem to be suitable to differentiate between



different samples as well as between fossil and background material (Fig. 2.5; Table 2.1). The “round sponge fossils” from the Chengjiang Biota show mean R_1 values of 0.79 (no.42952), 0.69 (no.42436), 0.81 (no.42981) and 0.74 (no.41407). The sample XYX from the Xiaoyanxi Formation is characterized by signals with higher D- than G-band, with an average R_1 value of 1.08. The different algal fossils from the Wenghui Biota have mean R_1 values of 0.90 (algae 1), 0.88 (algae 2), 0.91 (algae 3) and 0.97 (algae 4). In all samples except XYX, there is a clear difference between the R_1 values of the

Fig. 2.4 Representative Raman spectra measured on sponge fossils from the Chengjiang Biota (a) and the Xiaoyanxi Formation (b) as well as algal fossils from the Wenghui Biota (c); see Figs. 2–3 for position of sample spots. The small band centered at 462 cm^{-1} in b is attributed to the main SiO_2 vibration in quartz. Note the changing intensity relation of the D- and G-bands in each sample, resulting in different R_1 values (cf. Table 2.1).

fossils and those of the background material. When plotting the average Γ_D values over the average R1 values, this becomes even clearer (Fig. 2.5a). The carbonaceous remains of XYX seem too thin and discontinuous, so that the carbon signals of the fossil do not differ from those of the background. Additionally, this sample is the only one with a mean R1 value greater than 1, suggesting intensive diagenesis and/or metamorphism (cf. Wopenka and Pasteris 1993; Rahl et al. 2005; Bower et al. 2013; Foucher and Westall 2013), which may have caused an equalization between the fossil-derived carbon and the carbon from the matrix. Because the signals from this sample cannot reflect the nature of sponge-derived carbon, it is not considered in the further discussion of the Raman signals.

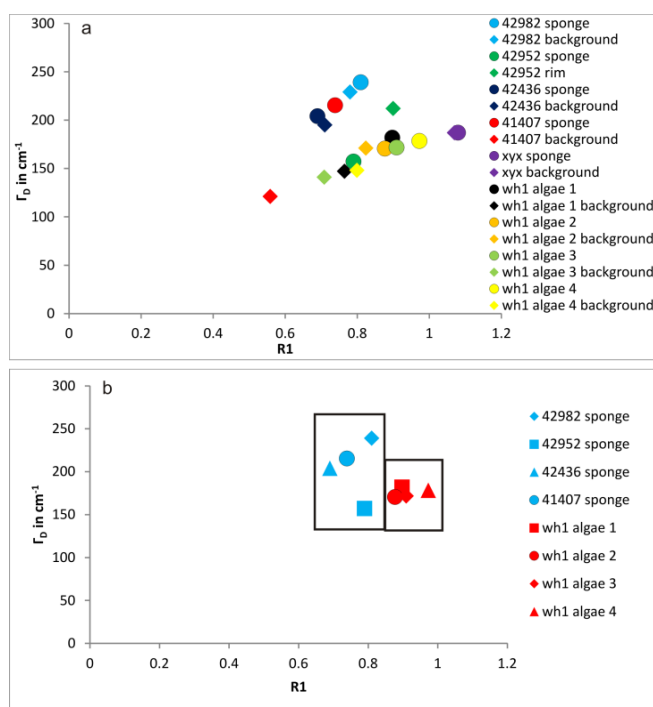


Fig. 2.5 Cross plots of the average values of the full width at half maximum of the D-band (Γ_D) over the intensity ratio of the D- and the G-band (R1) (cf. Table 2.1). **a**, values of the sponge fossils from Chengjiang and the Xiaoyanxi Formation (XYX), the algal fossils from the Wenghui Biota (WH), as well as the associated background materials. Fossil points are marked with circles and the associated background materials with diamonds. Except for samples from the Xiaoyanxi Formation, fossil values are clearly distinguishable from the respective background values. **b**, exclusively values of sponges from the Chengjiang Biota (blue symbols) and algae from the Wenghui Biotas (red symbols); note the apparent clustering of the data (see squares).

2.4 Discussion

BST preservation was firstly defined as “exceptional organic preservation of non-mineralizing organisms in fully marine siliciclastic sediments”, with “some degree of early diagenetic mineralization” (Butterfield 1995). Following this definition, the algal fossils studied in this paper should also be regarded as a representative of BST preservation, as what has been figured out by Xiao et al. (2002) for the algal fossils from the equivalent Miaohu Biota. Although the mechanisms causing exceptional BST preservation are still under debate (e.g. Butterfield 1990; Petrovich 2001; Gaines et al.

2005), it is obvious that materials of different taphonomical resistance are preserved in different states in BST Lagerstätten. It has been summarized by Butterfield et al. (2007) that the two-dimensional carbonaceous compressions represent relatively recalcitrant extracellular components (e.g., cuticles and chaetae), while former labile soft-tissues may result in three-dimensional mineralization of either carbonates or phosphates, and the early diagenetic pyrite incidentally distributes in all Burgess Shale fossils.

Table 2.1 Average Γ_D and R1 values measured on the investigated fossils and the associated background materials.

	Sample Point	Description	average Γ_D	average R1
Chengjiang Biota				
no. 42952	1 - 3	fossil	157	0.79
	4 - 5	rim	212	0.90
no. 42436	1	fossil + background	257	0.82
	2	fossil	204	0.69
	3	background	195	0.71
no. 42982	1 + 3	fossil	239	0.81
	4 - 5	background	229	0.78
no. 41407	1 - 3	fossil	215	0.74
	4 - 5	background	121	0.56
Xiaoyanxi				
	1 - 3	fossil	187	1.08
	4 - 5	background	187	1.07
Wenghui Biota				
algae 1	1 - 4 + 6	fossil	182	0.90
	5 + 7	background	147	0.76
algae 2	1 - 5	fossil	170	0.88
	6 - 7	background	171	0.82
algae 3	1 - 3	fossil	172	0.91
	4 - 5	background	141	0.71
algae 4	1 - 3	fossil	178	0.97
	4 - 5	background	148	0.80

In the Chengjiang Biota, most 2-D soft-bodied fossils are originally preserved in organic carbon, although due to intensive weathering the carbon material is largely diminished (Zhu et al. 2005). Compared with these fossils, the durability of carbonaceous material in the RSF appears unusual. As examples for diagenetically recalcitrant organic material, the taphonomy of collagenous periderm of *Rhabdopleura* (an extant close relative of graptolites) and the cuticle of arthropods composed of wax and chitin have been comprehensively studied (Gupta and Briggs 2011). Although received much less attention and having not been studied by taphonomical experiments, sponges possess diagenetic-

recalcitrant organic material as well. Collagen distribute pervasively in sponges as either supplementary or main components in the skeletal frame (Bergquist 1978). Furthermore, chitin was recently detected in the skeleton of some hexactinellids (Ehrlich et al. 2007) and as a scaffold material tangling with collagen in the spongin skeleton of Verongida (Ehrlich et al. 2010).

In the case of algae, algaenan has been identified as a material with high fossilizing potential. However, the known occurrence of this material is restricted to Chlorophyta and some unicellular algae (Collinson 2011). Because the phylogeny of these Ediacaran macroscopic algae is uncertain (Xiao and Dong 2006), it is currently impossible to postulate the original material of the algal carbonaceous remains from Wenghui Biota.

The Raman signals from these recalcitrant carbonaceous materials are clearly distinguishable from those of their backgrounds in the Γ_D –R1 diagram (Fig. 2.5a), supporting the fossil-derived nature of these carbon remains. When the data points of the background material are removed, it is obvious that the signals from Chengjiang sponge fossils and those from Wenghui algal fossils do cluster separately (Fig. 2.5b).

Comparing with the data published by Bower et al. (2013), all our fossil signals fall into the region in which other samples containing compositionally complex precursor material plot (Γ_D between 100 and 250 cm^{-1} ; R1 0.5 to 1.4). Bower et al. (2013) suggested that an extensive analysis of the carbon signature can reveal information on the precursor material, when other influences like a high thermal maturity can be ruled out. In our data, the Γ_D and R1 values of the algal fossils are very similar to each other, while the carbon of the sponge fossils shows a greater variability. Since the sponge fossils are from the same age and region, and preserved in similar yellowish-green shales, indicating a similar thermal diagenetic impact, it could be possible that a bigger variance of precursor material is responsible for the higher variance in the Raman signal of the carbonaceous remains. The values of the sponge sample no. 42952 show a higher similarity to those of the algae, with a slightly narrower D-band. The narrowing of the D-band could mean that this sample was either influenced by a thermal event (Wopenka and Pasteris 1993; Bower et al. 2013) or that the thick carbon cover has a different origin than the thinner covers of the other sponge fossils. Although these data show a clear

differentiation between the carbon cover of the BST sponge fossils and the Ediacaran algal fossils, it is still hard to judge whether this phenomenon is caused by a divergent diagenetic history or the different source of organic carbon (sponge vs. algae).

Anyhow, the data presented here, support the observations of Bower et al. (2013) that the evaluation of the D- and G-band parameters of carbonaceous material can give a clue on different precursor materials. For a more detailed evaluation it would be necessary to apply Raman spectroscopy on a greater variety of sponge and algae fossils from different environments and, if possible, with known precursor materials.

Despite the information revealed by Raman spectroscopy, the unordinary occurrence of the diagenetically robust organic material in RSF raises questions. In sponges, the enrichment of diagenetic-durable organic material (collagen and chitin) varies between taxa and physiological structures. In keratose sponges, spongin composes the skeletal framework and collagen may be enriched as a complement in the mesohyl (Bergquist 1978). In demosponges, the fibrillar collagen is still pervasive and often forms dense binds between spicules, while in hexactinellids, collagen only forms a thin sheath wrapping the spicules but does not occur massively (Bergquist 1978). Additionally, the shell of sponge gemmules and the sponge base which attaches to the substratum can also be specially enhanced by spongin (Ehrlich 2010). However, the RSF studied here yield indisputable hexactinellid spicules (Fig. 2.2), although RSF possessing only diactines have also been mentioned by Wu (2004).

Therefore, the thick carbonaceous remains on the hexactinellid RSF may indicate that either these fossils represent a special part or developing stage of the sponges, or some hexactinellids once possessed enriched collagen/spongin in the evolutionary history, or there is a special taphonomical mechanism in Chengjiang Biota, which selectively benefit the preservation of organic matter in RSF.

Wu (2004) regarded the RSF as sponge gemmules because of the exceptionally recalcitrant organic matter and the round shape. But this interpretation is not in line with the character of modern and confirmed fossil sponge gemmules, which are at largest only about 1 mm in diameter (Fell 1993; Petit and Charbonnier 2012) and thus much smaller than the RSF. When erecting some RSF from Sancha as

genera (*Triticispongia* and *Saetaspongia*), Steiner et al. (1993) interpreted *T. diagonata* as juveniles because their size hardly exceeds 10 mm, although adult forms have not been discovered then. But the juvenile theory cannot contribute directly to the interpretation of the thick carbon cover, because to our knowledge, the juvenile sponges do not necessarily have enriched spongin as in the case of gemmules.

On the other hand, based on the material from Chengjiang Biota, some other researchers tended to interpret *T. diagonata* as adult precursor of reticulosid sponges, considering the missing adults and its well-organized skeletal structures (Rigby and Hou 1995). Larger specimens of *T. diagonata* (2.5–3 cm) were further discovered in the Niutitang Formation in Guizhou (Zhao et al. 2006). They are more probably giant individuals relating to certain environment or evolutionary stage than adult forms of the Hunan and Chengjiang analogues, because none of these three fossil communities contain big and small specimens at the same time. However, interpreting *T. diagonata* as a specific evolutionary stage of hexactinellids also could not help to explain the intensive carbon preservation of RSF, because RSF are polyphylogenetic. Wu (2004) has described sponges which possess only diactinal spicules in the RSF, indicating a demosponge population in them. And in this study, the observed specimens appear to belong to different hexactinellid morphotypes (Fig. 2.2).

For these reasons, we prefer to suggest that the unusual preservation of the organic carbon in RSF is probably due to some specific processes during early diagenesis, e.g. more effective adsorption of clays relating to the specific size and shape of these fossils. Furthermore, we attribute the exclusively small and round shape of these sponges to similar environmental controls. It has been observed in modern examples, that the exterior morphology of sponges can be strongly affected by environment, while the skeletal construction is still controlled by gene expression. The juvenile theory cannot be completely excluded as an interpretation of the specific morphology of RSF. However, the difficulty here is that the RSF are composed of various biological taxa, and it seems unlikely to expect that the juvenile of all the sponges possessed a similar morphology when the influence from the environment is absent. Furthermore, there has not been any reconstruction on the ontogenies of Chengjiang sponges, which could relate RSF to any potential adult forms. Nevertheless, to test these postulations further investigations on the taxonomy of the RSF and precise observations in the outcrops are required.

2.5 Conclusions

Our observations show that the recalcitrant organic material from sponges, most probably being collagen and chitin according to current knowledge, can be preserved as dense carbonaceous remains in macroscopic fossils in BST Lagerstätten. The present application of Raman spectroscopy with the interpretation of the Γ_D and R1 values of the carbon signal still cannot directly reveal the nature of the precursor of the carbonaceous remains. However, our results confirmed suggestions by Bower et al. (2013) that carbonaceous material from complex precursor material with low thermal affection cluster in a certain area in the Γ_D -R1 plot (Γ_D between 100 and 250 cm^{-1} ; R1 0.5 to 1.4). As the study of Bower et al. (2013) deals with microfossils, our findings represent first evidence that this approach could also be applied to macrofossils. This method also appears to be able to differentiate several sources of carbon in macroscopic fossil samples: between the fossil and the background, between the fossil material from Cambrian RSF and Ediacaran algal fossils, and between different specimens of RSF. It is still uncertain whether the separate clustering of the RSF data and the algal data reflects the variance of precursor material or only the diagenetic or geological history. However, the larger variance within the RSF data compared to the algal data probably is caused by different precursor material, because the RSF derive from the same setting and thus have a similar diagenetic and geological history. Nonetheless, further measurements on other fossil algal and poriferan material must be involved in the future, in order to improve and testify the current interpretations.

The taphonomical mechanism of the dense carbonaceous material in RSF is also interesting. Because the RSF are polyphylogenetic and there is currently no evidence to support their nature as any special development stage of sponges, we infer that this unusual carbonaceous preservation is due to a diagenetic bias relating to their specific morphology, which in turn is possibly controlled by similar living environments. Again, to test these inferences, more detailed taxonomical and paleoecological studies are necessary.

Acknowledgement

We appreciate Prof. Dr Mao-Yan Zhu (NIGPAS) for providing the fossil material, and Dr. Michael Steiner (Freie Universität Berlin) for his beneficial review and precious suggestions for this text. We are also grateful for the help from Dr. Wen Wu (NIGPAS), Ms. Lan-Yun Miao (NIGPAS) and Mr. Han Zeng (Nanjing University) with the literature collecting.

References

- Beimforde C, Schäfer N, Dörfelt H, Nascimbene PC, Singh H, Heinrichs J, Reitner J, Rana RS, Schmidt AR (2011) Ectomycorrhizas from a Lower Eocene angiosperm forest. *New Phytologist* 192 (4):988–996
- Bergquist PR (1978) *Sponges*. University of California Press, Berkeley and Los Angeles. 267 pp
- Bower DM, Steele A, Fries MD, Kater L (2013) Micro Raman spectroscopy of carbonaceous material in microfossils and meteorites: improving a method for life detection. *Astrobiology* 13 (1):103–113
- Brain CB, Prave AR, Hoffmann K-H, Fallick AE, Botha A, Herd DA, Sturrock C, Young I, Condon DJ, Allison SG (2012) The first animals: ca. 760-million-year-old sponge-like fossils from Namibia. *South African Journal of Science* 108 (1–2):658–665
- Brasier MD, Green OR, Jephcoat AP, Kleppe AK, Van Kranendonk MJ, Lindsay JF, Steele A, Grassineau NV (2002) Questioning the evidence for Earth's oldest fossils. *Nature* 416 (6876):76–81
- Busemann H, Alexander MOD, Nittler LR (2007) Characterization of insoluble organic matter in primitive meteorites by microRaman spectroscopy. *Meteoritics & Planetary Science* 42 (7–8):1387–1416
- Butterfield NJ (1990) Organic preservation of non-mineralizing organisms and the taphonomy of the Burgess Shale. *Paleobiology* 16 (3):272–286
- Butterfield NJ (1995) Secular distribution of Burgess-Shale-type preservation. *Lethaia* 28 (1):1–13
- Butterfield NJ, Balthasar UWE, Wilson LA (2007) Fossil diagenesis in the Burgess Shale. *Palaeontology* 50 (3):537–543
- Collinson M (2011) Molecular taphonomy of plant organic skeletons. In: Allison P, Bottjer D (eds) *Taphonomy: Process and Bias through time*. Topics in Geobiology, vol 32. Springer, Dordrecht etc., pp 223–247
- Condon D, Zhu M, Bowring S, Wang W, Yang A, Jin Y (2005) U-Pb ages from the Neoproterozoic Doushantuo Formation, China. *Science* 308 (5718):95–98
- Ehrlich H (2010) Spongin. In: Ehrlich H (ed) *Biological Materials of Marine Origin. Biologically-Inspired Systems*, vol 1. Springer, Dordrecht etc., pp 245–256
- Ehrlich H, Ilan M, Maldonado M, Muricy G, Bavestrello G, Kljajic Z, Carballo JL, Schiaparelli S, Ereskovsky A, Schupp P, Born R, Worch H, Bazhenov VV, Kurek D, Varlamov V, Vyalikh D, Kummer K, Sivkov VV, Molodtsov SL, Meissner H, Richter G, Steck E, Richter W, Hunoldt S, Kammer M, Paasch S, Krasokhin V, Patzke G, Brunner E (2010) Three-dimensional chitin-based scaffolds from Verongida sponges (Demospongiae: Porifera). Part I. Isolation and identification of chitin. *International Journal of Biological Macromolecules* 47 (2):132–140
- Ehrlich H, Krautter M, Hanke T, Simon P, Knieb C, Heinemann S, Worch H (2007) First evidence of the presence of chitin in skeletons of marine sponges. Part II. Glass sponges (Hexactinellida: Porifera). *Journal of Experimental Zoology Part B: Molecular and Developmental Evolution* 308B (4):473–483
- Fell PE (1993) Porifera. In: Adiyodi KG, Adiyodi RG (eds) *Reproductive Biology of Invertebrates VI (A: Asexual propagation and reproductive strategies)*. Wiley, Chichester, pp 1–44
- Foucher F, Westall F (2013) Raman imaging of metastable opal in carbonaceous microfossils of the 700–800 Ma old Draken Formation. *Astrobiology* 13 (1):57–67
- Gaines RR, Kennedy MJ, Droser ML (2005) A new hypothesis for organic preservation of Burgess Shale taxa in the Middle Cambrian Wheeler Formation, House Range, Utah. *Palaeogeography, Palaeoclimatology,*

Palaeoecology 220 (1–2):193–205

- Guo Q, Shields GA, Liu C, Strauss H, Zhu M, Pi D, Goldberg T, Yang X (2007) Trace element chemostratigraphy of two Ediacaran–Cambrian successions in South China: Implications for organosedimentary metal enrichment and silicification in the Early Cambrian. *Palaeogeography, Palaeoclimatology, Palaeoecology* 254 (1–2):194–216
- Gupta N, Briggs DEG (2011) Taphonomy of animal organic skeletons through time. In: Allison P, Bottjer D (eds) *Taphonomy: Process and Bias through time. Topics in Geobiology*, vol 32. Springer, Dordrecht etc., pp 199–221
- Hu S (2005) Taphonomy and palaeoecology of the Early Cambrian Chengjiang Biota from eastern Yunnan. *Berliner Paläobiologische Abhandlungen* 7:1–189
- Jiang G, Shi X, Zhang S, Wang Y, Xiao S (2011) Stratigraphy and paleogeography of the Ediacaran Doushantuo Formation (ca. 635–551 Ma) in South China. *Gondwana Research* 19 (4):831–849
- Jiang G, Wang X, Shi X, Xiao S, Zhang S, Dong J (2012) The origin of decoupled carbonate and organic carbon isotope signatures in the early Cambrian (ca. 542–520 Ma) Yangtze platform. *Earth and Planetary Science Letters* 317–318 (0):96–110
- Kudryavtsev AB, Schopf JW, Agresti DG, Wdowiak TJ (2001) In situ laser-Raman imagery of Precambrian microscopic fossils. *Proceedings of the National Academy of Sciences* 98 (3):823–826
- Li C-W, Chen J-Y, Hua T-E (1998) Precambrian sponges with cellular structures. *Science* 279 (5352):879–882
- Maloof AC, Rose CV, Beach R, Samuels BM, Calmet CC, Erwin DH, Poirier GR, Yao N, Simons FJ (2010) Possible animal-body fossils in pre-Marinoan limestones from South Australia. *Nature Geosci* 3 (9):653–659
- Marshall AO, Wehrbein RL, Lieberman BS, Marshall CP (2012) Raman spectroscopic investigations of Burgess Shale–type preservation: A new way forward. *Palaios* 27 (5):288–292
- Marshall CP, Edwards HGM, Jehlicka J (2010) Understanding the application of raman spectroscopy to the detection of traces of life. *Astrobiology* 10 (2):229–243
- Pasteris JD, Wopenka B (2002) Laser-Raman spectroscopy (Communication arising): Images of the Earth's earliest fossils? *Nature* 420 (6915):476–477
- Pasteris JD, Wopenka B (2003) Necessary, but not sufficient: Raman identification of disordered carbon as a signature of ancient life. *Astrobiology* 3 (4):727–738
- Peterson KJ, Cotton JA, Gehling JG, Pisani D (2008) The Ediacaran emergence of bilaterians: Congruence between the genetic and the geological fossil records. *Philosophical Transactions of the Royal Society of London B: Biological Sciences* 363 (1496):1435–1443
- Petit G, Charbonnier S (2012) Fossil sponge gemmules, epibionts of *Carpopenaeus garassinoi* n. sp. (Crustacea, Decapoda) from the Sahel Alma Lagerstätte (Late Cretaceous, Lebanon). *Geodiversitas* 34 (2):359–372
- Petrovich R (2001) Mechanisms of fossilization of the soft-bodied and lightly armored faunas of the Burgess Shale and of some other classical localities. *American Journal of Science* 301 (8):683–726
- Philippe H, Derelle R, Lopez P, Pick K, Borchellini C, Boury-Esnault N, Vacelet J, Renard E, Houliston E, Quéinnec E, Da Silva C, Wincker P, Le Guyader H, Leys S, Jackson DJ, Schreiber F, Erpenbeck D, Morgenstern B, Wörheide G, Manuel M (2009) Phylogenomics revives traditional views on deep

- animal relationships. *Current Biology* 19 (8):706–712
- Pisera A (2006) Palaeontology of sponges — a review. *Canadian Journal of Zoology* 84 (2):242–261. doi:10.1139/z05-169
- Quirico E, Montagnac G, Rouzaud JN, Bonal L, Bourrot-Denise M, Duber S, Reynard B (2009) Precursor and metamorphic condition effects on Raman spectra of poorly ordered carbonaceous matter in chondrites and coals. *Earth and Planetary Science Letters* 287 (1–2):185–193
- Rahl JM, Anderson KM, Brandon MT, Fassoulas C (2005) Raman spectroscopic carbonaceous material thermometry of low-grade metamorphic rocks: Calibration and application to tectonic exhumation in Crete, Greece. *Earth and Planetary Science Letters* 240 (2):339–354
- Rigby JK, Collins D (2004) Sponges of the Middle Cambrian Burgess Shale and Stephen Formations, British Columbia. *ROM Contributions in Science* 1:1–155
- Rigby JK, Hou X-G (1995) Lower Cambrian demosponges and hexactinellid sponges from Yunnan, China. *Journal of Paleontology* 69 (6):1009–1019
- Robertson J (1986) Amorphous carbon. *Advances in Physics* 35 (4):317–374
- Schopf JW, Kudryavtsev AB, Agresti DG, Czaja AD, Wdowiak TJ (2005) Raman imagery: A new approach to assess the geochemical maturity and biogenicity of permineralized Precambrian fossils. *Astrobiology* 5 (3):333–371
- Schopf JW, Kudryavtsev AB, Agresti DG, Wdowiak TJ, Czaja AD (2002) Laser-Raman imagery of Earth's earliest fossils. *Nature* 416 (6876):73–76
- Sperling EA, Peterson KJ, Pisani D (2009) Phylogenetic-signal dissection of nuclear housekeeping genes supports the paraphyly of sponges and the monophyly of Eumetazoa. *Molecular Biology and Evolution* 26 (10):2261–2274
- Sperling EA, Robinson JM, Pisani D, Peterson KJ (2010) Where's the glass? Biomarkers, molecular clocks, and microRNAs suggest a 200-Myr missing Precambrian fossil record of siliceous sponge spicules. *Geobiology* 8 (1):24–36
- Steiner M, Mehl D, Reitner J, Erdtmann B-D (1993) Oldest entirely preserved sponges and other fossils from the lowermost Cambrian and a new facies reconstruction of the Yangtze Platform (China). *Berliner Geowissenschaftliche Abhandlungen (E: Paläobiologie)* 9:293–329
- Steiner M, Wallis E, Erdtmann B-D, Zhao Y, Yang R (2001) Submarine-hydrothermal exhalative ore layers in black shales from South China and associated fossils — insights into a Lower Cambrian facies and bio-evolution. *Palaeogeography, Palaeoclimatology, Palaeoecology* 169 (3–4):165–191
- Steiner M, Zhu M, Zhao Y, Erdtmann B-D (2005) Lower Cambrian Burgess Shale-type fossil associations of South China. *Palaeogeography, Palaeoclimatology, Palaeoecology* 220 (1–2):129–152
- Tuinstra F, Koenig JL (1970) Raman spectrum of graphite. *The Journal of Chemical Physics* 53 (3):1126–1130
- Wang A, Valentine RB (2002) Seeking and identifying phyllosilicates on mars- a simulation study. In: 33rd annual lunar and planetary science conference, Houston, Texas, March 11–15, 2002. Abstract no 1370
- Wang Y, Wang X, Huang Y (2007) Macroscopic algae from the Ediacaran Doushantuo formation in northeast Guizhou, South China. *Earth Science (Journal of China University of Geosciences)* 32 (6):828–844

- Wopenka B, Pasteris JD (1993) Structural characterization of kerogens to granulite-facies graphite: applicability of Raman microprobe spectroscopy. *American Mineralogist* 78:533–557
- Wu W (2004) Fossil sponges from the Early Cambrian Chengjiang Fauna, Yunnan, China. Unpublished PhD-thesis, Nanjing Institute of Geology and Palaeontology, Chinese Academy of Sciences. Nanjing. 179 pp
- Xiao S, Dong L (2006) On the morphological and ecological history of Proterozoic macroalgae. In: Xiao S, Kaufman A (eds) *Neoproterozoic Geobiology and Paleobiology*. Topics in Geobiology 27. Springer Netherlands, pp 57–90
- Xiao S, Yuan X, Steiner M, Knoll AH (2002) Macroscopic carbonaceous compressions in a terminal Proterozoic shale: A systematic reassessment of the Miaohu Biota, South China. *Journal of Paleontology* 76 (2):347–376
- Zhao F, Caron J-B, Hu S, Zhu M (2009) Quantitative analysis of taphofacies and paleocommunities in the Early Cambrian Chengjiang Lagerstätte. *Palaios* 24 (12):826–839
- Zhao Y, He M, Chen M, Peng J, Yu M, Wang Y, Yang R, Wang P, Zhang Z (2004) Discovery of a Miaohu-type biota from the Neoproterozoic Doushantuo Formation in Jiangkou County, Guizhou Province, China. *Chinese Science Bulletin* 49 (18):1916–1918
- Zhao Y, Yang R, Yang X, Mao Y (2006) Globular sponge fossils from the Lower Cambrian in Songlin, Guizhou Province, China. *Geological Journal of China Universities* 12 (1):106–110
- Zhu M, Babcock LE, Steiner M (2005) Fossilization modes in the Chengjiang Lagerstätte (Cambrian of China): testing the roles of organic preservation and diagenetic alteration in exceptional preservation. *Palaeogeography, Palaeoclimatology, Palaeoecology* 220 (1–2):31–46
- Zhu M, Yang A, Yang X, Peng J, Zhang J, Lu M (2012) Ediacaran succession and the Wenghui Biota in the deep-water facies of the Yangtze Platform at Wenghui, Jiangkou County, Guizhou. *Journal of Guizhou University (Natural Sciences)* 29 (1):133–138
- Zhu M, Zhang J, Yang A (2007) Integrated Ediacaran (Sinian) chronostratigraphy of South China. *Palaeogeography, Palaeoclimatology, Palaeoecology* 254 (1–2):7–61

- Chapter 3 -

First report of fossil “keratose” demosponges in Phanerozoic carbonates: preservation and 3-D reconstruction

(*Naturwissenschaften* (2014) 101: 467–477, doi: 10.1007/s00114-014-1176-0)

Cui Luo, Joachim Reitner

Abstract

Fossil record of Phanerozoic non-spicular sponges, beside of being important with respect to the lineage evolution *per se*, could provide valuable references for the investigation of Precambrian ancestral animal fossils. However, although modern phylogenomic studies resolve non-spicular demosponges as the sister group of the remaining spiculate demosponges, the fossil record of the former is extremely sparse or unexplored compared to that of the latter; the Middle Cambrian Vauxiidae Walcott, 1920, is the only confirmed fossil taxon of non-spicular demosponges. Here, we describe carbonate materials from Devonian (Upper Givetian to Lower Frasnian) bioherms of northern France and Triassic (Anisian) microbialites of Poland that most likely represent fossil remnants of keratose demosponges. These putative fossils of keratose demosponges are preserved as automicritic clumps. They are morphologically distinguishable from microbial fabrics but similar to other spiculate sponge fossils, except that the skeletal elements consist of fibrous networks instead of assembled spicules. Consistent with the immunological behavior of sponges, these fibrous skeletons often form a rim at the edge of the automicritic aggregate, separating the inner part of the aggregate from foreign objects. To confirm the architecture of these fibrous networks, two fossil specimens and a modern thorectid sponge for comparison were processed for three-dimensional (3-D) reconstruction using serial grinding tomography. The resulting fossil reconstructions are three-dimensionally anastomosing, like modern keratose demosponges, but their irregular and nonhierarchical meshes indicate a likely verongid affinity, although a precise taxonomic conclusion cannot be made based on the skeletal architecture alone. This study is a preliminary effort, but an important start to identify fossil non-spicular demosponges in carbonates and to reevaluate their fossilization potential.

Keywords

Keratose demosponges; Fossil sponges; Carbonates; Automicrite; Devonian; Triassic

3.1 Introduction

Sponges are the known most basic multicellular animals, and are expected to have originated long before the Cambrian, based on molecular-clock investigations (e.g., Peterson et al. 2008; Sperling et al. 2009; Erwin et al. 2011), biomarker studies (e.g., Love et al. 2009) and the fossil record of other animal lineages around the Precambrian-Cambrian boundary (cf. Shu et al. 2014). However, generally accepted fossils of early sponges, which were identified primarily according to the appearance of different sorts of spicules, started no earlier than the beginning of Cambrian (e.g., Steiner et al., 1993; Wu et al., 2005; Xiao et al., 2005; Reitner et al. 2012; Yang et al. 2014). This is probably because animals did not evolve the ability to build mineral skeletons until only a few million years before the Cambrian (Wood 2011). The Precambrian sponges may well be non-spicular and thus either not preserved, or preserved but not recognized. For this reason, it seems necessary and practical to check first the Phanerozoic fossil record for how non-spicular sponges could be preserved and in which environment they tend to survive and thrive. Then this knowledge could be used as a reference point to seek the ancestral animals.

The first formal taxonomic category for non-spicular sponges is “Keratosa”, which was established by early researchers to encompass those sponges whose skeletons consist of “horny” or “keratose” fibers and lack siliceous or calcareous spicules (Grant 1861; Bowerbank 1864). Based on increased knowledge of sponges, Minchin (1900, p.153–154) later refined the term “Keratosa” to mean “Demospongiae in which the skeleton consists of fibers of spongin, without ‘proper’ spicules”, apart from “Myxospongida”, which “is devoid of a skeleton in any form”. Although “Keratosa” was abolished as a formal taxonomic group after Levi (1957), it has recently been revived based on phylogenomic data (e.g., Borchiellini et al. 2004; Lavrov et al. 2008; Erpenbeck et al. 2012; reviewed in Wörheide et al. 2012). A consensus has been reached to assign the name “Keratosa” to the group formed by Dictyoceratida and Dendroceratida (G1) in the new phylogenetic tree. Simultaneously, the name “Myxospongiae” is applied to the branch composed of Verongida and Chondrosida + *Halisarca* (G2) (reviewed by Cárdenas et al. 2012). Furthermore, G1 + G2 has been identified as the sister group of the spiculate demosponges, indicating a similarly deep evolutionary history for the non-spicular demosponges. Although given the existence of siliceous skeletons in Hexactinellida, it is still under

debate whether the absence of mineral skeletons in the demosponge group G1 + G2 is apo- or plesiomorphic, the fossil record of these non-spicular sponges could be regarded as an analogue of that of the Precambrian sponges because they share similar physiological characters.

However, compared to the abundant fossils of siliceous demosponges from Cambrian to Cenozoic (e.g., Pisera 2002; Reitner and Wörheide 2002), Keratosa and Myxospongiae are poorly represented in the geological record. To date, the only confirmed non-spicular taxon is family Vauxiidae Walcott, 1920 with a single genus *Vauxia* from the Middle Cambrian (Rigby 1986; Rigby and Collins 2004). Although a recent study found chitin of 505-years-old in one of the *Vauxia* specimens (Ehrlich et al. 2013), indicating very high preservation quality of fossils in this Lagerstätte, the diversity and distribution of non-spicular sponge fossils have not been amplified in this, and other relevant shale facies. Here, we make the first report of possible keratose demosponges in Phanerozoic carbonate facies, in Middle Devonian bioherms and Middle Triassic microbialites, which may extend our knowledge about the taphonomy and distribution of fossil non-spicular sponges.

In this paper, we preferentially define “Keratosa” or “keratose demosponges” in the sense of Minchin (1900). In other words, Verongida is also included in this group in addition to Dictyoceratida and Dendroceratida. This is because in fossil material, most of the taxonomically important features of non-spicular sponges, such as the microscopic structure of the skeletal fibers and the type of choanocyte chambers, are obscured or obliterated by the fossilization process. In most cases, only the architecture of the skeletal frame is available for taxonomic identification. In this situation it is difficult or impossible to clearly distinguish dendroceratids, dictyoceratids and verongids in fossil material.

3.2 Material and geological background

3.2.1 Middle Devonian bioherms from Boulonnais, northern France

The studied Devonian materials are small bioherms collected from the “Banc Noir” quarry, located 3 km NE of Ferques. In the Ferques area, Paleozoic sediments developed in the so-called Bas-

Boulonnais in the western extension of the Namur Basin (Brice and Colbeaux 1976). The “Banc Noir” quarry exhibits a section of the entire Blacourt Formation (Middle to Upper Givetian) and the base of the Beaulieu Formation (Upper Givetian to Lower Frasnian). The sampled small bioherms are associated with black carbonates and marls at the base of the Middle Givetian “Membre du Grisè” of the Blacourt Formation (*P. varcus* zone) (Fig. 3.1). This facies is related to the initial development of the Devonian carbonate platform and most likely represents a fore-reef environment.

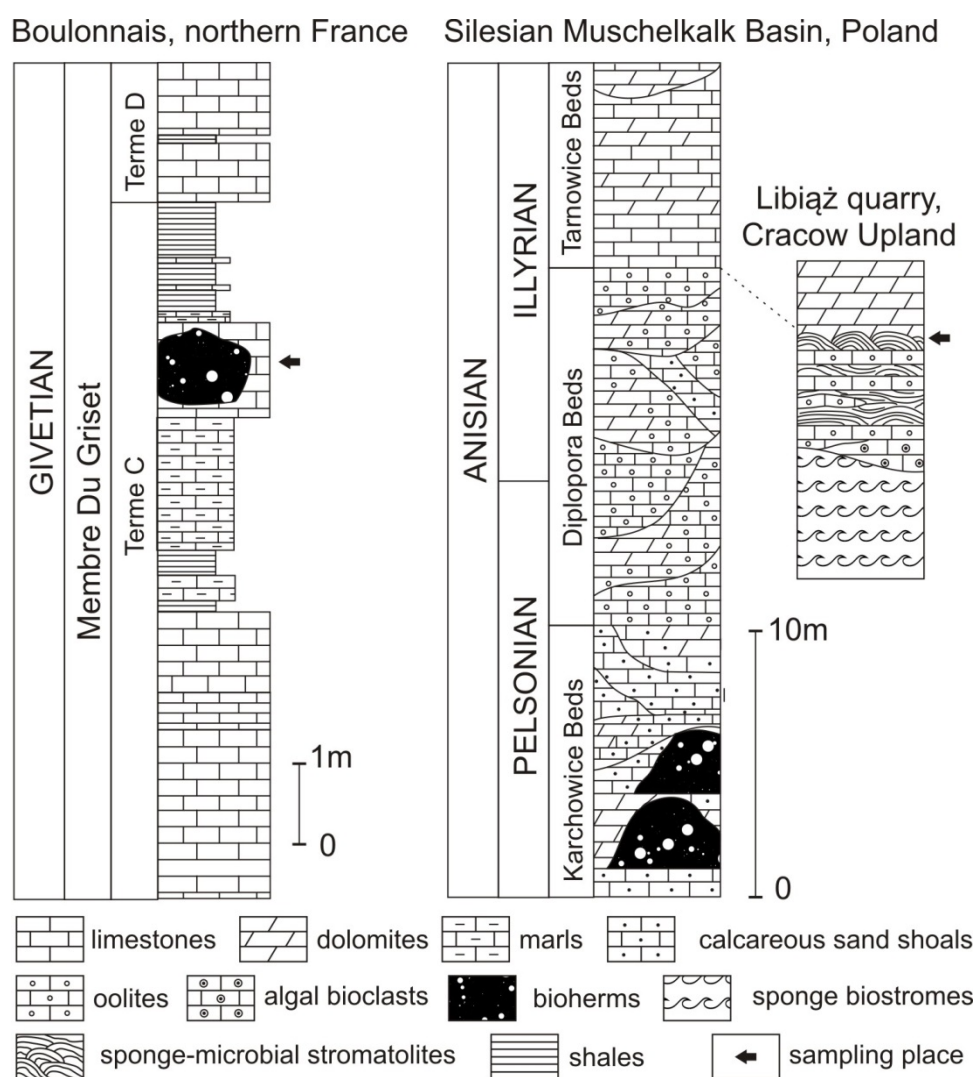


Fig. 3.1 Stratigraphy of the outcrops where the investigated fossil materials were sampled. The column for Boulonnais, northern France, is modified from Mistiaen and Poncet (1983). The column for the Silesian Muschelkalk Basin is modified from Szulc (1997a), and the column for the Libiąż quarry is modified from Szulc (1997b). Because the *Diplopore* Beds were deposited in highstand system tracts, the facies change rapidly according to the local paleotopography. The correlation shown in this figure is based on the description given in Szulc (1997a).

These small bioherms are often formed by single specimens of large colonial rugose corals of the *Hexagonaria-Disphyllum* group that were overgrown by *Rothpletzella* and abundant axinellid/halichondrid demosponges. *Rothpletzella* is a calcimicrobe traditionally interpreted as a cyanophyte, although its true systematic relationships remain unclear (Feng et al. 2010). However, Adachi et al. (2007) have concluded that these microbes normally grew under harsh environmental conditions. The abundant sponges growing on top and between the branches of the *Rothpletzella* crusts are well preserved and complete, with either various types of dark, pyrite-rich automicrites or peloidal textures. Both spiculate and keratose demosponges are common.

3.2.2 Triassic microbialites from the Middle Muschelkalk, Poland

Stromatolites and other microbialites are common in the Middle Muschelkalk facies of Poland and southern Germany. The best known are stromatolites from the Silesian-Krakow Upland, Poland (Szulc 1997a, b; Myszkowska 1992). The investigated material was collected in a quarry near Libiąż, which is close to Krakow. Anisian carbonates of Pelsonian and Illyrian age are exposed in this quarry; the sampled microbialites are from the uppermost part of the so-called “*Diplopora* Beds”, which are of Illyrian age (Fig. 3.1). The “*Diplopora* Beds” consist of shallow marine carbonates with dasycladacean algae (dominantly *Diplopora* and *Physoporella*), *Girvanella* oncoids and commonly occurring oolites underlying the stromatolitic build ups (Fig. 3.1). The stromatolites are planar and sometimes domal and are up to 40 cm thick. The domal stromatolites are rich in putative keratose-demosponge remains, which alternate with lithified microbial mats, whereas the planar stromatolites lack metazoan remains.

3.2.3 Dried skeletons of modern keratose demosponges

Recent non-spiculate demosponges were collected as dried specimens from a storm beach near Port Hedland, Western Australia. Remains of keratose and other demosponges are often enriched in the upper distal areas of beaches, clearly above the normal tidal range. In these materials, the organic

skeletons are fully macerated and separated from other soft tissues by tidal action and are subsequently preserved by natural dehydration.

3.3 Methods

Routine lithological and paleontological observations were initially performed on thin sections and polished surfaces of the Triassic and Devonian samples using a Zeiss SteREO Discovery.V8 microscope, which can be operated in both transmitted- and reflected-light modes.

Based on these microscopic observations (see Fig. 3.2–3.3), fossil structures from one Devonian sample (hereafter called “Boul”; Fig. 3.4c) and one Triassic sample (“Pol”; Fig. 3.4b) were selected for three-dimensional (3-D) reconstruction. These two samples were selected because the target fossil structures in them are better preserved and show stronger colour contrast with respect to the background. To control the efficiency and quality of the reconstruction method and to compare the fossil structures to the skeletal meshes of modern keratose demosponges, a piece of dried sponge belonging to the family Thorectidae (“Au”; Fig. 3.4a) was embedded in white-stained araldite and then prepared according to the same procedure as Boul and Pol.

The 3-D reconstruction was based on manual serial grinding tomography. The popular non-destructive method X-ray micro-tomography (XMT) was not applied basically because of the difficulty to access to the equipment. Besides, because the suspected skeletal structures and their background (automicritic clumps, see descriptions below) are both preserved as carbonates, we did not expect an adequate X-ray absorption contrast between the two facies, although a trial test with XMT is still worthy in the future when possible. Serial grinding tomography is a classic method having been used by paleontologist since more than 100 years ago (Sollas 1904; also reviewed in Sutton 2008) until today (e.g., Kiel et al. 2012; Pascual-Cebrian et al. 2013). The automatic grinding machines used by recent tomographic studies (e.g. Pascual-Cebrian et al. 2013) could achieve a maximum vertical resolution of 10 μm with a precision of 3 μm . Since the old machine in our lab could not guarantee such a precision, which is required by our small-sized samples, we carried out the grinding process manually. A Mitutoyo

digimatic micrometer with a resolution of 1 μm was used to control the vertical inter-plane distances. Processed in this way, the average shift of the inter-plane distances of each sample was less than 5 μm as calculated from the final experimental data (the exact value varied among samples; see below).

The target regions were first cut into 5-mm-thick sections and fixed in the center of standard thin-section glass slides. The shape of the glass slide matched a frame that was specially made to ensure that the target region would always be located in the same position under the microscope. The samples were then ground stepwise by hand using sandpaper (1000, 2400 and 4000 grit) and polished by a polishing machine. After each pre-determined thickness was abraded away, the remaining thickness of the target region was measured using a Mitutoyo micrometer, and the new surface was photographed using an AxioCam MRc 5-megapixel camera attached to the Zeiss SteREO Discovery.V8 microscope. For Boul, a total thickness of 564 μm was processed, with 49 planes and an average inter-plane distance of $12 \pm 3 \mu\text{m}$. For Pol, the total processed thickness was 624 μm , with 37 planes and an average distance of $17 \pm 4 \mu\text{m}$. For Au, the total processed thickness was 1005 μm , with 60 planes and an average distance of $17 \pm 3 \mu\text{m}$.

In the next step, the captured images were transformed into 8-bit gray-scale TIFF files and aligned to each other using the “automatic alignment” function of Adobe Photoshop CS 5.1. The aligned pictures were built into TIFF stacks using ImageJ 1.46r (<http://imagej.nih.gov/ij>) (Supp. 3.1a, 3.2a and 3.3a). Then the stacks were processed in Voreen 4.4 (<http://voreen.uni-muenster.de>) with the “single volume ray caster” processor, which finally visualized the 3-D structures (Fig. 3.4d–e, Supp. 3.1b, 3.2b and 3.3b). In order to better illustrate the 3-D construction of the skeletal networks, part of each TIFF stack was cropped out and reconstructed independently. The selected regions are a $0.679 \times 0.413 \text{ mm}$ area from Boul, a $1.636 \times 1.410 \text{ mm}$ area from Pol and a $1.986 \times 1.657 \text{ mm}$ area from Au (Fig. 3.4a–c, g–i; Supp. 3.1c–e, 3.2c and 3.3c).

The partial reconstruction is especially important for Boul, which needs a manual interpretation to further reveal the skeletal structures, because the target structures were strongly interfered by background noises due to their similar brightness. The selected small region made this interpreting work manageable. Here we offer the interpretations with three levels of intensities (Fig. 3.5, Supp.

3.1c–d). First, the dataset was visualized as a 3-D model without any interpretation. It was possible to check which elements on each plane were visualized using the clipping function in Voreen 4.4. By comparing the exposed sections in Voreen 4.4 and serial images in ImageJ 1.46r, we managed to identify the non-visualized skeletal elements and the visualized noises. Then operated in ImageJ 1.46r, the skeletal elements of very high brightness were manually coloured in black, whereas the very dark noises were erased. In the “moderate interpretation”, only the main fibers of the suspected skeletal scaffold were enhanced; doubtful or ambiguously preserved elements were deleted to better represent the main scaffold. In the “intensive interpretation”, every details of possible biological origin were enhanced to avoid missing any morphological information. Then the interpreted volumes were imported to Voreen 4.4 again for a new reconstruction. Different from Boul, the other two samples (Pol and Au) show very sound contrast between skeleton and background. The dataset from them were presented without additional interpretation.

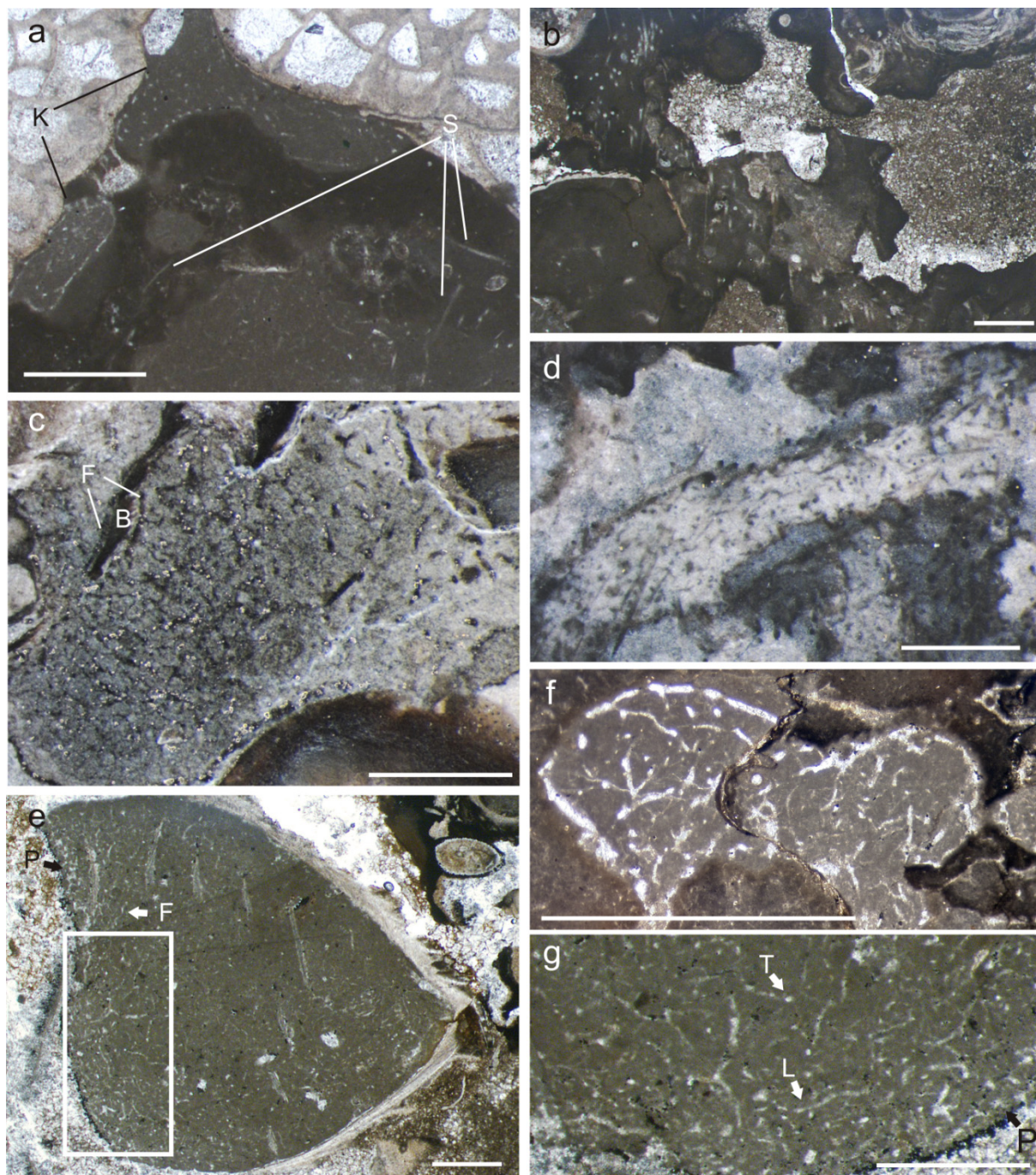


Fig. 3.2 Sponge fossils in a Devonian bioherm. All scale bars represent 1 mm. **a** An automicritic clump between coral skeletons, containing different generations of automicrites. The upper to upper-left portion shows putative keratose sponge structures (*K*), and the dark portion in the lower-right preserves a few monaxonic spicules (*S*). **b** A halichondrid sponge fossil preserved in an automicritic clump, observed under transmitted light. **c** A putative fossil keratose sponge individual, observed under reflected light. In the upper left, a piece of foreign bioclast (*B*) is enclosed by fibrous structures (*F*) and separated from the remainder of the clump. **d** A halichondrid sponge individual, observed under reflected light. **e** An automicritic clump within a completely preserved brachiopod, showing fibrous structures similar to keratose sponge skeletons. The transition between the fibrous structures (*F*) and peloidal fabrics (*P*) appears at the edge of the clump. The area within the white rectangle is further magnified in **g**. **f** A putative keratose sponge individual with hierarchical skeletons. **g** Magnification of the area inside the white rectangle in **e**. Longitudinal (*L*) and transverse (*T*) sections of the fibers and the branching pattern are visible. Marks in the pictures: *B*, bioclast; *F*, putative sponge skeletal fibers; *K*, putative keratose

sponge fossils; *L*, longitudinal section of a skeletal fiber; *P*, peloidal fabrics; *S*, spicules; *T*, transverse section of a skeletal fiber. ←

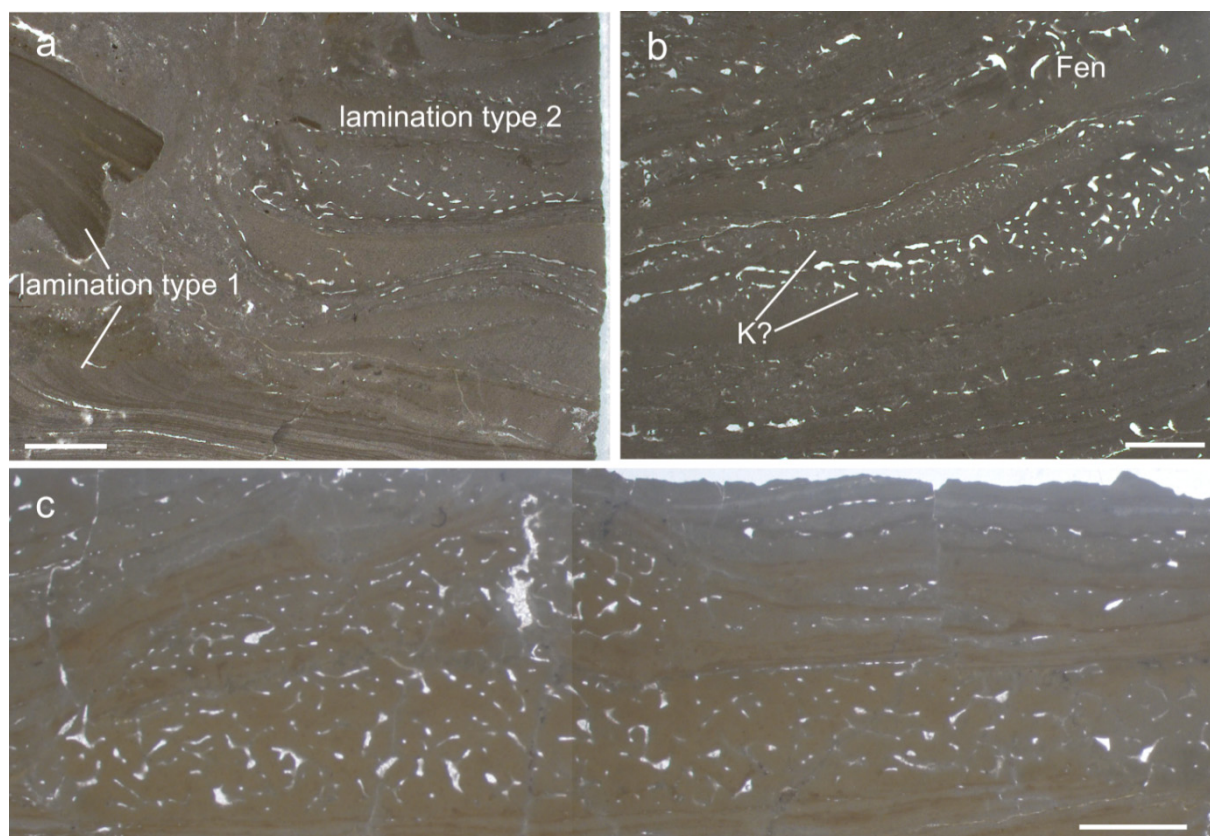


Fig. 3.3 Fossils and microbial fabrics in the Triassic microbialites. All scale bars represent 2 mm. **a** The two types of lamination. The finely laminated microbialites (*lamination type 1*) exhibit brittle eroded surfaces underlying the accretion of the sponge-related microbialites (*lamination type 2*). **b** Sponge-related microbialites. The cavities of the two laminates in the center of the image (*K?*) resemble sponge skeletons more closely than the other fenestral fabrics of abiotic origin (e.g. *Fen*). **c** A putative keratose sponge. The cavity morphology strongly indicates an anastomosing fibrous network, although some of the cavities have been modified by diagenesis. Marks in the pictures: *Fen*, fenestral structures; *K?*, structures similar to remnants of keratose sponges.

3.4 Results

The Middle Devonian material from Boulonnais, northern France, consists of small metazoan-microbialitic bioherms (Mistiaen and Poncet 1983; Reitner et al. 2001; Brice 2003; Hühne 2005). The main frame of each bioherm is formed by rugose corals and encrusting *Rothpletzella*. The spaces inside the corals are normally cemented by sparite (Fig. 3.2a), except where the skeleton is penetrated by automicrite patches. Allochthonous and autochthonous sediments are heterogeneously distributed in the interspaces of the frame. The allochthonous sediments are mainly calcitic silts and bioclasts (Fig.

3.2b). The autochthonous elements include excellently preserved gastropods and brachiopods (e.g., Fig. 3.2e) and automicrite aggregates that are partly related to various demosponge remnants (Fig. 3.2; Reitner et al. 2001). All of these features reflect a light-poor sedimentary environment affected by sporadic currents.

The siliceous-spicular demosponges are preserved as automicritic clumps with the calcite-cemented structures left by spicules. These clumps are normally bright under reflected light and dark under transmitted light (Fig. 3.2). The micrites within a single clump sometimes show different colors, indicating different precipitation mechanisms and/or diagenetic generations (Fig. 3.2a–b). The putative keratose demosponges exhibit the same preservation pattern as the spiculate demosponges, except that their skeletal elements are fibrous networks instead of spicules (Fig. 3.2a–d). These structures are considered “fibrous” because they show soft deformation and a more-or-less constant thickness in longitudinal section and an approximately round shape in transverse section (Fig. 3.2f–g). Framboidal pyrites are scattered within some clumps and show a tendency to accumulate along the fibrous trails (Fig. 3.2c).

In contrast to the Devonian material, the Anisian microbialites are characterized by stromatolitic fabrics. Two types of lamination are present, both composed of micrites (Fig. 3.3a). Type 1 is finely laminated, forming planar or slightly domal structures at the macro- and mesoscopic scales. Erosions and brittle breakages are evident on the top of these laminations, indicating that they formed hard surfaces before the accretion of the overlying type 2 laminations. Type 2 laminations are cloudy and irregularly undulate and host abundant fenestral fabrics (Fig. 3.3a–b). Certain lenticular micritic clumps within these type 2 laminations are here interpreted as fossil keratose sponges (Fig. 3.3c). These clumps are similar to those associated with the Devonian sponges described above and stand out from the surrounding microbialitic fabrics due to the following features: 1) they are composed of homogeneous automicrites without any lamination or other texture, except the anastomosing fibrous cavities; and 2) the fibrous cavities are distributed with a consistent density within each clump and never extend beyond the boundary of the clump. However, unlike their Devonian analogs, the fibrous cavities of these Triassic specimens are not fully cemented, and pyrite is absent in the automicrites.

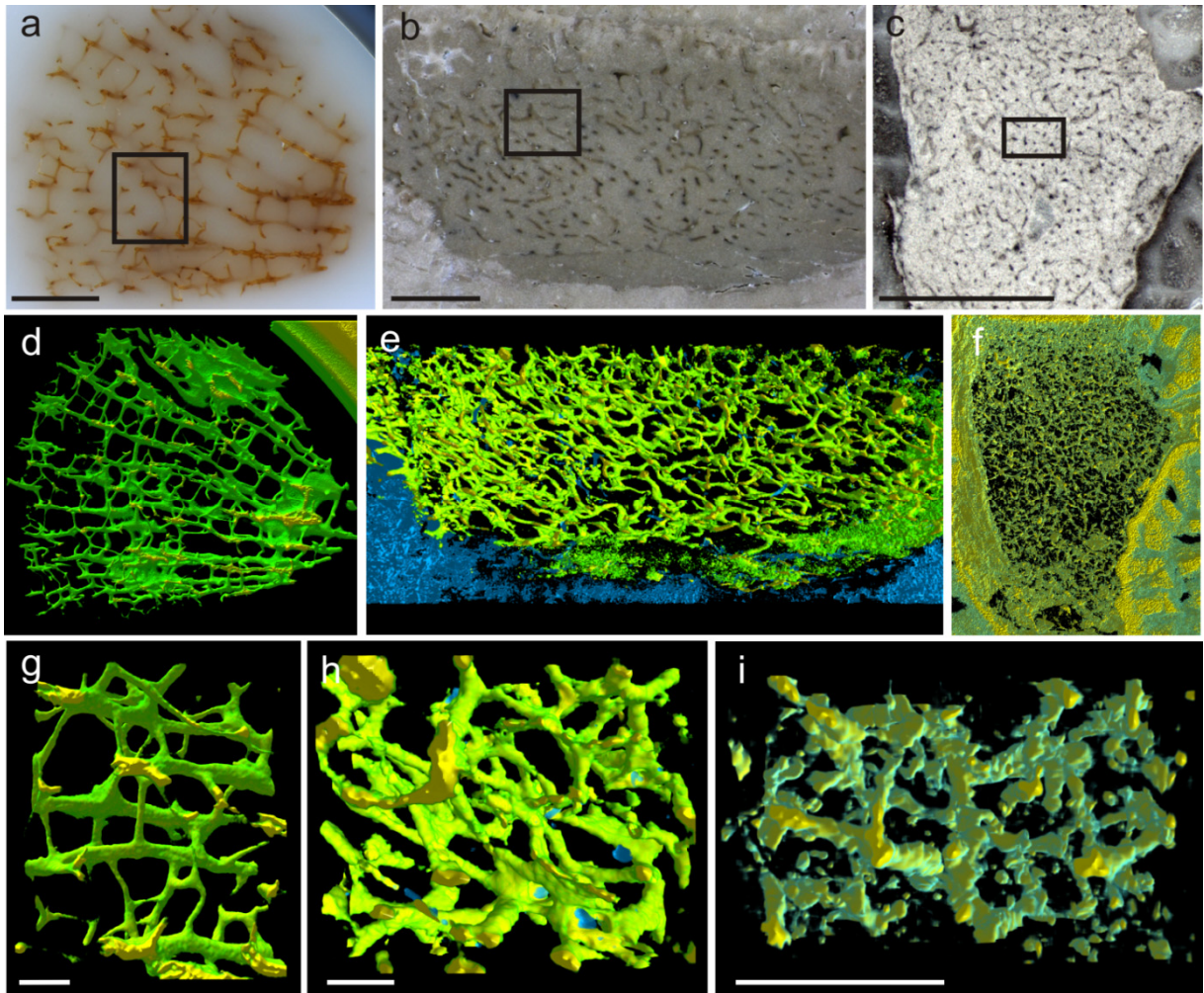


Fig. 3.4 Samples selected for 3-D reconstruction and snapshots of the respective 3-D models. Black scale bars represent 2 mm; white scale bars represent 300μm. **a**, **b** and **c** show Au, Pol and Boul, respectively, under reflected light. The rectangles in **a–c** indicate the selected areas used for the final 3-D reconstruction. **d–f** are the 3-D reconstructions of the fossils in **a–c**, respectively. **g–i** are snapshots of the 3-D models corresponding to the selected areas in **a–c**, respectively. **d–i** are shown in pseudo-color, with yellow representing the darker parts of the original images.

The 3-D reconstruction successfully portrays the skeletal structure of the modern thorectid specimen (Au), with identifiable anastomosing primary and secondary fibers (Fig. 3.4d, g; Supp. 3.3b–c), indicating the effectiveness of the method we applied. For the Devonian (Boul) and Triassic (Pol) samples, this method further demonstrates the anastomosing fibrous architecture of the fossil material (Fig. 3.4e–f, h–i; Supp. 3.1b–e, 3.2b–c). The 3-D reconstruction of the Devonian specimen shows fibers of differentiated thicknesses (Fig. 3.4i, Supp. 3.1b–e). This phenomenon, however, is not necessarily an authentic biological feature; instead, as explained in the method description, this could

be an artifact of diagenesis combined with the 3-D-reconstruction method. Additionally, in the consecutively polished surfaces of this specimen, no size hierarchy was evident among the fibers (Supp. 3.1a). For these three samples, the size of the fibers was measured under microscope along the minor axis of the elliptical transverse section. The primary and secondary skeletons of Au show the sizes of around 60–90 μm and 30–50 μm respectively; the fibers of Pol mainly fall into the size-space of 50–80 μm ; the fibers of Boul show the sizes around 30–50 μm .

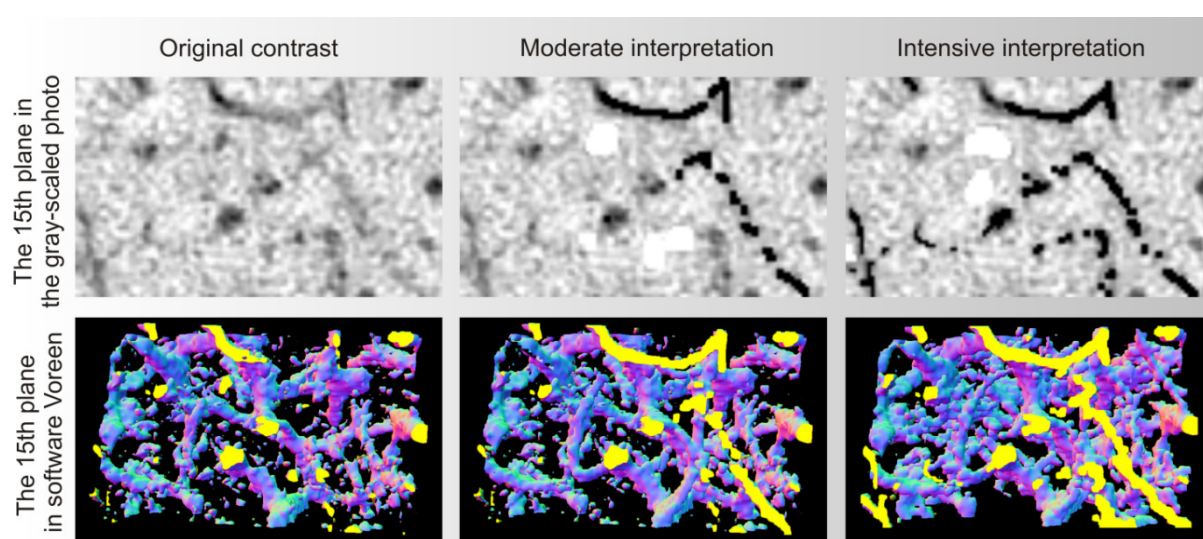


Fig. 3.5 Manual interpretations of the Devonian sample Boul during 3-D reconstruction. In the original image, some fibrous structures are preserved with the same brightness as the micrites in the background. In the moderate interpretation, only the main fibers were enhanced, and some doubtful or ambiguously preserved elements were deleted to better represent the main scaffold. In the intensive interpretation, every small detail of possible biological origin was enhanced to avoid missing any important morphological information. The 3-D models of all three levels of interpretations are provided in Supp. 3.1c–e.

3.5 Discussion

Given the observations above, we argue that the micritic clumps with anastomosing fibrous structures represent rapidly permineralized remnants of keratose demosponges rather than inorganic sedimentary structures or fossils of other organisms.

First, the anastomosing fibrous network revealed by both the lithological thin sections and the 3-D reconstructions contradicts an affinity to sedimentary structures. Some fenestral structures may form networks in rocks, but the spaces in these structures do not form a regular fibrous shape. When peloids are compacted, some of the inter-grain spaces may remain. However, fibrous cavities with a regular shape and consistent thickness, as seen in our samples, would be difficult to achieve in randomly piled peloids. Further, the inter-spaces among three adjoining peloidal grains are normally Y-shaped, whereas true skeletal fibers are clearly round or elliptical in transverse section. Nonetheless, skeletal fibers and peloidal inter-spaces cannot always be clearly distinguished. The former may gradually grade into the latter in some cases due to local diagenetic alterations (Fig. 3.2e, g).

Second, when these specimens are regarded as biogenic structures, their physiological and ecological features best match those of sponges. For example, some cyanobacteria grow as branching filaments. To our knowledge, however, cyanobacterial filaments are not known to form well-organized 3-D-extending networks, as seen in our samples. Further, calcification of the outer cyanobacterial sheath is normally driven by photosynthesis and CO₂ uptake (Arp et al. 2001). This process could not occur in a poorly illuminated depositional environment like that of the Devonian material. Fungal hyphae can also produce anastomosing fibrous networks, and it has been revealed in recent years that fungi can survive even in deep-sea environments (e.g., Schumann et al. 2004; Edgcomb et al. 2011). However, our samples do not exhibit structures that would directly imply a fungal affinity, such as septa, spores or sporocarps. On the contrary, the distribution of the fibrous structures within our samples contradicts the hyphal growth habit. Fungi are saprotrophs or parasites; therefore, if they lived contemporaneously with the other organisms, the hyphae should appear to penetrate the body from which they obtained nutrients. In our samples, however, the fibrous structures are restricted to automicritic clumps and often form a ring at the boundary of the clump (e.g., Fig. 3.2a, c, f; Fig. 3.3c; Fig. 3.4c) or wrap around

the grains inside the clump (Fig. 3.2c, Fig. 3.4c) to isolate the inner part from foreign materials. Alternatively, these specimens might represent a type of endolithic fungi that favored micrites and created the fibrous cavities after the lithification of the rocks. However, then it would be difficult to explain why such fungi did not bore through the micritic clumps of the completely preserved spiculate sponges. In fact, compared to fungal hyphae, sponge behavior better explains the distribution of the fibrous structures. As multicellular animals, sponges can immunologically recognize and react to non-self material at the cell and tissue levels (Müller and Müller 2003). In one example from Lizard Island, a sponge was observed secreting organic phragma to separate the living part from the decaying part (Reitner 1993, Plate 4, Fig. 3.4). Later, a sponge from the Bahama bank was observed enclosing agglutinated sediment particles with collagen-enriched tissue (Neuweiler et al., 2007, Fig. 4), and a *Geodia barretti* specimen was found to isolate sedimentary inclusions within its body by building a cortex of microscleres resembling the surface cortex (Hoffmann et al. 2004).

Furthermore, the preservation of these fossils is consistent with that of other known sponges. This is best demonstrated by the Devonian material, in which the preservation of the keratose demosponges is similar to that of the other siliceous demosponges. In Phanerozoic carbonates, siliceous sponges are commonly preserved by rapid carbonate permineralization, or so-called “mummification”, with the skeletal scaffold remaining nearly intact (e.g., Reitner et al. 1995, the brief review in Neuweiler et al. 2007). Many previous studies of both the fossil record (e.g., Lang 1991; Warnke 1995) and modern analogs (e.g., Reitner 1993; Neuweiler and Burdige 2005; Neuweiler et al. 2007) have confirmed that under restricted microenvironments, automicritic permineralization of the necrotic soft tissues can occur at a very early stage, even when the sponge individual is still alive, and that the opal in the spicules is replaced by calcitic cements slightly later in the process. Sulfate reduction and ammonification during the anaerobic microbial degradation of sponge tissues are regarded as the main causes of this rapid automicritization (Fritz 1958; Reitner et al. 1995; Reitner and Schumann-Kindel 1997), although some researchers have emphasized the importance of the dismantling collagen bundles as a sorbent in this process (Neuweiler et al. 2007). However, in either model, a basic prerequisite for this type of preservation is that the skeletal elements must be more resistant to decay

than the other tissues; otherwise, the skeletal scaffold could not be molded intact in fossils (Brachert 1991).

In this regard, the organic skeletons of keratose demosponges are at least as competent as siliceous skeletons. The organic skeletons of horny sponges are composed of spongin, a sponge-specific collagen type that is resistant to enzymes including proteases, collagenases, amylases and lysozymes (Gross et al. 1956; Junqua et al. 1974). Recently, chitin has been documented as a scaffold-building component in the organic skeletons of modern Verongida (Ehrlich et al. 2007, 2010), and was also detected from an exceptionally preserved sponge fossil of 505 Ma old (Ehrlich et al. 2013). Although in normal situations chitin and collagen are biodegradable and can be consumed rapidly in some cases (e.g., Gaino and Pronzato 1989; Poulicek and Jeuniaux 1991), they are more durable than other soft tissues under degradation (see, also, the review in Butterfield 1990). By comparison, siliceous skeletons can also dissolve rapidly under certain hydrological conditions, such as a warm and alkaline environment (Laschet 1984). The dissolution of spicules during early diagenesis and even in living individuals due to biological processes has also been reported (e.g., Land 1976; Bavestrello et al. 1996). In a decaying boring sponge on Lizard Island, collagen fibers were still preserved while other soft tissues had begun the process of permineralization and the siliceous spicules had been partly replaced by calcite (Reitner 1993, Reitner et al. 1995). Taken together, current taphonomic knowledge supports the possibility that the organic skeletons of horny sponges can be preserved in the same way as the rapidly calcified siliceous sponges found in Phanerozoic carbonates. This is consistent with the characteristics of our fossils.

As discussed above, these micritic clumps with anastomosing fibrous structures most likely represent fossil keratose sponges; however, it is difficult to determine their precise taxonomic affinity because many important morphological characteristics used to classify modern keratose sponges, including the microscopic structure of the skeletal fibers, the type of choanocyte chambers and the color of tissues, are not available in fossils. In our fossil specimens, the only applicable taxonomic character is the architecture of the skeletal framework. Because we reconstructed the 3-D structure of the skeletons from only two fossil specimens, the Devonian Boul and the Triassic Pol, the taxonomic discussion

below focuses on these specimens. The affinity of the other specimens observed in the thin sections and on the polished rock surfaces (e.g., Fig. 3.2f, e) should be discussed only after more data are acquired.

The 3-D reconstructions of the Devonian and Triassic specimens show an anastomosing skeletal architecture. According to the taxonomic system of Hooper and van Soest (2002), keratose demosponges with anastomosing skeletons include all taxa within the order Dictyoceratida, the family Dictyodendrillidae within the order Dendroceratida and the families Ianthellidae and Aplysiniidae within the order Verongida. However, the skeletal fibers of Dictyodendrillidae always interlace to form “perfectly regular to slightly irregular meshes” (Bergquist and Cook 2002), in contrast to the irregular architecture of both fossil specimens. The skeletal meshes of dictyoceratids differ from those of anastomosing verongids in exhibiting hierarchically differentiated fibers, except in the two genera *Dactylospongia* and *Narrabeena*. The hierarchy of spongin fibers is generally defined by both size and construction. In addition to being thicker, the primary fibers provide the main supporting force for the sponge body and usually extend to the sponge surface at right angles (cf. Boury-Esnault and Rützler 1997; Hooper 2003). Here, the 3-D reconstructed modern sample Au gives a nice example how a hierarchical skeletal scaffold looks like. By comparison, the skeletons of Pol and Boul are obviously not hierarchical. Thus, it appears more likely that the analyzed Devonian and Triassic specimens are the remnants of ancient verongids.

3.6 Conclusion

The observations and discussion above demonstrate that the automicritic clumps with anastomosing fibrous structures in the investigated Devonian and Triassic microbialites are taphonomically comparable to spiculate sponges and morphologically akin to keratose demosponges. Therefore, we attribute these fossil structures to the remnants of ancient keratose demosponges, although it is currently impossible to confirm the exact taxonomic placement of these organisms based on the preserved skeletal architecture of the fossils. This taxonomic difficulty is due partly to the loss of information during diagenesis and partly to our lack of knowledge about fossil keratose demosponges.

As this study indicates, the scarcity of non-spicular sponges in the fossil record may be due largely to our previous underestimation of their fossilization potential. Thus, further exploration for fossil non-spicular sponges is likely to be fruitful. Such exploration is important not only to enhance our knowledge about the evolution, historical diversity and paleoecology of sponges, but also to elucidate the early evolution of animals in the Precambrian.

Acknowledgements

We thank Dr. Steffen Kiel (University of Göttingen) for his help and suggestions concerning the grinding tomography method, Axel Hackmann and Wolfgang Dröse for the laboratory support. The beneficial comments from Dr. Imran Rahman (University of Bristol) are also appreciated. This research was sponsored by the Excellence Initiative, DFG, Courant Research Centre of Geobiology, Göttingen. The China Scholarship Council (CSC) financially supported the doctoral studies of the first author at the University of Göttingen.

References

- Adachi N, Ezaki Y, Pickett JW (2007) Interrelations between framework-building and encrusting skeletal organisms and microbes: more refined growth history of Lower Devonian bindstones. *Sedimentology* 54: 89–105
- Arp G, Reimer A, Reitner J (2001) Photosynthesis-Induced biofilm calcification and calcium concentrations in Phanerozoic oceans. *Science* 292 (5522):1701–1704
- Bavestrello G, Cattaneo-Vietti R, Cerrano C, Sarà, M (1996) Spicule dissolution in living *Tethya omanensis* (Porifera: Demospongiae) from a tropical cave. *Bulletin of Marine Science* 58 (2):598–601
- Bergquist PR, Cook SdC (2002) Family Dictyodendrillidae Bergquist, 1980. In: Hooper JNA, Van Soest RWM (eds) *Systema Porifera: A Guide to the Classification of Sponges*. Kluwer Academic/Plenum Publishers, New York, pp 1072–1076
- Borchiellini C, Chombard C, Manuel M, Alivon E, Vacelet J, Boury-Esnault N (2004) Molecular phylogeny of Demospongiae: implications for classification and scenarios of character evolution. *Molecular Phylogenetics and Evolution* 32 (3):823–837
- Boury-Esnault N, Rützler K (eds) (1997) *Thesaurus of sponge morphology*. Smithsonian Contributions to Zoology Number 596. Smithsonian Institution Press, Washington, D.C., 55 pp
- Bowerbank JS (1864) *A monograph of the British Spongiidae*, vol 1. Robert Hardwicke, London, 290 pp
- Brachert TC (1991) Environmental control on fossilization of siliceous sponge assemblages: A proposal. In: Reitner J, Keupp H (eds) *Fossil and Recent Sponges*. Springer Berlin Heidelberg, pp 543–553
- Brice D (2003) Brachiopod assemblages in the Devonian of Ferques (Boulonnais, France). Relations to palaeoenvironments and global eustatic curves. *Bulletin of Geosciences* 78: 405–417
- Brice D, Colbeaux JP (1976) Serie Devonienne du massif de Ferques s.s. tectonique du massif primaire du Bas-Boulonnais. *Guide Géologique Reunion Spécialisée de la Service Géologique National*. Orléans, pp 3–30
- Butterfield NJ (1990) Organic preservation of non-mineralizing organisms and the taphonomy of the Burgess Shale. *Paleobiology* 16 (3):272–286
- Cárdenas P, Pérez T, Boury-Esnault N (2012) Chapter two - Sponge Systematics Facing New Challenges. In: Becerro MA, Uriz MJ, Maldonado M, Turon X (eds) *Advances in Marine Biology*, vol 61. Academic Press, pp 79–209
- Edgcomb VP, Beaudoin D, Gast R, Biddle JF, Teske A (2011) Marine subsurface eukaryotes: the fungal majority. *Environmental Microbiology* 13 (1):172–183
- Ehrlich H, Ilan M, Maldonado M, Muricy G, Bavestrello G, Kljajic Z, Carballo JL, Schiaparelli S, Ereskovsky A, Schupp P, Born R, Worch H, Bazhenov VV, Kurek D, Varlamov V, Vyalikh D, Kummer K, Sivkov VV, Molodtsov SL, Meissner H, Richter G, Steck E, Richter W, Hunoldt S, Kammer M, Paasch S, Krasokhin V, Patzke G, Brunner E (2010) Three-dimensional chitin-based scaffolds from Verongida sponges (Demospongiae: Porifera). Part I. Isolation and identification of chitin. *International Journal of Biological Macromolecules* 47 (2):132–140
- Ehrlich H, Maldonado M, Spindler KD, Eckert C, Hanke T, Born R, Goebel C, Simon P, Heinemann S, Worch H (2007) First evidence of chitin as a component of the skeletal fibers of marine sponges. Part I. Verongidae (Demospongia: Porifera). *Journal of Experimental Zoology Part B: Molecular and Developmental Evolution* 308 (4):347–356

- Ehrlich H, Rigby JK, Botting JP, Tsurkan MV, Werner C, Schwille P, Petrášek Z, Pisera A, Simon P, Sivkov VN, Vyalikh DV, Molodtsov SL, Kurek D, Kammer M, Hunoldt S, Born R, Stawski D, Steinhof A, Bazhenov VV, Geisler T (2013) Discovery of 505-million-year old chitin in the basal demosponge *Vauxia gracilentia*. *Scientific Reports* 3:3497. doi:10.1038/srep03497
- Erpenbeck D, Sutcliffe P, Cook SdC, Dietzel A, Maldonado M, van Soest RWM, Hooper JNA, Wörheide G (2012) Horny sponges and their affairs: On the phylogenetic relationships of keratose sponges. *Molecular Phylogenetics and Evolution* 63 (3):809–816
- Erwin DH, Laflamme M, Tweedt SM, Sperling EA, Pisani D, Peterson KJ (2011) The Cambrian Conundrum: Early Divergence and Later Ecological Success in the Early History of Animals. *Science* 334 (6059):1091–1097
- Feng Q, Gong YM, Riding R (2010) Mid-Late Devonian calcified marine algae and Cyanobacteria, South China. *Journal of Paleontology* 84: 569–587
- Fritz GK (1958) Schwammstotzen, Tuberoide und Schuttbreccien im Weißen Jura der Schwäbischen Alb. *Arbeiten des Geologisch-Paläontologischen Instituts TH Stuttgart*, NF 13: 1–118
- Gaino E, Pronzato R (1989) Ultrastructural evidence of bacterial damage to *Spongia officinalis* fibers (Porifera, Demospongiae). *Diseases of Aquatic Organisms* 6:67–74
- Grant RE (1861) *Tabular view of the primary divisions of the Animal Kingdom*. Walton and Maberly, London, 91 pp
- Gross J, Sokal Z, Rougvié M (1956) Structural and chemical studies on the connective tissue of marine sponges. *Journal of Histochemistry & Cytochemistry* 4 (3):227–246
- Hoffmann F, Rapp HT, Pape T, Peters H, Reitner J (2004) Sedimentary inclusions in the deep-water sponge *Geodia barretti* (Geodiidae, Demospongiae) from the Korsfjord, western Norway. *Sarsia* 89 (4):245–252
- Hooper JNA (2003) *Spongguide: Guide to sponge collection and identification*. Queensland Museum, South Brisbane, pp 1–26
- Hooper JNA, van Soest RWM (eds) (2002) *Systema Porifera: A Guide to the Classification of Sponges*. Kluwer Academic/Plenum Publishers, New York, 1763 pp
- Hühne C (2005) *Geochemie Porifera-reicher Mud Mounds und Mikrobialithe des Mittel- und Oberdevons (Westaustralien, Nordfrankreich)*. Unpublished dissertation, University of Göttingen, 133 pp
- Junqua S, Robert L, Garrone R, Pavans de Ceccatty M, Vacelet J (1974) Biochemical and morphological studies on collagens of horny sponges. *Ircinia* filaments compared to spongins. *Connective Tissue Research* 2 (3):193–203
- Kiel S, Götz S, Pascual-Cebrian E, Hennhöfer DK (2012) Fossilized digestive systems in 23 million-year-old wood-boring bivalves. *Journal of Molluscan Studies* 78 (4):349–356
- Land LS (1976) Early dissolution of sponge spicules from reef sediments, North Jamaica. *Journal of Sedimentary Research* 46 (4):967–969
- Lang B (1991) Baffling, binding, or debris accumulation? Ecology of Upper Jurassic sponge-bacterial buildups (Oxfordian, Franconian Alb, Southern Germany). In: Reitner J, Keupp H (eds) *Fossil and Recent Sponges*. Springer Berlin Heidelberg, pp 516–521
- Laschet C (1984) On the origin of cherts. *Facies* 10:257–290

- Lavrov DV, Wang X, Kelly M (2008) Reconstructing ordinal relationships in the Demospongiae using mitochondrial genomic data. *Molecular Phylogenetics and Evolution* 49 (1):111–124
- Levi C (1957) Ontogeny and systematics in sponges. *Systematic Biology* 6 (4):174–183
- Love GD, Grosjean E, Stalvies C, Fike DA, Grotzinger JP, Bradley AS, Kelly AE, Bhatia M, Meredith W, Snape CE, Bowring SA, Condon DJ, Summons RE (2009) Fossil steroids record the appearance of Demospongiae during the Cryogenian period. *Nature* 457 (7230):718–721
- Minchin EA (1900) Chapter III. Sponges. In: Lankester ER (ed) *A treatise on zoology. Part II. The Porifera and Coelenterata*. Adam & Charles Black, London, pp 1–178
- Mistiaen B, Poncet J (1983) Evolution sédimentologique des petits biohermes a Stromatolithes et Vers dans le Givétien de Ferques (Boulonnais). *Annales Société Géologique du Nord* 102 (4):205–216
- Müller WEG, Müller IM (2003) Origin of the metazoan immune system: Identification of the molecules and their functions in sponges. *Integrative and Comparative Biology* 43 (2):281–292
- Myszkowska J (1992). Lithofacies and sedimentation of *Diplopore* Dolomite (Middle Muschelkalk) in the east part of the Cracovian-Silesian region. *Annales Societatis Geologorum Poloniae* 62, 19–62
- Neuweiler F, Burdige DJ (2005) The modern calcifying sponge *Spheciospongia vesparium* (Lamarck, 1815), Great Bahama Bank: Implications for ancient sponge mud-mounds. *Sedimentary Geology* 175 (1–4):89–98
- Neuweiler F, Daoust I, Bourque P-A, Burdige DJ (2007) Degradative calcification of a modern siliceous sponge from the Great Bahama Bank, the Bahamas: A guide for interpretation of ancient sponge-bearing limestones. *Journal of Sedimentary Research* 77 (7):552–563
- Pascual-Cebrian E, Hennhöfer DK, Götz S (2013) High resolution and true colour grinding tomography of rudist bivalves, exemplified with the taxonomic revision of *Mathesia darderi* (Astre). *Caribbean Journal of Earth Science* 45:35–46
- Peterson KJ, Cotton JA, Gehling JG, Pisani D (2008) The Ediacaran emergence of bilaterians: Congruence between the genetic and the geological fossil records. *Philosophical Transactions of the Royal Society B: Biological Sciences* 363:1435–1443
- Pisera A (2002) Fossil 'Lithistids': An overview. In: Hooper JNA, van Soest RWM (eds) *Systema Porifera: A guide to the classification of sponges*. Kluwer Academic/Plenum Publishers, New York, pp 388–402
- Poulicek M, Jeuniaux C (1991) Chitin biodegradation in marine environments: An experimental approach. *Biochemical Systematics and Ecology* 19 (5):385–394
- Reitner J (1993) Modern cryptic microbial/metazoan facies from Lizard Island (Great Barrier Reef, Australia): Formation and concepts. *Facies* 29:3–40
- Reitner J, Gautret P, Marin F, Neuweiler F (1995) Automicrites in a modern marine microbialite: Formation model via organic matrices (Lizard Island, Great Barrier Reef, Australia). *Bulletin de l'Institut océanographique, Monaco, n° spécial* 14 (2): 237–263
- Reitner J, Hühne C, Thiel V (2001) Porifera-rich mud mounds and microbialites as indicators of environmental changes within the Devonian/Lower Carboniferous critical interval. *Terra Nostra* 4:60–65
- Reitner J, Luo C, Duda JP (2012) Early sponge remains from the Neoproterozoic-Cambrian phosphate deposits of the Fontanarejo area (Central Spain). *Proceedings of the 17th Field Conference of the Cambrian Stage Subdivision Working Group, International Subcommission on Cambrian Stratigraphy & Celebration of*

- the 30th Anniversary of the Discovery of the Kaili Biota. Guizhou. Journal of Guizhou University (Natural Sciences) 29 (Sup. 1): 184–186
- Reitner J, Schumann-Kindel G (1997) Pyrite in mineralized sponge tissue. Product of sulfate reducing sponge-related bacteria? *Facies* 36:272–276
- Reitner J, Wörheide G (2002) Non-lithistid fossil Demospongiae - origins of their palaeobiodiversity and highlights in history of preservation. In: Hooper JNA, van Soest RWM (eds) *Systema Porifera: a guide to the classification of sponges*. Kluwer Academic/Plenum Publishers, New York, pp 52–68
- Rigby JK (1986) Sponges of the Burgess shale (Middle Cambrian), British Columbia. *Palaeontographica Canadiana* 2: 1–105
- Rigby JK, Collins D (2004) Sponges of the Middle Cambrian Burgess Shale and Stephen Formations, British Columbia. *ROM Contributions in Science* 1:1–155
- Schumann G, Manz W, Reitner J, Lustrino M (2004) Ancient fungal life in North Pacific Eocene oceanic crust. *Geomicrobiology Journal* 21: 241–246
- Shu D, Isozaki Y, Zhang X, Han J, Maruyama S (2014) Birth and early evolution of metazoans. *Gondwana Research* 25 (3):884–895
- Sollas WJ (1904) A method for the investigation of fossils by serial sections. *Philosophical Transactions of the Royal Society of London Series B* 196 (214-224):259–265
- Sperling EA, Peterson KJ, Pisani D (2009) Phylogenetic-signal dissection of nuclear housekeeping genes supports the paraphyly of sponges and the monophyly of Eumetazoa. *Molecular Biology and Evolution* 26 (10):2261–2274
- Steiner M, Mehl D, Reitner J, Erdtmann B-D (1993) Oldest entirely preserved sponges and other fossils from the lowermost Cambrian and a new facies reconstruction of the Yangtze Platform (China). *Berliner Geowissenschaftliche Abhandlungen* E (9):293–329
- Sutton MD (2008) Tomographic techniques for the study of exceptionally preserved fossils. *Proceedings of the Royal Society B: Biological Sciences* 275 (1643):1587–1593
- Szulc J (1997a) Middle Triassic (Muschelkalk) sponge-microbial stromatolites, diplopores and *Girvanella*-oncolites from the Silesian Cracow Upland. In: 3rd IFAA Regional Symposium and IGCP 380 International Meeting, Guidebook. Cracow, pp 10–15
- Szulc J (1997b) Stop 3 Libiąż, active dolomite quarry, Cracow Upland. In: 3rd IFAA Regional Symposium & IGCP 380 International Meeting, Guidebook. Cracow, pp 42–43
- Walcott CD (1920) Cambrian geology and paleontology IV, No.6 Middle Cambrian Spongiae. *Smithsonian Miscellaneous Collections* 67 (6):261–364
- Warnke K (1995) Calcification processes of siliceous sponges in Viséan Limestones (Counties Sligo and Leitrim, Northwestern Ireland). *Facies* 33 (1):215–227
- Wood RA (2011) Paleoecology of the earliest skeletal metazoan communities: Implications for early biomineralization. *Earth-Science Reviews* 106 (1-2):184–190
- Wörheide G, Dohrmann M, Erpenbeck D, Larroux C, Maldonado M, Voigt O, Borchellini C, Lavrov DV (2012) Chapter One - Deep Phylogeny and evolution of sponges (Phylum Porifera). In: Becerro MA, Uriz MJ, Maldonado M, Turon X (eds) *Advances in Marine Biology*, Volume 61. Academic Press, pp 1–78

- Wu W, Yang AH, Janussen D, Steiner M, Zhu MY (2005) Hexactinellid sponges from the Early Cambrian black shale of South Anhui, China. *Journal of Paleontology* 79 (6):1043–1051
- Xiao SH, Hu H, Yuan XL, Parsley RL, Cao R (2005) Articulated sponges from the Lower Cambrian Hetang Formation in southern Anhui, South China: their age and implications for the early evolution of sponges. *Palaeogeography, Palaeoclimatology, Palaeoecology* 220 (1–2):89–117
- Yang B, Zhang L, Danelian T, Feng Q, Steiner M (2014) Chert-hosted small shelly fossils: Expanded tool of biostratigraphy in the Early Cambrian. *GFF* 00 (1):1–6

Supplementary material

(Please find in the attached CD)

- Supp. 3.1a** Consecutively ground planes of Boul (Devonian)
- Supp. 3.1b** 3-D reconstruction of sample Boul (Devonian) without manual interpretation.
- Supp. 3.1c** 3-D reconstruction of a part of Boul (Devonian) with minimum interpretation. See Fig. 3.4c for the exact location of the reconstructed area
- Supp. 3.1d** 3-D reconstruction of a part of Boul (Devonian) with moderate manual interpretation. See Fig. 3.4c for the exact location of the reconstructed area
- Supp. 3.1e** 3-D reconstruction of a part of Boul (Devonian) with intensive manual interpretation. See Fig. 3.4c for the exact location of the reconstructed area
- Supp. 3.2a** Consecutively ground planes of Pol (Triassic)
- Supp. 3.2b** 3-D reconstruction of sample Pol (Triassic)
- Supp. 3.2c** 3-D reconstruction of a part of Pol (Triassic). See Fig. 3.4b for the exact location of the reconstructed area
- Supp. 3.3a** Consecutively ground planes of Au (thorectid Keratosa, Recent)
- Supp. 3.3b** 3-D reconstruction of sample Au (thorectid Keratosa, Recent)
- Supp. 3.3c** 3-D reconstruction of a part of Au. See Fig. 3.4a for the exact location of the reconstructed area

- Chapter 4 -

“Stromatolites” built by sponges and microbes – a new type of Phanerozoic bioconstruction

(Submitted to *Lethaia* on Dec. 10, 2014)

Cui Luo, Joachim Reitner

Abstract

Investigations on the sponge-related bioconstructions, especially the sponge-microbial buildups and the buildups related to non-spicular sponges, may enhance the knowledge about sponge paleoecology and help to search for early sponge fossils in the Precambrian. Here we analyze two bioconstructions from Triassic and Carboniferous carbonates which were previously regarded as stromatolites, and reinterpret them as sponge-microbial buildups. The automicritic aggregations in these buildups are similar to the previously reported fossils of keratose sponges in showing moulded anastomosing filamentous structures. All the studied columnar or domal constructions were formed in turbulent water with considerable sedimentary inputs. The Triassic rocks precipitated in a slightly evaporitic environment, showing a transition from planar microbial laminations to stacked sponge clumps which constructed the stromatolite-like columns and domes. Variation of salinity may have played an important role in controlling the sponge-microbe alternation and inducing laminations in the stromatolite-like constructions. The Carboniferous buildups were constructed in the shallow subtidal zone of an open shelf or a ramp. The laminations within the stromatolite-like columns are composed of alternating dark micritic laminae of sponge fossils and pale laminae of neomorphic microspars. The accretion of these columns is probably related to repeated cycles of sponge growth, burial and rapid lithification, re-exposure and erosion and settlement of the new generation. Congruent with other recent studies, this work shows again that sponge-related bioconstruction can mimic microbialites.

Keywords

Keratose sponge, Stromatolite, Microbialite, Triassic, Carboniferous.

4.1 Introduction

The first metazoan-bearing reef in the Phanerozoic was constructed by sponge-like archaeocyaths and calcimicrobes in the Tommotian, subsequent to the dominance of calcimicrobe constructions at the beginning of the Cambrian (Riding and Zhuravlev 1995; Rowland and Shapiro 2002). From then till the end of the Mesozoic, the sponge-microbe association was pervasive and active in building reefs and mounds (e.g. Brunton and Dixon 1994; Reitner et al. 1995b; Höfling and Scott 2002). The high adaptability of both microbes and sponges enables this association proliferating in the aftermath of extinction events (e.g. Delecat et al. 2011) and conditions unfavorable for other animals (e.g. Heckel 1974).

In recent years, increasing workers started to hypothesize that sponges or sponge-like organisms probably presented in the Ediacaran sea and their filter feeding may have contributed to the ventilation of the water column by removing organic particles; this in turn provoked the rapid evolution of animals at the Precambrian-Cambrian transitional interval (e.g. Erwin and Tweedt 2012; Lenton et al. 2014; Zhang et al. 2014). However, although molecular clock predicts that sponges have a long evolutionary history deep into Cryogenian (e.g., Peterson et al. 2008; Sperling et al. 2009; Erwin et al. 2011), the first unequivocal sponge fossil is not older than the Early Cambrian (e.g. Reitner and Wörheide 2002; Reitner et al. 2012; Antcliff et al. 2014). The known Precambrian bioconstructions were characterized by microbial structures except the presence of secondary dwellers like calcified *Namacalathus* and *Cloudina* at the end of the Ediacaran (e.g. Grotzinger et al. 2000; Penny et al. 2014).

If ancestral sponges have developed in the Precambrian, how were they like? In the microbe-dominated ancient ecosystem, did they live in consortia with microbes like their Phanerozoic descendants?

It may help to find out the answers, if we know better the (paleo-) ecology and taphonomy of the Phanerozoic sponge-microbial buildups. Of special importance are these aspects related to the non-spicular sponges, because animals started to build mineral skeletons only shortly before the Cambrian (Wood 2011). Antiquity of the non-spicular character in sponges has been supported by the Middle

Cambrian occurrence of the fossil taxon *Vauxia* (possible verongid) (Rigby 1986; Rigby and Collins 2004; Ehrlich et al. 2013), as well as the modern phylogenomic studies which indicate that spicular and non-spicular taxa diverged at the very base of the lineage Demospongiae (Cárdenas et al. 2012; Wörheide et al. 2012). In recent years, advances on the listed aspects are emerging. New occurrences of sponge-microbe associations are reported from the intervals of critical evolutionary events (e.g. Hong et al. 2012; Kruse and Reitner 2014). Keratose sponges, a group of non-spicular demosponges in which “the skeleton consists of fibers of spongin, without ‘proper’ spicules” (*sensu* Minchin 1900, p.153–154), have been described from the Phanerozoic carbonates for the first time (Luo and Reitner 2014). Furthermore, demosponges, beside of calcimicrobes, were found as a main component of the “maze-like microbialites” (Lee et al. 2014).

Continuing with the previous work, here we describe two carbonate bioconstructions from the Triassic and Carboniferous. They were previously regarded as stromatolites, but now seem to be constructed mainly by keratose sponges and to a lesser content by associated microbial mats. This study may enrich our knowledge about paleoecology of sponges and diversity of their buildups, and may also provide a new angle to look at the Precambrian fossil record.

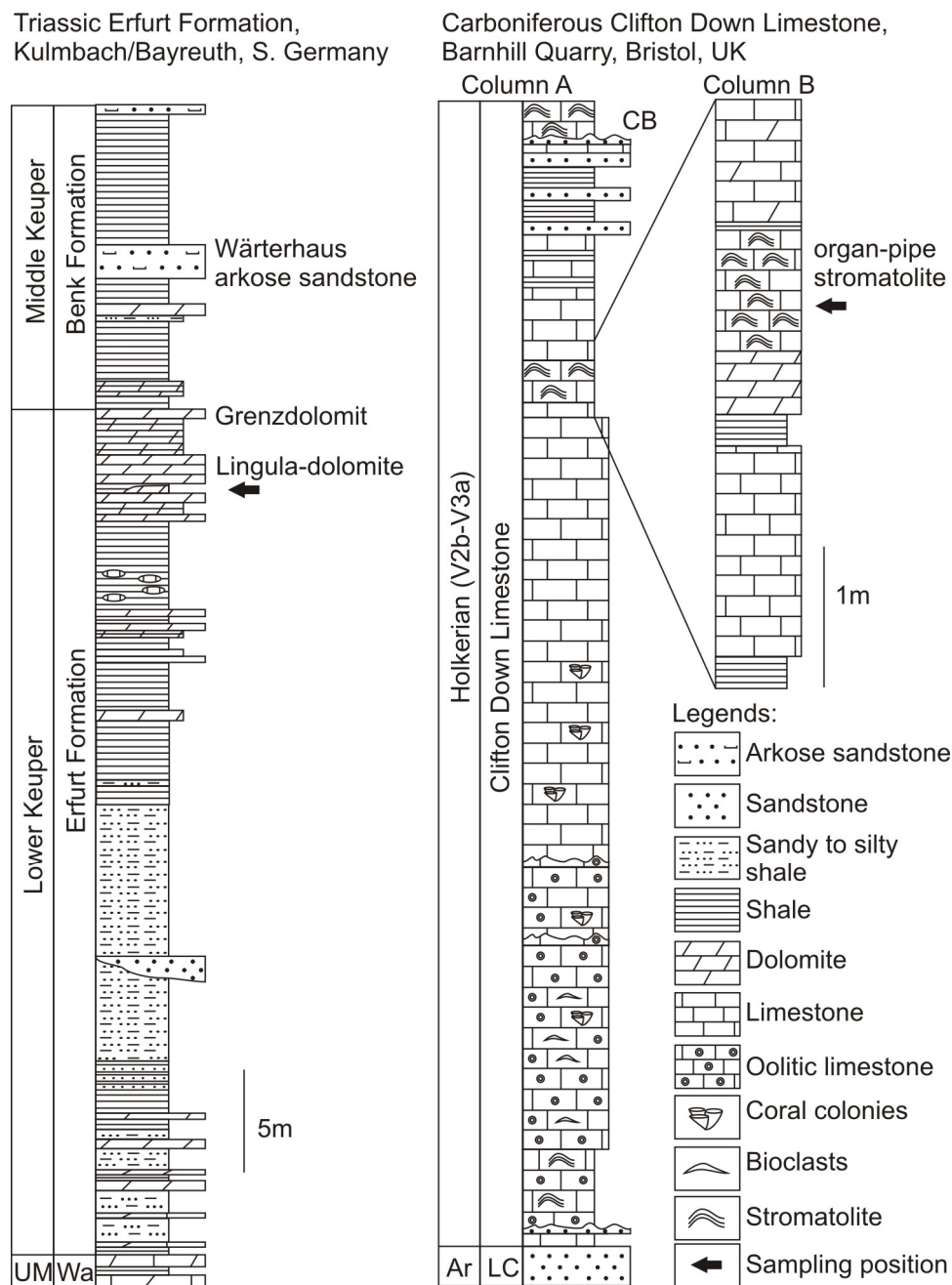


Fig. 4.1 Stratigraphy of the outcrops where the studied samples were taken. The Triassic stratigraphic column was modified from Bachmann (2002). The Carboniferous column A is modified from Cossey et al. (2004), while column B is drawn according to the description in Murray and Wright (1971). Abbreviations (in alphabetic order): Ar, Arundian; CB, Concretionary Beds; LC, Lower Cromhall Sandstone; UM, Upper Muschelkalk; Wa, Warburg Formation.

4.2 Material

The Triassic materials were collected from an outcrop at the junction of the A9 and A70 high ways in South Germany, between the towns Kulmbach and Bayreuth (Bachmann et al. 1999). In ascending order, the outcrop exhibits the Meissner, Warburg, Erfurt and Benk Formations. Samples were taken near to the top of the Erfurt Formation, which represents the lithostratigraphic unit Lower Keuper (c.a. 238–239 Ma according to Kozur and Bachmann 2005, 2008) and is generally characterized by cyclically alternating sandy-muddy and muddy-carbonate horizons, representing fluvial, palustrine, brackish to marine facies (Nitsch 2005). In the investigated section, this formation is dominated by greenish-gray and reddish-brown shales with several intercalated dolomite beds (Fig. 4.1). This was interpreted as coastal plain facies interrupted by several intervals of restricted environments, while the succeeding Benk Formation (Middle Keuper) exhibits fluvial to lacustrine deposits (Fig. 4.1; Bachmann 2002). The boundary between the Erfurt and Benk formations is marked by the Grenzdolomit and the 2 m-thick *Lingula*-dolomite at the top of the former. Some domal *Placunopsis*-stromatolite bioherms, capped by a layer of gray shale, occur below the *Lingula*-dolomite. These bioherms are around 25 cm high and 70 cm across, consisting of a core of stacked *Placunopsis* shells and overgrowing stromatolitic crusts. The samples investigated in this paper are from these crusts. Bachmann (2002, p. 86) figured out that the “nodular textures” in these crusts are similar to those structures from the Buntsandstein and Middle Muschelkalk which were interpreted as relics of hexactinellid sponges by Hagdorn et al. (1999). The abbreviation “PB” will be used in the following text to designate the samples from these *Placunopsis*-stromatolite bioherms.

The Carboniferous materials are from Barnhill Quarry (in earlier literatures also mentioned as Arnold’s Quarry), which is immediately located northwest to the present Chipping Sodbury Golf Club, Bristol, UK. Samples were collected in the 1990s during the execution of the DFG research projects of Dr. Klaus Warnke (Wa 980/1-1 and Wa 980/1-2). This quarry was abandoned in 1950s and is now under a filling-back project, but a few of previous studies have described the geology of this area in a detailed way. In ascending order, the quarry exposed the upper part of the Lower Cromhall Sandstone (Arundian), the whole succession of the Clifton Down Limestone (Holkerian or V2b–V3a, Middle

Viséan) except an abruptness near to the top, and the lower part of the Middle Cromhall Sandstone (Asbian) (Fig. 4.1; Murray and Wright 1971; Kirkham 1977, 2005). In this locality, the Clifton Down Limestone is around 130 m thick and featured by a complete transgression-regression sedimentary cycle: beginning with intertidal facies, then grading into subtidal open shelf facies (or ramp, according to Wright 1986), and finally returning to an intertidal situation represented by the stromatolite-rich “Concretionary Beds” at the top (Fig. 4.1; Murray and Wright 1971; Kirkham 1977; Cossey et al. 2004). The samples studied in this paper belong to the “organ-pipe stromatolites” which are more than 20 m below the “Concretionary Beds” (Holkerian / V3a, according to Kirkham 2005). These stromatolites form a c.a. 80 cm thick bed; each individual column can reach a height of over 30 cm (Kirkham 1977) with a width of 3–8 cm. These columns resemble organ pipes by showing steep-falling edges, large height/width ratios and close inter-column distances. According to Murray and Wright (1971), stromatolites of this form are restricted to this particular single bed in Chipping Sodbury and are absent from contemporaneous rocks in the neighboring Wick region. Compared with the gradual change of facies observed in the Wick region, the rapid appearance of these stromatolites above the stable, massive pelmicrite beds in Barnhill Quarry is believed indicating a relatively sudden switch from transgressive to regressive phase, which was probably controlled by the local elevation of the sea floor (Murray and Wright 1971). For convenience, the abbreviation “OS” will be used in the following text to designate the samples of these “organ-pipe stromatolites”.

All the PB and OS samples are now deposited in the Department of Geobiology, Centre of Geosciences of the University of Göttingen.

4.3 Methods

4.3.1 *Microscope observation*

To study the lithological and sedimentary features, all samples were prepared into polished slabs and 10×15 cm thin sections. These slabs and thin sections were checked under reflected and transmitted

light respectively, using a Zeiss SteREO Discovery.V8 microscope. Photos of the microscopic structures were taken using the AxioCam MRc 5-megapixel camera combined with this microscope.

4.3.2 *LA-ICP-MS*

Based on the microscope observation, parts of the samples were selected for LA-ICP-MS measurement, so that the elemental composition of different microstructures can be detected *in situ* rapidly and precisely. The selection was based on the criterion that as various lithological facies as possible should be included in each tested sample. These selected areas, including one from the PB and two from the OS samples, were cut into $4.5 \times 2.5 \times 0.5$ cm chips, polished and then sent to the LA-ICP-MS lab in the Institute of Geochemistry, University of Göttingen. The samples were measured using a PerkinElmer SCIEX ELAN 6100 DRC II ICP-MS coupled with a 193 nm ArF excimer laser ablation system (GeoLas, COMpex 110 from Lamda Physik). Elemental composition was measured along lines, including three lines from the OS samples (L1, L2 and L3) and one line from the PB sample (L5). The scanning speeds are 30.2–31.3 $\mu\text{m/s}$, varying from line to line. The maximum width of the lines is 120 μm and the sampling depth is 30 μm . Acquired data were then processed using Igor Pro 6.3.4.1 combined with Iolite 2.2. The external calibration was done with silicate glass NIST 610 and Ca was set as internal standard.

4.3.3 *Carbon and oxygen isotopes*

Beside of the samples measured by LA-ICP-MS, other rock materials were prepared to study the carbon and oxygen isotope composition of different lithological facies. Powder samples were taken *in situ* on the polished slabs using a PROXXON Professional drill IBS/E No. 28481 (borehole diameter c.a. 1 mm) and then sent to the Department of Isotope Geology, University of Göttingen. Measurement was done using a Thermo Kiel IV equipped with Finnigan Delta plus gas mass spectrometer. The resulted $\delta^{13}\text{C}$ data were originally relative to VPDB and $\delta^{18}\text{O}$ to VSMOW. In this

paper, the $\delta^{18}\text{O}$ values are converted to VPDB standard according to the formula $\delta^{18}\text{O}_{\text{PDB}} = 0.97002 \delta^{18}\text{O}_{\text{SMOW}} - 29.98$ (Coplen et al. 1983), because many publications dealing with the sea water geochemistry in geological time use PDB or VPDB standard for $\delta^{18}\text{O}$.

4.4 Results

4.4.1 Description of the Triassic material

The samples are the yellow to brownish laminated crusts up to 10 cm thick within the *Placunopsis*-stromatolite bioherms (Fig. 4.2a–b). They are strongly dolomitized and the porosity is high. Larger fractures, fenestral structures and pseudomorphs of evaporative minerals are commonly filled by pink carbonate cements, while smaller fractures and pores within and between the laminations are pervasively stained by Fe-Mn oxides. Though the samples seem to be intensively affected by diagenesis, the microstructures are still preserved and could provide clues to resolve their origin. Morphological and sedimentological features of the laminations vary within small scales in the transection of these crusts. For the convenience of discussion, they are classified into 4 types and described as below.

PB laminated structure a (PBLa, Fig. 4.2a–b; Fig. 4.3a)

This type of lamination is slightly undulated, composed of alternating darker and brighter laminae which show high lateral continuity and vertical inheritance. Though all the laminae are generally micritic, the brighter ones seem contain larger crystals. The thickness of each single lamina varies from about 100 μm to 200 μm . These laminations are typical microbially-induced structures.

PB laminated structure b (PBLb, Fig. 4.2a–b; Fig. 4.3c–f)

In this part, the parallel laminae, like those described in PBLa, are disturbed by some intercalated lenticular clumps. The base of these clumps templates the underlying substrate, but their concave lenticular shape creates a quite uneven upper surface, which destroys the overall inheritance of these laminations.

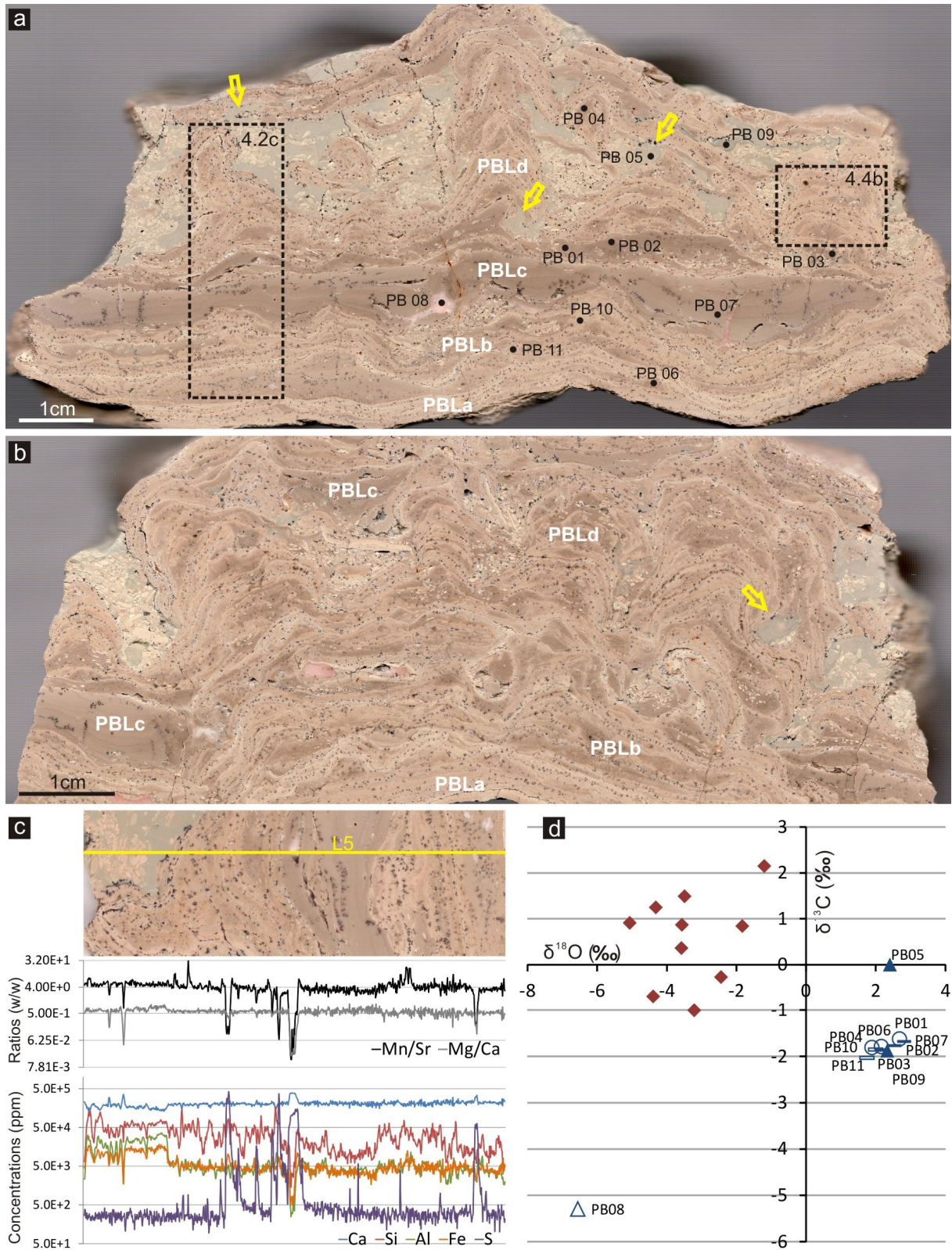


Fig. 4.2 a–b, transection of the stromatolitic crusts of the *Placunopsis*-stromatolite bioherms in polished slabs. Four types of laminations are marked with white letters. Black dots show the positions where the isotope samples were drilled. Regions in the rectangles correspond to the pictures in Fig. 4.2c and Fig. 4.4b, respectively. Hollow arrows point to syndimentary fragmentation of the laminates. **c**, result of the LA-ICP-MS measurement along Line 5. **d**, $\delta^{13}\text{C}$ and $\delta^{18}\text{O}$ of carbonates from different sources. Diamonds: values of contemporaneous sea water acquired from literature; circles: values from lenticular micritic clumps; solid

triangles: allochthonous sediments; hollow triangle: pink cement; solid bars: structureless micrite aggregations; hollow bars: microbial laminates between lenticular micritic clumps. ←

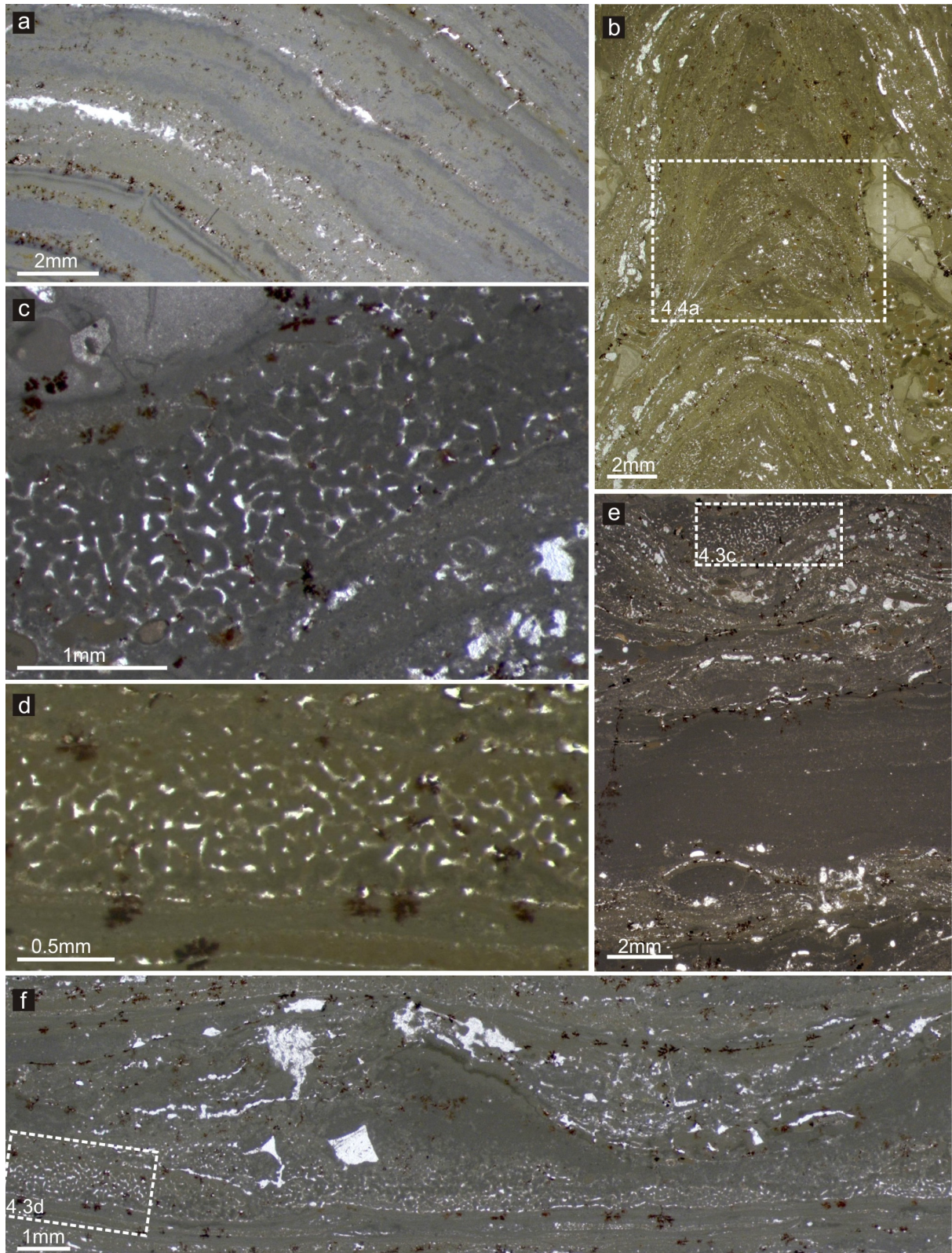


Fig. 4.3 The four types of PB laminations in thin section: **a**, PBLa; **b**, PBLd; **e**, PBLb and PBLc; **f**, PBLb. **c–d** are magnified from the rectangles in **e** and **f** respectively, illustrating automicritic clumps with anastomosing filamentous microstructures. The rectangle in **b** is magnified in Fig. 4.4a.

These clumps are millimeters thick and characterized by the microstructure of filamentous networks embedded in an automictic matrix. The filaments are slightly curved and about 20–40 μm in diameter. Their transections, if not at the conjunction point, are round or elliptical. The interconnected network fills up the clump with a constant density but never extends beyond it. Instead, the network can form a boundary near and parallel to the clump margin (Fig. 4.3c–d). Some of these clumps can be traced laterally across a whole hand specimen (e.g. Fig. 4.3f). However, the tracing work can be achieved only when using the overlying and/or underlying microbial lamina as references, because compared with these referential microbial lamina, the thickness and preservation quality of the clumps are quite unstable.

PB laminated structure c (PBLc, Fig. 4.2a–b; Fig. 4.3e)

These laminations are micritic lenses of millimeter-scale to centimeter-scale thickness. Appearing as fillings in depressions, their lateral extension is controlled by the topography of the underlying surface. Vague sedimentary laminae with good inheritance can be identified within these micritic aggregations according to slightly differentiated brightness.

Structureless bulk accumulation of micrites occurs also in some lenticular clumps in PBLb. For example, the clumps in Fig. 4.3f show well preserved filamentous networks at the basal part, which grade upward into structureless micrites with halite pseudomorphs (cf. Warren 2006) at the grading boundary. However, different from PBLc, the clumps in PBLb lack any form of finer laminae and show a convex outline protruding upwards; their shape is independent from the topography of the underlying surfaces.

PB laminated structure d (PBLd, Fig. 4.2a–b; Fig. 4.3b; Fig. 4.4)

On the basis of PBLb, when the lenticular clumps become dominant and stack up, a stromatolite-like columnar or domal buildup is formed. There's no abrupt boundary between PBLb and PBLd. The stromatolite-like buildups are about 2–3 cm high and 1–2 cm wide, closely spaced and partially linked. Their morphology is quite unstable, from domal to columnar, straight to curved, but normally the buildups do not branch. The morphological variability of the buildups probably originates from their

main components, the stacked micritic clumps, which are irregular in shape and tend to accrete without following the same symmetrical axis.

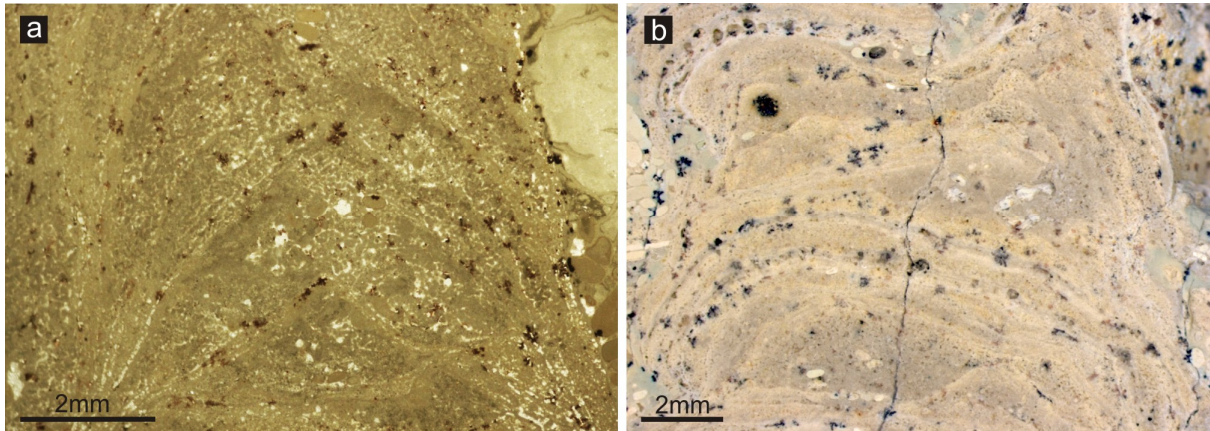


Fig. 4.4 Stacking pattern of the micritic clumps in the PB buildups: **a**, in transmitted light, magnified from part of Fig. 4.3b; **b**, in reflected light, magnified from part of Fig. 4.2a.

Spaces between the columns are filled by wacke- to packstones, which are composed of greenish clay-rich matrix and millimeter-scale pale-coloured grains. Many of these grains show elongated or even tabular shape. Some of them probably are fragments from vicinal or local laminated constructions; these can be identified by darker colour, less rounded shape, better preserved inner structures, and even the continuity with the neighboring laminations. Similar clastic grains appear also in PBLb and are incorporated into the base of the overgrowing laminations.

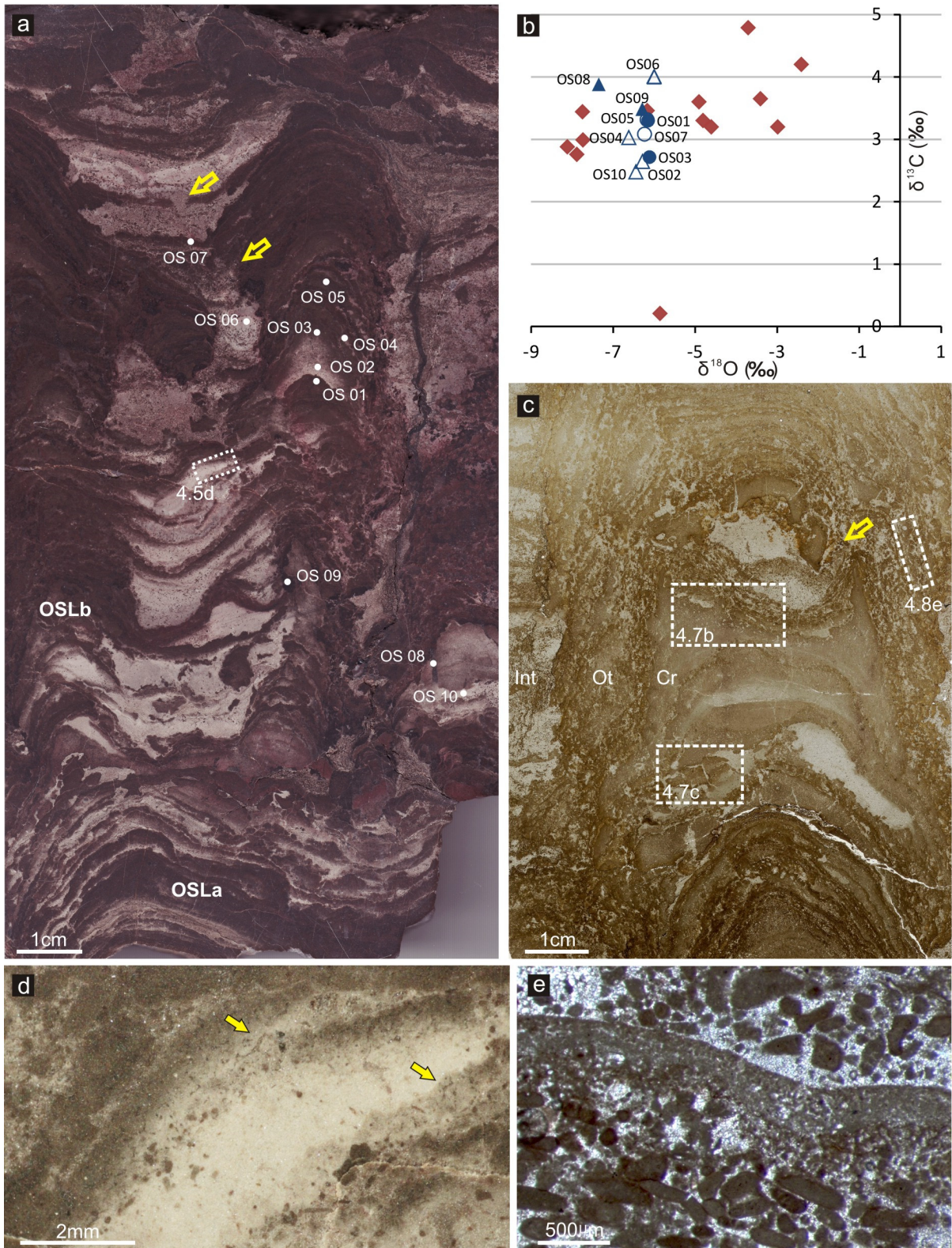


Fig. 4.5 **a**, transection of the “organ-pipe stromatolites” in a polished slab. White dots mark the positions where powder samples were drilled for carbon and oxygen isotope measurements. The region in the rectangle is magnified in **d**. **b**, $\delta^{13}\text{C}$ and $\delta^{18}\text{O}$ of carbonates from different sources. Diamonds: values of contemporaneous sea water acquired from literature; solid circles: values from the automicritic aggregations with filamentous microstructures; hollow circles: elongated grains cemented by black or white cements; solid triangles: black cements; hollow triangles: microspars. **c**, thin section of an OS specimen showing the structure within the stromatolite-like columns. Abbreviations: Cr, the coring part; Ot, the outer part; Int, inter-column space. Regions in rectangles are magnified in Fig. 4.7b–c and 8e respectively. Hollow arrows in **a** and **c** point to synsedimentary

breakage and fragmentation of the bioconstructions. **d**, part of an inter-column lamination in reflected light, showing structures similar to the diagenetically altered automicritic clumps in the coring part of the columns. Solid arrows point to the remnant micrites and plausible filamentous structures, cf. the solid arrow in Fig. 4.7a. **e**, elongated grains wrapped by a layer of peloidal micrites, from an inter-column bridging layer, in transmitted light. ←

4.4.2 Description of the Carboniferous material

The “organ-pipe stromatolites” are preserved in organic-rich calcitic carbonates. The laminated mesostructure is characterized by alternating dark brown and pale grey laminations. Two types of laminated structures are distinguished:

OS laminated structure a (OSLa, Fig. 4.5a)

These are the waved laminations underlying the stromatolites. The alternating darker and brighter laminae are millimeters thick, composed of micrites and microspars respectively. The darker laminae may well be autochthonous precipitations which were eroded and fragmented after a rapid lithification in the early diagenetic process. In contrast, the microspars distribute in the fractures of the dark micritic aggregations like cements or pore-fillings. Inheritance of the laminations is medium.

OS laminated structure b (OSLb, Fig. 4.5a, c)

This type designates the so called “organ-pipe stromatolites”. The buildups are columnar and closely spaced. Columns are about 10 cm high or even higher, 3–6 cm wide with 1–3 cm inter-column spaces. There are bridges or linkages between neighboring columns, which can be eroded and broken. Accordingly, the edges of the columns also show features of strong erosion (Fig. 4.5a, c; Fig. 4.7d). Each column consists of two parts (Fig. 4.5c). The one that we call “coring part” is composed of well-preserved automicritic aggregations, while the “outer part” is strongly fragmented. However, the spatial relationship of the two phases is not always inner-outer, but can also be superposition (Fig. 4.5a, c).

The automicritic aggregations in the coring part can be in shape of either centimeter-scaled chunks (e.g. the chunk near the point OS 08 in Fig. 4.5a), or continuous thick laminae (Fig. 4.5c; Fig. 4.7a). Regardless of the overall shape, all these aggregations show the microstructure of filamentous

networks embedded in automicritic matrix, similar to that described in the lenticular clumps in the PB material. Most of the filaments are around 20 μm thick. However, in some clumps there are thicker ones of 30–70 μm across, representing another hierarchy (Fig. 4.7g). Besides, there are some cylindrical, branching canals in the OS micritic aggregations which are not seen in the PB samples (Fig. 4.7b, e, h). The filaments and the canals are both cemented by microspars.

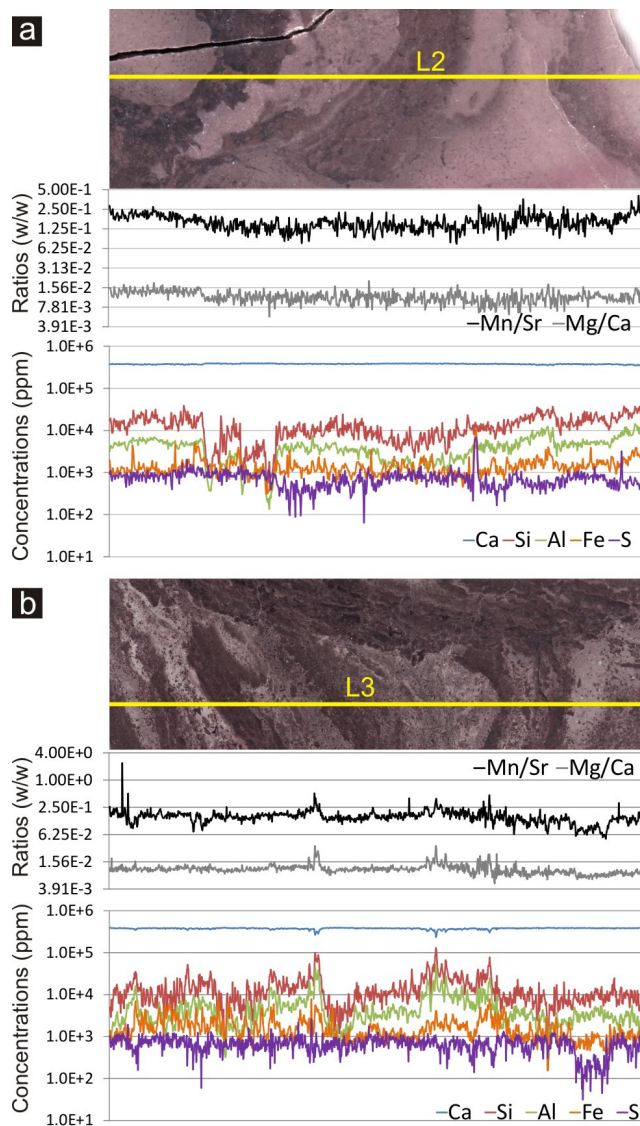
Between the micritic aggregations are some intercalated crescentic regions which are filled by microspars and showing pale colour. Some of these crescentic regions have distinct contacts with the surrounding micritic aggregations. They may well have been cavities for quite a long time before being filled by microspars or their precursors, because 1) there are elastic grains deposited in these regions and the surrounding micritic aggregations are eroded (Fig. 4.5c; Fig. 4.7a; Fig. 4.8a); 2) some fragments of the overlying micritic aggregations are preserved in the crescentic regions in the manner of falling into a pre-existed space (Fig. 4.7a, c). Additionally, there are some brachiopod fossils preserved as “floating” in the microspars in these crescentic regions; the shells are enclosed in thick structureless micritic wraps which have a flat edge facing and parallel to the “wall” of the crescentic region (Fig. 4.8a, c). It appears like that the animals were attaching on the wall and overgrown by microbes before they were finally torn down by another force. Existence of these syndimentary cavities indicates a very rapid lithification of the micritic aggregations.

Origin of these crescentic cavities is probably related to the erosion and corrosion induced by the turbulent water. There are a few “developing cavities” in which the relicts of pre-existed micritic materials are still visible (solid arrow in Fig. 4.7a), or the materials from the ceiling is still falling down (Fig. 4.7a). The arched ceilings of the crescentic regions are probably inherited from the outline of pre-existed micritic laminations. In this scenario, the branched canals mentioned above may have provided a “weak point” in the buildups where the preferential erosion and corrosion started (e.g. Fig. 4.7h).

Compared with the coring part, the laminations in the outer part are much more intensively affected by water movement. They are strongly fragmented and even rounded (Fig. 4.5c; the upper-right part in Fig. 4.8a). Fractures are cemented by microspars. In the micritic fragments, the filamentous networks

and canals described above are either absent or badly preserved, except for a few exceptions (e.g. Fig. 4.8e). Sometimes erosion can be strong enough to remove all the laminations in the outer part and reach the core of the column (Fig. 4.7d).

Sediments among the columns are also characterized by alternating brighter and darker layers (Fig. 4.5a). Some of these laminations probably originated from diagenetically altered autochthonous constructions (Fig. 4.5d). In this situation, the pale parts were formed in the same processes as those created the crescentic regions. However, more frequently, the inter-column spaces are filled by allochthonous deposits. The bright parts are grainstones with cements of anhedral to subhedral, equi- to inequigranular microspars. The predominant grains are brown micritic clasts, less frequent are larger fragments from local constructions and very rare are recrystallized fossil fragments (Fig. 4.7f). These microspars are obvious neomorphic products. Their precursors are hard to trace, but perhaps are



allochthonous carbonate silts. Many of the brown clasts show elongated shape, resembling fecal pellets (Fig. 4.5e; Fig. 4.7f). However, the fragments washed down from the stromatolite columns are more possible to be the source of them, because erosional products of the filaments-baring micritic aggregations can show similar morphology to these grains (Fig. 4.8d), and phosphor concentration is very low in the samples (Table S4.1), contradicting the fecal pellet interpretation. The darker laminations represent denser accumulations of the brown grains, which are sometimes overlain by a

Fig. 4.6 Elemental composition of the OS samples measured by LA-ICP-MS along lines inside of a column (a) and in the inter-column space (b).

layer of micritic peloids (Fig. 4.5e), indicating sediment fixation by microbial films.

Identifiable fossils are not common in these samples. Except the aforementioned wrapped shells in the crescentic cavities and the recrystallized fragments embedded in microspars, another relatively frequent fossil type is some empty tubes (Fig. 4.8b–c). These tubes are around 20–50 μm thick and normally do not show the full length. Different from the anastomosing filaments within the micritic aggregations, the tubes have explicit walls and never branch or interconnect. They are commonly incorporated in the micritic aggregations, but can also appear in the allochthonous sediments. Additionally, there are some regularly round or elliptical hollow structures within and often near to the bottom of the micritic aggregations (Fig. 4.8d–e). They are not necessarily related to the branched canals which have more irregular transection and can extend parallel, oblique or vertical to the laminations (Fig. 4.7b, e, h). Some of these structures are possibly the space left by some kind of dwelling worms (e.g. Fig. 4.8d).

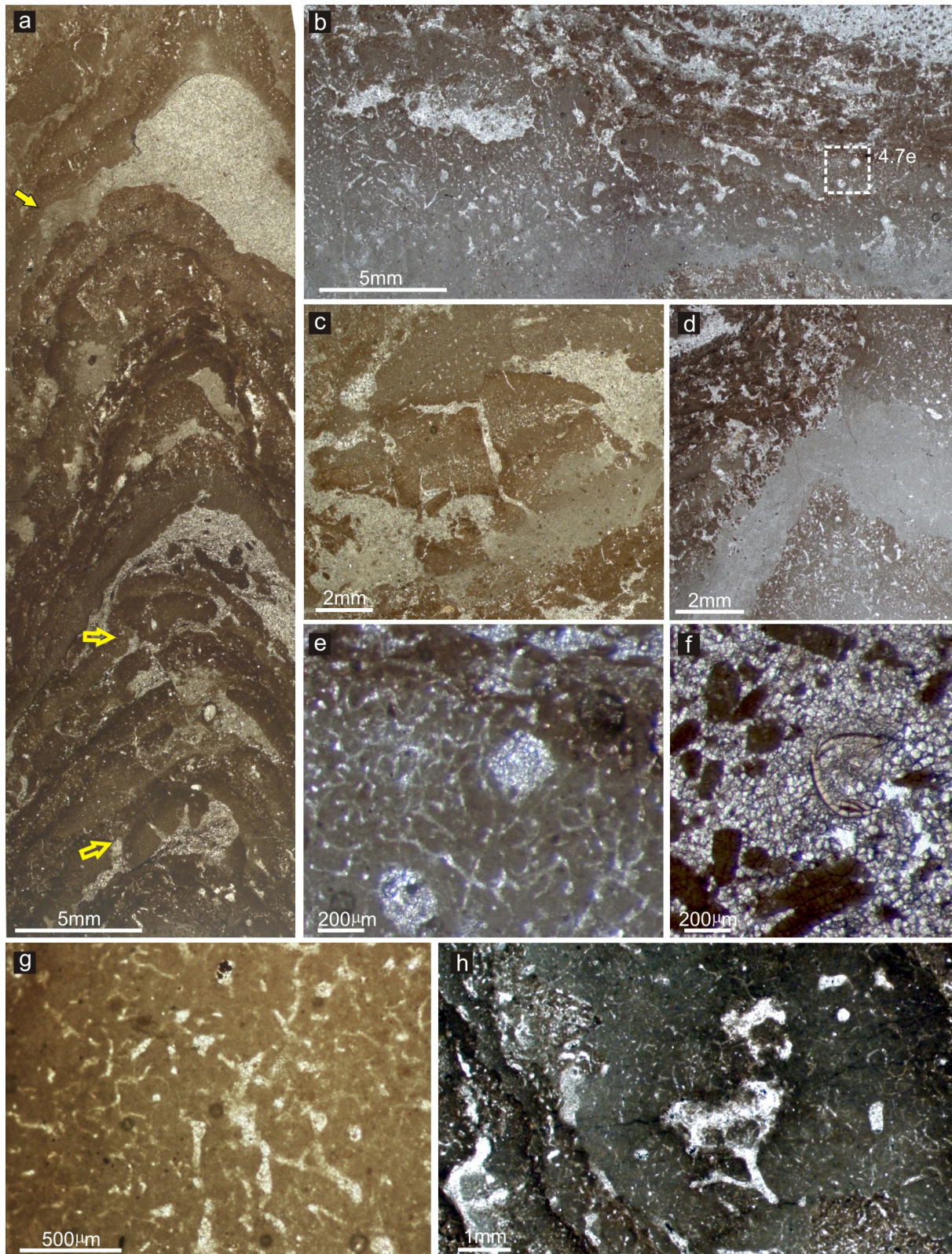


Fig. 4.7 **a**, **c** and **d** show erosion and corrosion in the columns. Hollow arrows point to synsedimentary breakage and fragmentation, the solid arrow marks the grading area between microspars and the remnant micrities. **b**, **e** and **h** show the branching canals within the automicritic aggregations along with the filamentous networks. **e** is a closer view of the rectangle in **b**. **f**, the allochthonous grains and microspar cements in the inter-column space. **g**, an automicritic aggregation containing hierarchical filaments.

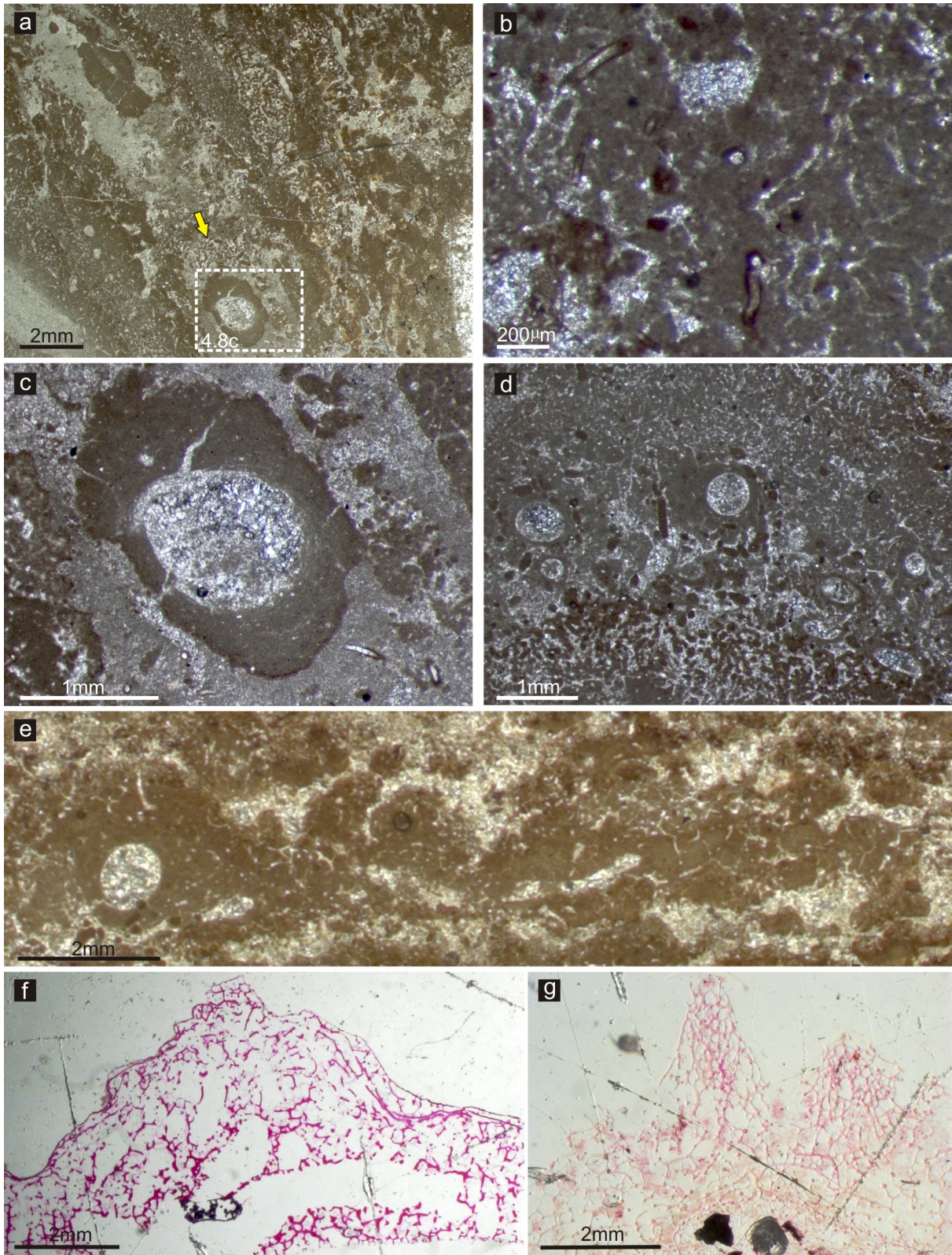


Fig. 4.8 **a**, a crescentic region in the column, which contains wrapped brachiopod fossils and is partly filled by grains (arrow). The region in the rectangle is magnified in **c**. **b**, unidentified tubular fossils embedded in the automicrites, along with the filamentous network. **c**, a closer view of the rectangle in **a**. **d**, the round structures within an automicritic aggregation; they may have been left by dwelling organisms. **e**, a closer look at the microstructures in the outer part of the columns, modified from part of Fig. 4.5c. **f–g**, two forms of modern keratose skeletons from Lizard Island, stained by fuchsin.

4.4.3 LA-ICP-MS data

Consistent with the lithological observations, the PB samples yield high Mg/Ca ratios which are generally over 0.5 (Fig. 4.2c, Table S4.1), while the Mg/Ca ratio of a stoichiometric dolomite is 0.6. Mn/Sr ratio is a commonly adopted indicator for the diagenetic alteration of carbonates. Though some authors suggested that $Mn/Sr < 10$ already indicates acceptable preservation quality of carbon isotope signals (Kaufman and Knoll 1995), the more strict value $Mn/Sr < 2$ is used by other authors to screen geochemical data (e.g. Korte et al. 2005; Guo et al. 2013). Among all the obtained Mn/Sr ratios from the PB samples, 7.0% of them are < 2 , 21.6% are < 3 and 98.3% are < 10 (Fig. 4.2c, Table S4.1). However, the other lithological features of the rocks, including high porosity, pervasive stain of Fe-Mn oxides and also the $\delta^{13}C$ and $\delta^{18}O$ values (see below), all indicate strong diagenetic overprint. The high strontium concentration of these rocks is probably controlled by the facies. The halite pseudomorphs indicate an evaporitic environment (Fig. 4.3f), while rocks precipitated in hypersaline environments are expected to be enriched in strontium (Veizer and Demovič 1974). Additionally, some of the pore cements show very high sulfur concentration decoupled with the enrichment of iron (Fig. 4.2b); this may originate from the relicts of evaporitic sulfates. Compared with the micritic aggregations, the greenish allochthonous sediments between the columns and domes are enriched in Si, Al and Fe, showing stonger affection of terrestrial inputs.

Characterized by very low Mn/Sr (mostly < 0.5) and Mg/Ca ratios (mostly < 0.03) (Fig. 4.6; Table S4.1), the OS samples appear to be almost unaltered calcitic carbonates. Although apparent diagenetic features, such as erosion, corrosion and recrystallization, have been described above, these processes probably happened in syn-sedimentary stage, hence the geochemical signals were stabilized within the same fluid environment as the depositional one. No matter inside or outside of the “organ-pipe stromatolite” columns, the brighter part of the samples are generally richer in Si and Al (Fig. 4.6). This pattern is observed even within each single micritic clump or lamination (Fig. 4.6a). As described above, the bright regions are related to different intensities of neomorphism or recrystallization. Depositional clay minerals may have played a role in inducing or promoting these diagenetic processes (Longman 1977).

4.4.4 Carbon and oxygen isotopes

The acquired isotope values were plotted on $\delta^{13}\text{C}$ - $\delta^{18}\text{O}$ diagrams with a few referential values of the contemporaneous sea water in the respective geological intervals (Fig. 4.2d; Fig. 4.5d; Table S4.2). The referential data for the PB samples are taken from Korte et al. (2005) based on bio- and lithostratigraphy. Meanwhile, the sea water carbon and oxygen isotope composition of the Upper Holverian reported by Bruckschen and Veizer (1997) and Bruckschen et al. (1999) were selected as a reference for the OS data.

Compared with the referential values, the PB samples show generally lighter carbon but heavier oxygen isotope composition, except the single plot representing the later cements, which is extremely light in both carbon and oxygen composition, indicating a diagenetic fluid depleted in both ^{13}C and ^{18}O (Fig. 4.2d). The generally low $\delta^{13}\text{C}$ in the PB samples are probably derived from post-burial water-rock interaction. However, although oxygen isotope is theoretically more sensitive to post-burial alteration (e.g. Marshall 1992), $\delta^{18}\text{O}$ of the PB samples are still much heavier than the referential values. In evaporitic environments, the water column can be intensively enriched in ^{18}O because of kinetic disequilibrium fractionation and this can be recorded by the precipitates. Therefore, the high $\delta^{18}\text{O}$ values in the PB samples are congruent with the lithological observation and measured Mn/Sr ratios, indicating an evaporative sedimentary environment. But the evaporation was probably not quite intensive because the occurrence of evaporative mineral pseudomorphs is not very pervasive in the samples.

Different from the Triassic samples, $\delta^{13}\text{C}$ and $\delta^{18}\text{O}$ of the Carboniferous materials fit well within the variation range of the Holverian referential values (Fig. 4.5b). This indicates that the water column from which the OS materials precipitated had a good connection to the open ocean.

Neither PB nor OS samples yield any significant clustering of $\delta^{13}\text{C}$ and $\delta^{18}\text{O}$ values among different carbonate sources like the micritic clumps with filamentous networks, microbial laminations and allochthonous carbonates, etc.

4.5 Discussion

4.5.1 *Sponge origin of the micritic aggregations*

The micritic clumps and laminations which contain filamentous networks were interpreted in different ways in previous studies. Bachmann (2002) suggested that the structures in the Triassic bioherms are similar to the relicts of hexactinellids as discussed in Hagdorn et al. (1999). However, according to our observation, the filamentous networks in the PB samples never show the symmetric characters of hexactinellid skeletons. Similar microstructure in the “organ-pipe stromatolites” were either considered as of “algal origin” (Murray and Wright 1971) or compared to the vermiform microstructure in the stromatolites described by Walter (1972) (Warnke 1996).

Vermiform microstructure is known from several Neoproterozoic (Vendian) and Cambrian stromatolites (Walter 1972; Bertrand-Sarfati 1976). However, based on the literature that we could reach, the term “vermiform microstructure” seems have been used for microstructures of different appearances and origins. For example, the one in *Acaciella angepena* Preiss, 1972 was described as “irregularly tubular” and distributing “crossing the dark laminae” which are only 30–70 µm thick (Preiss 1972, p. 73). This microstructure was not very well-illustrated in the original figure plates of Preiss (1972), but it looks rather like fractures or degassing structures than filaments. On the contrary, the Middle to Late Cambrian stromatolite *Madiganites mawsoni* Walter, 1972 closely resembles the “organ-pipe stromatolites” in both meso- and microstructures, although the former has branching columns. *M. mawsoni* shows alternating pale and dark laminae of millimetric thickness; the dark laminae are composed of micrites and containing “vermiform structures”, while the pale ones are structureless and composed of large or small microspars; laminations are dark at top and pale at bottom and the vermiform filaments “parallel laminae borders for some distance” (Walter 1972, p. 159). The origin of vermiform microstructure was not resolved (summarized in Bertrand-Sarfati 1976). Walter (1972, p.160) argued that they are similar to “*Girvanella* but lack the microgranular boundaries of that form”.

In recent years, filamentous microstructures similar to those seen in the PB and OS samples and in *M. mawsoni* were also reported from Ordovician and Cambrian sponge-microbial bioherms. They were

interpreted by different authors as fossil lithistid sponges (Ordovician, Kwon et al. 2012), siliceous sponges (Middle Cambrian, Hong et al. 2012) and siliceous demosponges (Upper Cambrian, Lee et al. 2014), respectively.

Here we suggest that these anastomosing filamentous microstructures can be compared to the possible keratose sponge fossils described by Luo and Reitner (2014) because of the following reasons:

1) All fossils are preserved as microspar-cemented filamentous networks embedded in aggregations of homogeneous automicrites, or peloidal fabrics in worse preservation. This is congruent with the preservation of sponges in carbonates (e.g. Brachert 1991; Warnke 1995). During the decay of the soft tissue, microbial activity induces rapid precipitation of micrites, which moulds the morphology of skeletons before the original skeletal composition is dissolved and replaced by cements (e.g. Fritz 1958; Reitner et al. 1995a; Reitner and Schumann-Kindel 1997). It has been observed from fossil and modern examples that the organic skeleton of sponges can also be very durable in diagenesis (Ehrlich et al. 2013; the discussion in Luo and Reitner 2014).

2) The filaments do not show any sheaths like those *Girvanella* or other calcified cyanobacteria have.

3) There are no features like spores or sporocarps which could lead to a fungal interpretation.

4) The filaments branch and connect to each other, forming an anastomosing network which fills up the micritic aggregation with a more or less consistent density but never extend beyond the aggregation. We did not know any algal or bacterial filaments growing and being preserved in this way. The typical growth patterns of many calcimicrobes are radial, dendritical and parallel to or encrust on each other (cf. Riding 1991a). In the PB samples, the filaments can form a clear border parallel to the margin of the clump (e.g. Fig. 4.3c–d), similar to the phenomenon described in Walter (1972) and illustrated in Lee et al. (2014) and Luo and Reitner (2014). This was compared to the self-recognizing behavior of multicellular organisms by Luo and Reiter (2014). However, this phenomenon is not clearly observed from the OS samples, partly because of the intensive erosion and corrosion on the margins of the micritic laminations.

5) Within the micritic clumps and among the filamentous networks, no proper spicules are observed. Lithistid sponges with heloclone and megaclone desmas are able to form skeletal frameworks with smooth, sinuous and filament-like elements as well. However, the sinuous filaments of high length/width ratios (e.g. Fig. 4.7e, g–h) seem hard to be achieved by heloclones, although the networks constructed by shorter filaments (e.g. Plate 1, Fig. 1–2 in Walter 1972; Fig. 4.3c) do resemble lithistid skeletons in some extent. Furthermore, zygomes and zygoxis were not identified from these samples. Compared with skeletons of most fossil and extant lithistids (cf. lithistids-related chapters in Hooper and Van Soest 2002 and Kaesler 2004), the filaments illustrated here are thinner and their networks are more irregular.

Therefore, without further contradictory evidences, the PB and OS fossils are regarded as keratose sponges here. The fossils in the PB buildups seem belong to a single morpho-type, while those in the OS materials are morphologically more diversified: at least some of them show clearly hierarchical skeletons (Fig. 4.7g) while others do not. The branching canals observed in the OS material (Fig. 4.7b, e, h) are interpreted here as water canals of sponges. Their irregular transection shapes and variable widths on branches look different from burrows (cf. Buatois and Mángano 2011).

4.5.2 Construction of the columnar buildups

The stromatolite-like bioconstructions in both the PB and OS materials were constructed in a very turbulent water body by sponge communities of low diversity and high abundance. An ecologically comparable example has been reported from the Pleistocene tidal-channels in Florida, where a single species of haplosclerid sponges flourished as opportunists in the developing tidal channels and each individual forms 1–2 m high barrel- to vase-shaped columns (Cunningham et al. 2007; Rigby and Cunningham 2007). The unfavorable environment may have prohibited competitors and predators. However, different from the Pleistocene example, the PB and OS buildups are constructed by superposed individuals of encrusting sponges. Encrustation is a strategy to withstand turbulent water other than increasing skeletal rigidity (Finks 2003). Besides, both PB and OS materials show bridging between vicinal columns or domes; this is not reported from the Pleistocene example. These bridging

layers seem have been rapidly lithified and then partly destroyed before the deposition of the overlying sediments (Fig. 4.2a; Fig. 4.5a), indicating cyclically changing deposition rate and water dynamic conditions.

The variation of water dynamics and sediment influx may be the major factor controlling the construction of the OS buildups. Fig. 4.9 demonstrates a suggested model of the construction process, which consists of repeated cycles of sponge growth, burial and lithification, re-exposure and erosion and settlement of new generations. In a period with relatively low deposition rate, sponges could settle down and grow to a certain size (Fig. 4.9a). When deposition rate increased, the sponges were partly or completely buried. The buried tissue became dead and was then rapidly lithified due to the carbonate precipitation induced by anaerobic degradation (Fig. 4.9b). According to the observation on modern examples, lithification can happen to the buried part of a sponge even when the upper part is still living (e.g. Reitner 1993; Reitner et al. 1995a). In the burial period, if the current energy was high enough to prevent the deposition of finer sediments, the coarser pellet-like grains were accumulated and formed a “bridging” dark layer covering sponges and the spaces among them. Microbial films could be developed to stabilize these grains (Fig. 4.9f). In the next stage, when a stronger current came, the non- or weakly lithified sediments could be removed and the lithified sponges could be excavated and exposed to erosion (Fig. 4.9c). This phenomenon, that sponges are lithified while the surrounding sediments are still loose, is also known from modern Great Bahama Bank (Wiedenmayer 1978; Neuweiler and Burdige 2005). Lithification of these modern sponges starts at a few centimeters below the sediment surface. Re-exposure of the buried parts was directly observed. The superposing way of growth seen in the fossil buildups is still not attentively described from the modern sponges. However, it is conceivable. The fossil sponges lived as encrusting organisms and lack root-like structures or tufts, thus they seem to be adapted to hard substrate. Compared with the non-lithified sediments or the thin microbial mats, the re-exposed lithified sponge bodies could provide a more stable substrate for the larva to settle on.

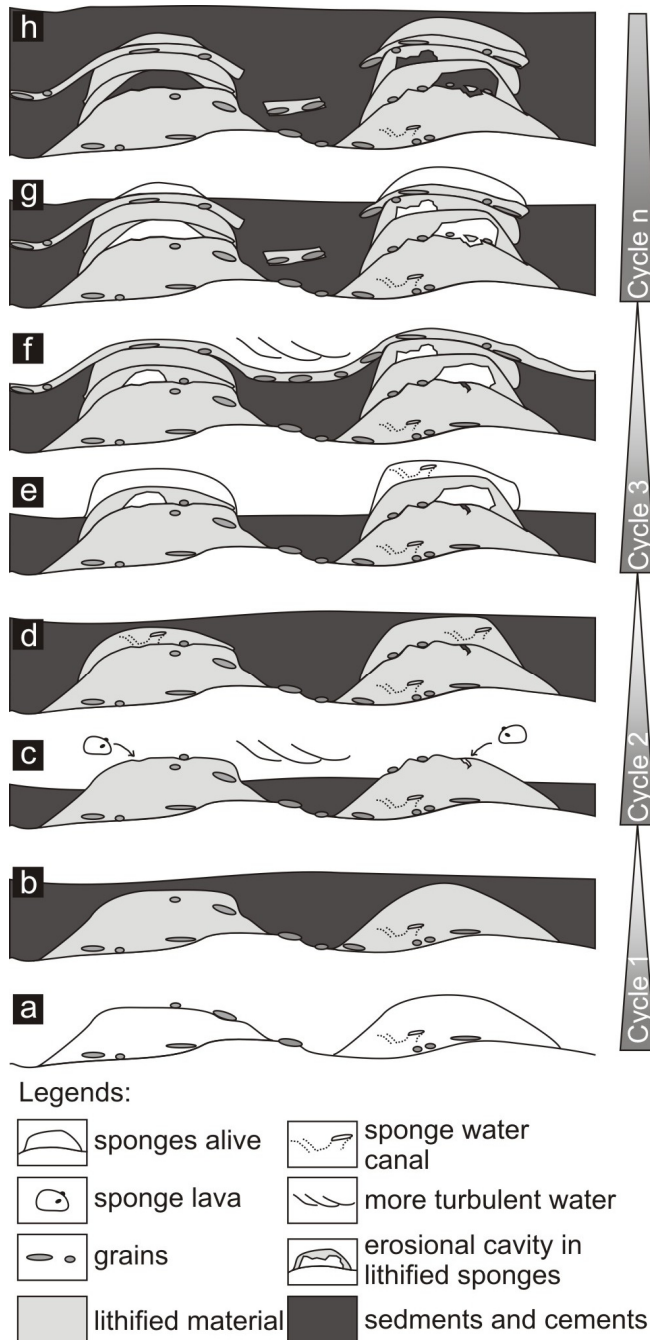


Fig. 4.9 Hypothesized model on the construction of the “organ-pipe stromatolites”, demonstrated by three example burial-exposure cycles. Each of these cycles starts with the settlement of a generation of sponges. **a**, first generation of sponges grow on the substrate. **b**, after a period of growth, sponges are buried and lithified. **c**, lithified sponges are excavated by agitated water and eroded; the second generation of sponges settles down. **d**, growth, burial and lithification of the second generation of sponges. **e**, Re-exposure of the lithified sponges; erosion creates cavities in the lithified part; the third generation settles on and grows. **f**, the third generation of sponges are buried and lithified again; bridging layers may form in the turbulent water. **g**, increased water energy destroys the bridges between columns and even eroded and expanded the non-cemented cavities within the columns; settlement of the fourth generation of sponges. **h**, the burial-exposure cycles repeat until the final burial of the columns.

The PB materials show a transition from microbe-dominated to sponge-dominated laminations. As the proportion of sponge increases, the laminations become more and more undulate and finally form the columnar or domal constructions. Reflected by the syndimentary erosion and fragmentation (Fig. 4.2a–b), the construction of the PB buildups were possibly also accompanied by burial-excitation cycles. However, different from the situation in the OS material, breakages and other erosional structures are not so prominent in the PB columns or domes: many micritic clumps have smooth margins (Fig. 4.3b; Fig. 4.4). Boundaries between superposing clumps are not defined by erosional

surfaces or crescentic cavities, but by some laminae which look brighter in reflected light and show densely packed micrites in thin section (Fig. 4.2a–b; Fig. 4.3b; Fig. 4.4). These laminae are perhaps of microbial origin. Probably, beside of burial, fluctuation of salinity played a more important role in driving the local accretion cycles. Sponges can survive in a wide range of salinities (e.g. Barnes 1999) with an upper limit up to 40‰ or even higher (e.g. Leamon and Fell 1990). Growth of the fossil sponges may have ceased from time to time due to extreme salinities. Decay of sponge tissue may have provided loci for the precipitation of micrites from the oversaturated water. In the periods of extreme salinity, only micribes could survive. Repeat of the cyclic salinity variation and the piling up of allochthonous sediments are probably the causes of the PB stromatolite-like buildups.

Water canals are not identified within the Triassic sponge fossils, although some fenestral structures (e.g. the lower part of Fig. 4.3b) may represent suspicious ones. This can be simply because water canals were not so developed in these sponges, especially considering their smaller size. Even when checking the skeletons of modern keratose sponges, water canals can be either obvious or not (Fig. 4.8f–g). An alternative possibility is that the fossil sponges have undergone tissue regression before death; this is a common reaction of modern sponges to unfavorable salinity (e.g. Leamon and Fell 1990).

4.6 Conclusion and implications

The observations and discussions above lead to the conclusion that sponges, specifically the possible keratose sponges interpreted here, can construct stromatolite-like buildups. This result forms a mirror image to the study of Lee et al. (2014), which revealed that sponges of this type can be builders of the “maze-like microbialites” or the previously considered thrombolites. The popular definition of the term “stromatolite” is “laminated benthic microbial deposits” (Riding 1991b, p. 30). The buildups discussed here obviously meet the criteria “laminated” and “benthic”. They even meet the last criterion “microbial” in some extent, because the preservation of these sponges is related to the micritization induced by microbial activities during decay. The inorganic geochemical data of the micrites within sponge-related clumps and of those in microbial laminations do not show recognizable differences.

These realities indicate a possibility that some of the Precambrian early animals may also be preserved in such structures which are similar to microbial products in both morphology and inorganic geochemistry. Bearing this consideration in mind, hopefully the future paleontological investigations of Precambrian materials will result in new discoveries and understandings.

Acknowledgment

Special appreciation is dedicated to Dr. K. Warnke for permitting us to study his old collections and Prof. Dr. Gerhard Bachmann (University of Halle, Germany) who has allocated us his Keuper material from Franconia in Bavaria. We are heartily grateful to Dr. B. Schirrmeister (University of Bristol, UK) for organizing us the field excursion to Barnhill Quarry and to Mr. G. Owen (WYG Environment) for his support in collecting the local geological information. Also greatly appreciated is Prof. Dr. P.V. Wright's recommendation on the basic geological documents of the Barnhill Quarry, Mr. J. Ma's help with the literature collection and the suggestions from Mr. S. Wu and Prof. Dr. J. Veizer about the geochemical data interpretation. The China Scholarship Council (CSC) financially supported the doctoral study of the first author at the University of Göttingen.

References

- Antcliffe JB, Callow RHT, Brasier MD (2014) Giving the early fossil record of sponges a squeeze. *Biological Reviews* 89:972–1004
- Bachmann GH (2002) A lamellibranch–stromatolite bioherm in the Lower Keuper (Ladinian, Middle Triassic), South Germany. *Facies* 46 (1):83–88
- Bachmann GH, Beutler G, Hagdorn H (1999) Muschelkalk und Keuper am Autobahndreieck Bayreuth/Kulmbach, Nordost-Bayern. *Hallesches Jahrbuch für Geowissenschaften* B21:1–34
- Barnes DKA (1999) High diversity of tropical intertidal zone sponges in temperature, salinity and current extremes. *African Journal of Ecology* 37 (4):424–434
- Bertrand-Sarfati J (1976) An attempt to classify Late Precambrian stromatolite microstructures. In: Walter MR (ed) *Developments in Sedimentology*, vol 20. Elsevier, pp 251–259
- Brachert TC (1991) Environmental Control on Fossilization of Siliceous Sponge Assemblages: A Proposal. In: Reitner J, Keupp H (eds) *Fossil and Recent Sponges*. Springer Berlin Heidelberg, pp 543–553
- Bruckschen P, Oesmann S, Veizer J (1999) Isotope stratigraphy of the European Carboniferous: proxy signals for ocean chemistry, climate and tectonics. *Chemical Geology* 161 (1–3):127–163
- Bruckschen P, Veizer J (1997) Oxygen and carbon isotopic composition of Dinantian brachiopods: Paleoenvironmental implications for the Lower Carboniferous of western Europe. *Palaeogeography, Palaeoclimatology, Palaeoecology* 132 (1–4):243–264
- Brunton FR, Dixon OA (1994) Siliceous sponge-microbe biotic associations and their recurrence through the Phanerozoic as reef mound constructors. *Palaios* 9 (4):370–387
- Buatois LA, Mángano MG (2011) Ichnology of carbonate environments, rocky shorelines, and volcanic terrains In: *Ichnology: Organism-substrate interactions in space and time*. Cambridge University Press, Cambridge, New York, Melbourne, Madrid, Cape Town, Singapore, São Paulo, Delhi, Tokyo, Mexico City pp 217–227
- Cárdenas P, Pérez T, Boury-Esnault N (2012) Chapter two - sponge systematics facing new challenges. In: Becerro MA, Uriz MJ, Maldonado M, Xavier T (eds) *Advances in Marine Biology*, vol 61. Academic Press, pp 79–209
- Coplen TB, Kendall C, Hopple J (1983) Comparison of stable isotope reference samples. *Nature* 302 (5905):236–238
- Cossey PJ, Adams AE, Purnell MA, Whiteley MJ, Whyte MA, Wright VP (2004) *British Lower Carboniferous Stratigraphy*. Geological Conservation Review Series 29. Joint Nature Conservation Committee, Peterborough, 617 pp
- Cunningham KJ, Rigby JK, Wacker MA, Curran HA (2007) First documentation of tidal-channel sponge biostromes (upper Pleistocene, southeastern Florida). *Geology* 35 (5):475–478
- Delecat S, Arp G, Reitner J (2011) Aftermath of the Triassic–Jurassic boundary crisis: Spiculite formation on drowned Triassic steinplatte reef-slope by communities of hexactinellid sponges (Northern Calcareous Alps, Austria). In: Reitner J, Quéric N-V, Arp G (eds) *Advances in Stromatolite Geobiology*, vol 131. Heidelberg, pp 355–390
- Ehrlich H, Rigby JK, Botting JP, Tsurkan MV, Werner C, Schwille P, Petrášek Z, Pisera A, Simon P, Sivkov VN, Vyalikh DV, Molodtsov SL, Kurek D, Kammer M, Hunoldt S, Born R, Stawski D, Steinhof A, Bazhenov VV, Geisler T (2013) Discovery of 505-million-year old chitin in the basal demosponge

Vauxia gracilenta. Scientific Reports 3: 3497. doi:10.1038/srep03497

- Erwin D, Tweedt S (2012) Ecological drivers of the Ediacaran-Cambrian diversification of Metazoa. *Evolutionary Ecology* 26 (2):417–433
- Erwin DH, Laflamme M, Tweedt SM, Sperling EA, Pisani D, Peterson KJ (2011) The Cambrian Conundrum: Early divergence and later ecological success in the early history of animals. *Science* 334 (6059):1091–1097
- Finks RM (2003) Ecology and paleoecology of sponges. In: Kaesler RL (ed) *Treatise on Invertebrate Paleontology Part E Porifera Revised*, vol 2. The Geological Society of America, Inc. and The University of Kansas, Colorado, Kansas, pp 243–260
- Fritz GK (1958) Schwammstotzen, Tuberoide und Schuttbreccien im Weißen Jura der Schwäbischen Alb. *Arbeiten des Geologisch–Paläontologischen Instituts TH Stuttgart*, NF 13:1–118
- Grotzinger JP, Watters WA, Knoll AH (2000) Calcified metazoans in thrombolite–stromatolite reefs of the terminal Proterozoic Nama Group, Namibia. *Paleobiology* 26 (3):334–359
- Guo H, Du Y, Kah LC, Huang J, Hu C, Huang H, Yu W (2013) Isotopic composition of organic and inorganic carbon from the Mesoproterozoic Jixian Group, North China: Implications for biological and oceanic evolution. *Precambrian Research* 224 (0):169–183
- Hagdorn H, Szulc J, Bodzioch A, Morycowa E (1999) Riffe aus dem Muschelkalk. In: Hauschke N, Wilde V (eds) *Trias: Eine ganz andere Welt*. Verlag Dr. Friedrich Pfeil, München, pp 309–320
- Heckel PH (1974) Carbonate buildups in the geologic record: A review. In: Laporle LF (ed) *Reefs in Time and Space*, vol Special Publication No. 18. Society of Economic Paleontologists and Mineralogists, Tulsa, Oklahoma, USA, pp 90–154
- Höfling R, Scott RW (2002) Early and Mid-Cretaceous buildups. In: Kiessling W, Flügel E, Golonka J (eds) *Phanerozoic Reef Patterns*. SEPM Special Publication, vol 72. SEPM (Society of Sedimentary Geology), Tulsa, Oklahoma, USA, pp 521–548
- Hong J, Cho S-H, Choh S-J, Woo J, Lee D-J (2012) Middle Cambrian siliceous sponge-calcimicrobe buildups (Daegi Formation, Korea): Metazoan buildup constituents in the aftermath of the Early Cambrian extinction event. *Sedimentary Geology* 253–254 (0):47–57
- Hooper JNA, Van Soest RWM (eds) (2002) *Systema Porifera: A Guide to the Classification of Sponges*. Kluwer Academic/Plenum Publishers, New York, 1763 pp
- Kaufman AJ, Knoll AH (1995) Neoproterozoic variations in the C-isotopic composition of seawater: stratigraphic and biogeochemical implications. *Precambrian Research* 73 (1–4):27–49
- Kirkham A (1977) *Facies variations and diagenesis of the Upper Arudian–Holkerian (Lower Carboniferous) sediments of the Bristol area.*, University of Bristol, Bristol. 378 pp
- Kirkham A (2005) Thrombolitic-*Ortonella* reefs and their bacterial diagenesis, Upper Visian Clifton Down Limestone, Bristol area, SW England. *Proceedings of the Geologists' Association* 116 (3–4):221–234
- Korte C, Kozur HW, Veizer J (2005) $\delta^{13}\text{C}$ and $\delta^{18}\text{O}$ values of Triassic brachiopods and carbonate rocks as proxies for coeval seawater and palaeotemperature. *Palaeogeography, Palaeoclimatology, Palaeoecology* 226 (3–4):287–306
- Kozur HW, Bachmann GH (2005) Correlation of the Germanic Triassic with the international scale. *Albertiana* 32:21–35
- Kozur HW, Bachmann GH (2008) Updated relation of the germanic Triassic with the Tethyan scale and assigned

- numeric ages. *Berichte Geologische Bundes-Anstalt* 76:53–58
- Kruse PD, Reitner J (2014) Northern Australian microbial-metazoan reefs after the mid-Cambrian mass extinction. *Memoirs of the Association of Australasian Palaeontologists* 45:31–53
- Kwon S-W, Park J, Choh S-J, Lee D-C, Lee D-J (2012) Tetradiid-siliceous sponge patch reefs from the Xiazhen Formation (late Katian), southeast China: A new Late Ordovician reef association. *Sedimentary Geology* 267–268 (0):15–24
- Leamon J, Fell PE (1990) Upper salinity tolerance of and salinity-induced tissue regression in the estuarine sponge *Microciona prolifera*. *Transactions of the American Microscopical Society* 109 (3):265–272
- Lee J-H, Chen J-T, Choh S-J, Lee D-J, Han Z-Z, Chough SK (2014) Furongian (Late Cambrian) sponge-microbial maze-like reefs in the North China Platform. *Palaios* 29:27–37
- Lenton TM, Boyle RA, Poulton SW, Shields-Zhou GA, Butterfield NJ (2014) Co-evolution of eukaryotes and ocean oxygenation in the Neoproterozoic era. *Nature Geosci* 7 (4):257–265
- Longman MW (1977) Factors controlling the formation of microspar in the Bromide Formation. *Journal of Sedimentary Petrology* 47 (1):347–350
- Luo C, Reitner J (2014) First report of fossil “keratose” demosponges in Phanerozoic carbonates: Preservation and 3-D reconstruction. *Naturwissenschaften* 101 (6):467–477
- Marshall JD (1992) Climatic and oceanographic isotopic signals from the carbonate rock record and their preservation. *Geological Magazine* 129 (2):143–160
- Minchin EA (1900) Chapter III. Sponges. In: Lankester ER (ed) *A treatise on zoology. Part II. The Porifera and Coelenterata*. Adam and Charles Black, London, pp 1–178
- Murray JW, Wright CA (1971) The Carboniferous limestone of Chipping Sodbury and Wick, Gloucestershire. *Geological Journal* 7 (2):255–270
- Neuweiler F, Burdige DJ (2005) The modern calcifying sponge *Spherospongia vesparium* (Lamarck, 1815), Great Bahama Bank: Implications for ancient sponge mud-mounds. *Sedimentary Geology* 175 (1–4):89–98
- Nitsch E (2005) Der Keuper in der Stratigraphischen Tabelle von Deutschland 2002: Formationen und Folgen. *Newsletters on Stratigraphy* 41:159–171
- Penny AM, Wood R, Curtis A, Bowyer F, Tostevin R, Hoffman K-H (2014) Ediacaran metazoan reefs from the Nama Group, Namibia. *Science* 344 (6191):1504–1506
- Peterson KJ, Cotton JA, Gehling JG, Pisani D (2008) The Ediacaran emergence of bilaterians: Congruence between the genetic and the geological fossil records. *Philosophical Transactions of the Royal Society B* 363:1435–1443
- Preiss WV (1972) The systematics of South Australian Precambrian and Cambrian stromatolites. Part 1. *Transactions of the Royal Society of South Australia* 96 (Part 2):67–100
- Reitner J (1993) Modern cryptic microbial/metazoan facies from Lizard Island (Great Barrier Reef, Australia): Formation and concepts. *Facies* 29:3–40
- Reitner J, Gautret P, Marin F, Neuweiler F (1995a) Automicrites in a modern marine microbialite: Formation model via organic matrices (Lizard Island, Great Barrier Reef, Australia). *Bulletin de l'Institut océanographique, Monaco* 14 (2):237–303
- Reitner J, Luo C, Duda JP (2012) Early sponge remains from the Neoproterozoic–Cambrian phosphate deposits

- of the Fontanarejo Area (Central Spain). *Journal of Guizhou University (Natural Sciences)* 29 (Sup. 1):184–186
- Reitner J, Neuweiler F, Gautret P (1995b) Part II Modern and fossil automicrites: Implications for mud mound genesis. *Facies* 32 (1):4–17
- Reitner J, Schumann-Kindel G (1997) Pyrite in mineralized sponge tissue - Product of sulfate reducing sponge-related bacteria? *Facies* 36:272–276
- Reitner J, Wörheide G (2002) Non-lithistid fossil Demospongiae-origins of their palaeobiodiversity and highlights in history of preservation. In: Hooper JNA, Van Soest RWM (eds) *Systema Porifera: a guide to the classification of sponges*. Kluwer Academic/Plenum Publishers, New York, pp 52–68
- Riding R (1991a) Calcified cyanobacteria. In: Riding R (ed) *Calcareous Algae and Stromatolites*. Springer Berlin Heidelberg, pp 55–87
- Riding R (1991b) Classification of microbial carbonates. In: Riding R (ed) *Calcareous Algae and Stromatolites*. Springer, Berlin, Heidelberg, pp 21–51
- Riding R, Zhuravlev AY (1995) Structure and diversity of oldest sponge-microbe reefs: Lower Cambrian, Aldan River, Siberia. *Geology* 23 (7):649–652
- Rigby JK (1986) Sponges of the Burgess shale (Middle Cambrian), British Columbia. *Palaeontographica Canadiana* 2:1–105
- Rigby JK, Collins D (2004) Sponges of the Middle Cambrian Burgess Shale and Stephen Formations, British Columbia. *ROM Contributions in Science* 1. Royal Ontario Museum, Toronto. 155 pp
- Rigby JK, Cunningham KJ (2007) A New, large, Late Pleistocene demosponge from southeastern Florida. *Journal of Paleontology* 81 (4):788–793
- Rowland SM, Shapiro RS (2002) Reef patterns and environmental influences in the Cambrian and earliest Ordovician. In: Kiessling W, Flügel E, Golonka J (eds) *Phanerozoic Reef Patterns*. SEPM Special Publication, vol 72. SEPM (Society of Sedimentary Geology), Tulsa, Oklahoma, USA, pp 95–128
- Sperling EA, Peterson KJ, Pisani D (2009) Phylogenetic-signal dissection of nuclear housekeeping genes supports the paraphyly of sponges and the monophyly of Eumetazoa. *Molecular Biology and Evolution* 26 (10):2261–2274
- Veizer J, Demovič R (1974) Strontium as a tool in facies analysis. *Journal of Sedimentary Petrology* 44 (1):93–115
- Walter MR (1972) Stromatolites and the biostratigraphy of the Australian Precambrian and Cambrian. *Special Papers in Palaeontology* 11:1–256
- Warnke K (1995) Calcification processes of siliceous sponges in Viséan Limestones (Counties Sligo and Leitrim, Northwestern Ireland). *Facies* 33 (1):215–227
- Warnke K (1996) Sponge diagenesis and micrite formation in Lower Carboniferous carbonates. *Göttinger Arb Geol Paläont Sb* 2:339–343
- Wiedenmayer F (1978) Modern sponge bioherms of the Great Bahama Bank. *Eclogae Geologicae Helvetiae* 71 (3):699–744
- Wood RA (2011) Paleoecology of the earliest skeletal metazoan communities: Implications for early biomineralization. *Earth-Science Reviews* 106 (1–2):184–190
- Wörheide G, Dohrmann M, Erpenbeck D, Larroux C, Maldonado M, Voigt O, Borchellini C, Lavrov DV (2012)

Chapter one - Deep phylogeny and evolution of sponges (Phylum Porifera). In: Becerro MA, Uriz MJ, Maldonado M, Xavier T (eds) *Advances in Marine Biology*, vol Volume 61. Academic Press, pp 1–78

Wright VP (1986) Facies sequences on a carbonate ramp: The Carboniferous limestone of South Wales. *Sedimentology* 33:221–241

Zhang X, Shu D, Han J, Zhang Z, Liu J, Fu D (2014) Triggers for the Cambrian explosion: Hypotheses and problems. *Gondwana Research* 25 (3):896–909

Supplementary material

(Please find in the attached CD)

Table S4.1 Elemental concentrations along Line 2 (OS), Line 3 (OS) and Line 5 (PB), measured using LA-ICP-MS.

Table S4.2 Carbon and oxygen isotope data from PB and OS samples, together with the referential data from literature.

- Chapter 5 -

Secular occurrences of keratose sponge fossils

5.1 Introduction

As discussed in chapters 3 and 4, the organic skeleton of keratose sponges (*sensu* Minchin 1900) has the potential to be fossilized. Before the work of Luo and Reitner (2014), few occurrences of fossil keratose sponges have been reported, but only the Middle Cambrian taxon *Vauxia* Walcott, 1920 was widely acknowledged (Rigby 1986; Rigby and Collins 2004; Ehrlich et al. 2013). During this doctoral study, I encountered quite a few carbonate fossil materials in publications and collections which could also be assigned to keratose sponges according to the criteria stated in chapters 3 and 4, although they were not diagnosed in this way previously. All of these occurrences are piled together in this chapter, along with a few specimens which may represent Myxospongida (demosponges without any form of skeleton; *sensu* Minchin 1900; see 3.1). Many of these fossils are unpublished and still in the initial stages of investigation. It may require years of work to establish a comprehensive understanding on their paleobiology. Therefore, this chapter does not aim to provide such a deep understanding of them, but just: 1) to show the continuous occurrence and diversity of keratose sponges in geological record; 2) to underpin the keratose affinity of these fossils by distinguishing them from other co-occurring and morphologically similar fossils; 3) to figure out the most explicit common features shared by keratose sponge fossils by comparing them with each other; 4) to raise questions for future study.

The overall chronological distribution of these fossils is shown in Fig. 5.1 and the relevant details of each occurrence are given in 5.2. At the end of this chapter, all the information will be summarized and discussed (5.3).

All the unpublished fossil materials illustrated and discussed in this chapter are from the collection of Prof. Dr. Joachim Reitner. They are now deposited in the Department of Geobiology, Center of Geosciences of the University of Göttingen. Thin sections were studied using a Zeiss SteREO

Discovery.V8 microscope. Photographs were taken using the AxioCam MRc 5-megapixel camera combined with this microscope.

Q	Pleistocene																																																																																																																																																																																																																																																																																																																																																																																																																																																																																																																																																																																																																																																																																																																																																																																																																																																																																																																																																																																																																																																																																																																																																																																																																																																																																																																																																																																																																																																																																																																																																																																																								
---	-------------	--	--	--	--	--	--	--	--	--	--	--	--	--	--	--	--	--	--	--	--	--	--	--	--	--	--	--	--	--	--	--	--	--	--	--	--	--	--	--	--	--	--	--	--	--	--	--	--	--	--	--	--	--	--	--	--	--	--	--	--	--	--	--	--	--	--	--	--	--	--	--	--	--	--	--	--	--	--	--	--	--	--	--	--	--	--	--	--	--	--	--	--	--	--	--	--	--	--	--	--	--	--	--	--	--	--	--	--	--	--	--	--	--	--	--	--	--	--	--	--	--	--	--	--	--	--	--	--	--	--	--	--	--	--	--	--	--	--	--	--	--	--	--	--	--	--	--	--	--	--	--	--	--	--	--	--	--	--	--	--	--	--	--	--	--	--	--	--	--	--	--	--	--	--	--	--	--	--	--	--	--	--	--	--	--	--	--	--	--	--	--	--	--	--	--	--	--	--	--	--	--	--	--	--	--	--	--	--	--	--	--	--	--	--	--	--	--	--	--	--	--	--	--	--	--	--	--	--	--	--	--	--	--	--	--	--	--	--	--	--	--	--	--	--	--	--	--	--	--	--	--	--	--	--	--	--	--	--	--	--	--	--	--	--	--	--	--	--	--	--	--	--	--	--	--	--	--	--	--	--	--	--	--	--	--	--	--	--	--	--	--	--	--	--	--	--	--	--	--	--	--	--	--	--	--	--	--	--	--	--	--	--	--	--	--	--	--	--	--	--	--	--	--	--	--	--	--	--	--	--	--	--	--	--	--	--	--	--	--	--	--	--	--	--	--	--	--	--	--	--	--	--	--	--	--	--	--	--	--	--	--	--	--	--	--	--	--	--	--	--	--	--	--	--	--	--	--	--	--	--	--	--	--	--	--	--	--	--	--	--	--	--	--	--	--	--	--	--	--	--	--	--	--	--	--	--	--	--	--	--	--	--	--	--	--	--	--	--	--	--	--	--	--	--	--	--	--	--	--	--	--	--	--	--	--	--	--	--	--	--	--	--	--	--	--	--	--	--	--	--	--	--	--	--	--	--	--	--	--	--	--	--	--	--	--	--	--	--	--	--	--	--	--	--	--	--	--	--	--	--	--	--	--	--	--	--	--	--	--	--	--	--	--	--	--	--	--	--	--	--	--	--	--	--	--	--	--	--	--	--	--	--	--	--	--	--	--	--	--	--	--	--	--	--	--	--	--	--	--	--	--	--	--	--	--	--	--	--	--	--	--	--	--	--	--	--	--	--	--	--	--	--	--	--	--	--	--	--	--	--	--	--	--	--	--	--	--	--	--	--	--	--	--	--	--	--	--	--	--	--	--	--	--	--	--	--	--	--	--	--	--	--	--	--	--	--	--	--	--	--	--	--	--	--	--	--	--	--	--	--	--	--	--	--	--	--	--	--	--	--	--	--	--	--	--	--	--	--	--	--	--	--	--	--	--	--	--	--	--	--	--	--	--	--	--	--	--	--	--	--	--	--	--	--	--	--	--	--	--	--	--	--	--	--	--	--	--	--	--	--	--	--	--	--	--	--	--	--	--	--	--	--	--	--	--	--	--	--	--	--	--	--	--	--	--	--	--	--	--	--	--	--	--	--	--	--	--	--	--	--	--	--	--	--	--	--	--	--	--	--	--	--	--	--	--	--	--	--	--	--	--	--	--	--	--	--	--	--	--	--	--	--	--	--	--	--	--	--	--	--	--	--	--	--	--	--	--	--	--	--	--	--	--	--	--	--	--	--	--	--	--	--	--	--	--	--	--	--	--	--	--	--	--	--	--	--	--	--	--	--	--	--	--	--	--	--	--	--	--	--	--	--	--	--	--	--	--	--	--	--	--	--	--	--	--	--	--	--	--	--	--	--	--	--	--	--	--	--	--	--	--	--	--	--	--	--	--	--	--	--	--	--	--	--	--	--	--	--	--	--	--	--	--	--	--	--	--	--	--	--	--	--	--	--	--	--	--	--	--	--	--	--	--	--	--	--	--	--	--	--	--	--	--	--	--	--	--	--	--	--	--	--	--	--	--	--	--	--	--	--	--	--	--	--	--	--	--	--	--	--	--	--	--	--	--	--	--	--	--	--	--	--	--	--	--	--	--	--	--	--	--	--	--	--	--	--	--	--	--	--	--	--	--	--	--	--	--	--	--	--	--	--	--	--	--	--	--	--	--	--	--	--	--	--	--	--	--	--	--	--	--	--	--	--	--	--	--	--	--	--	--	--	--	--	--	--	--	--	--	--	--	--	--	--	--	--	--	--	--	--	--	--	--	--	--	--	--	--	--	--	--	--	--	--	--	--	--	--	--	--	--	--	--	--	--	--	--	--	--	--	--	--	--	--	--	--	--	--	--	--	--	--	--	--	--	--	--	--	--	--	--	--	--	--	--	--	--	--	--	--	--	--	--	--	--	--	--	--	--	--	--	--	--	--	--	--	--	--	--	--	--	--	--	--	--	--	--	--	--	--	--	--	--	--	--	--	--	--	--	--	--	--	--	--	--	--	--	--	--	--	--	--	--	--	--	--	--	--	--	--	--	--	--	--	--	--	--	--	--	--	--	--	--	--	--	--	--	--	--	--	--	--	--	--	--	--	--	--	--	--	--	--	--	--	--	--	--	--	--	--	--	--	--	--	--	--	--	--	--	--	--	--	--	--	--	--	--	--	--	--	--	--	--	--	--	--	--	--	--	--	--	--	--	--	--	--	--	--	--	--	--	--	--	--	--	--	--	--	--	--	--	--	--	--	--	--	--	--	--	--	--	--	--	--	--	--	--	--	--	--	--	--	--	--	--	--	--	--	--	--	--	--	--	--	--	--	--	--	--	--	--	--	--	--	--	--	--	--	--	--	--	--	--	--	--	--	--	--	--	--	--	--	--	--	--	--	--	--	--	--	--	--	--	--	--	--	--	--	--	--	--	--	--	--	--	--	--	--	--	--	--	--	--	--	--	--	--	--	--	--	--	--	--	--	--	--	--	--	--	--	--	--	--	--	--	--	--	--	--	--	--	--	--	--	--	--	--	--	--	--	--	--	--	--	--	--	--	--	--	--	--	--	--	--	--	--	--	--	--	--	--	--	--	--	--	--	--	--	--	--	--	--	--	--	--	--	--	--	--	--	--	--	--	--	--	--	--	--	--	--	--	--	--	--	--	--	--	--	--	--	--	--	--	--	--	--	--	--	--	--	--	--	--	--	--	--	--	--	--	--	--	--	--	--	--	--	--	--	--	--	--	--	--	--	--	--	--	--	--	--	--	--	--	--	--	--	--	--	--	--	--	--	--	--	--	--	--	--	--	--	--	--	--	--	--	--	--	--	--	--	--	--	--	--	--	--	--	--	--	--	--	--	--	--	--	--	--	--	--	--	--	--	--	--	--	--	--	--	--	--	--	--	--	--	--	--	--	--	--	--	--	--	--	--	--	--	--	--	--	--	--	--	--	--	--	--	--	--	--	--	--	--	--	--	--	--	--	--	--	--	--	--	--	--

5.2 Description

Most of the following fossils, except II, part of X, XVI and XVII, are recognized as keratose sponges preserved in carbonate facies basically according to the features which have been concluded in 4.5.1. Those are (with minor modification): 1) all of them are preserved as automicritic clumps with moulded filamentous structures which are cemented by microspars; 2) the filaments form an anastomosing network which fills up the micritic aggregation with a more or less consistent density but never extends beyond the aggregation; 3) the filaments are not associated with spicules, sheaths, spores or sporocarps, which may lead to other biological interpretations. In the following descriptions, these characters will not be repeatedly emphasized. Rather, more attention will be paid to the unique features of each example.

I. Middle Eocene; Boltaña, Spain (Fig. 5.2)

The rock material exhibits deep fore-reef mud mound facies but is now preserved in debris flows (Reitner and Keupp 1991). The recognized keratose sponge fossils are preserved as small micritic clumps occupying the cryptic spaces in the rigid frames which are

Fig. 5.1 Distribution of proposed non-spicular sponge fossils in geological history. Black circles, keratose sponge fossils; gray circles, myxospongid fossils; half-filled circles, specimens interpreted with lower assurance. Roman numbers correspond to the order of descriptions in 5.2. Italic roman numbers indicate data from literature.

formed by skeletal clasts and lithified deposits. These specimens can be preserved in a position as geopetal fillings in small cavities (e.g. Fig. 5.2c), or filling up the remaining spaces above other geopetal sediments (Fig. 5.2a–b). Nearly every observed specimen has a filamentous ring at the edge of the micritic clump. Filament thickness in some of the fossils is around 15–20 μm , while that in the others can reach 30 μm . However, within each individual, the filaments do not show obvious size hierarchies. These sponges do not seem to be very pervasive in the investigated samples, but this can be a phenomenon caused by poor preservation as well (e.g. Fig. 5.2d).

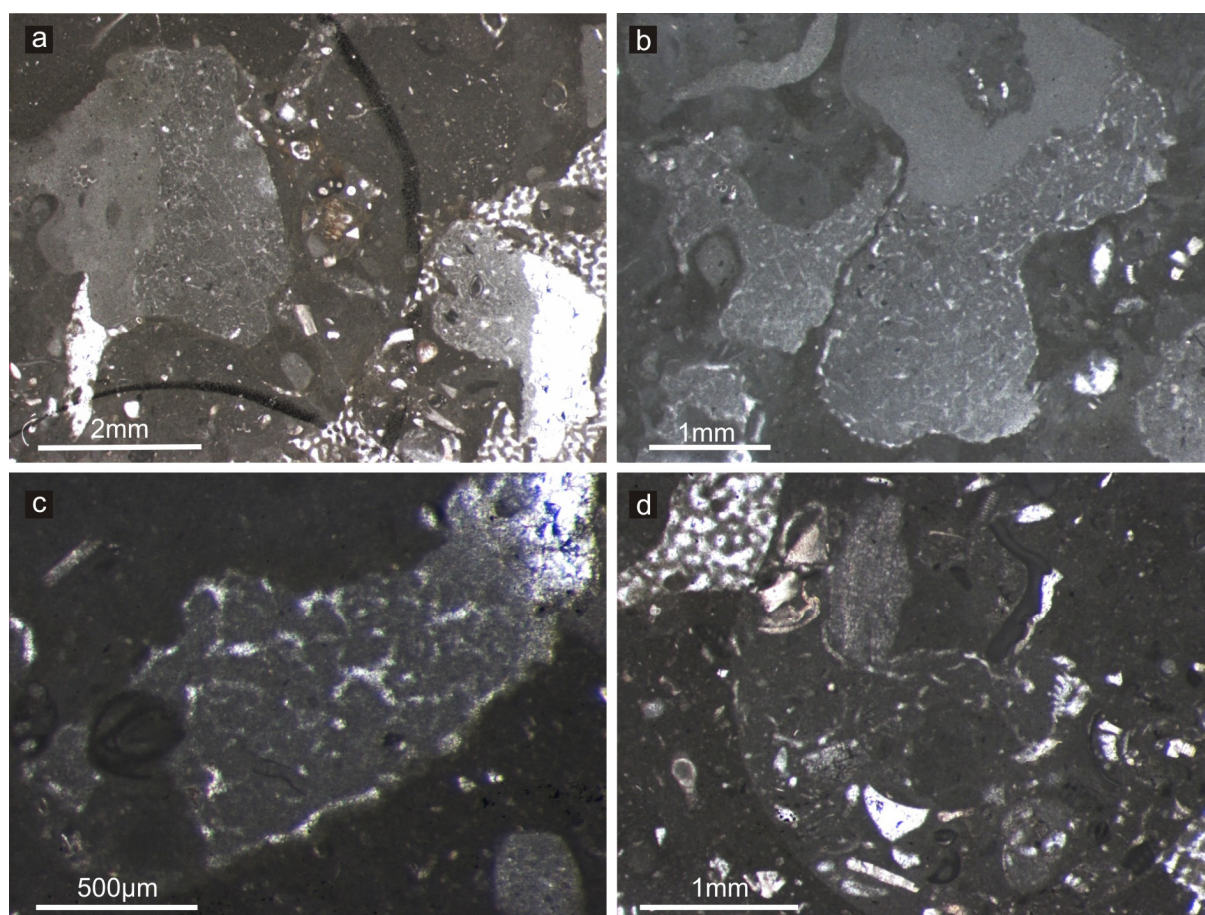


Fig. 5.2 Fossils from the Middle Eocene, Botaña, Spain.

Other samples from the same locality, but probably not the same facies, present a different reef consortium which is dominated by lithistids. Keratose sponges are absent in these samples. The skeletal frame of some lithistid sponges can resemble those of some keratose sponges to some extent (Fig. 5.3; cf. Fig. 4.3). However, zygomeres and zygores are conspicuous in most lithistid skeletons. They are recognizable even in the relatively worse preserved individuals (Fig. 5.3f). Besides, because

of the rigid skeletons, lithistid sponges are often reef builders and tend to maintain their own shape during growth, while the keratose sponges described above adapted their shape to the living spaces.

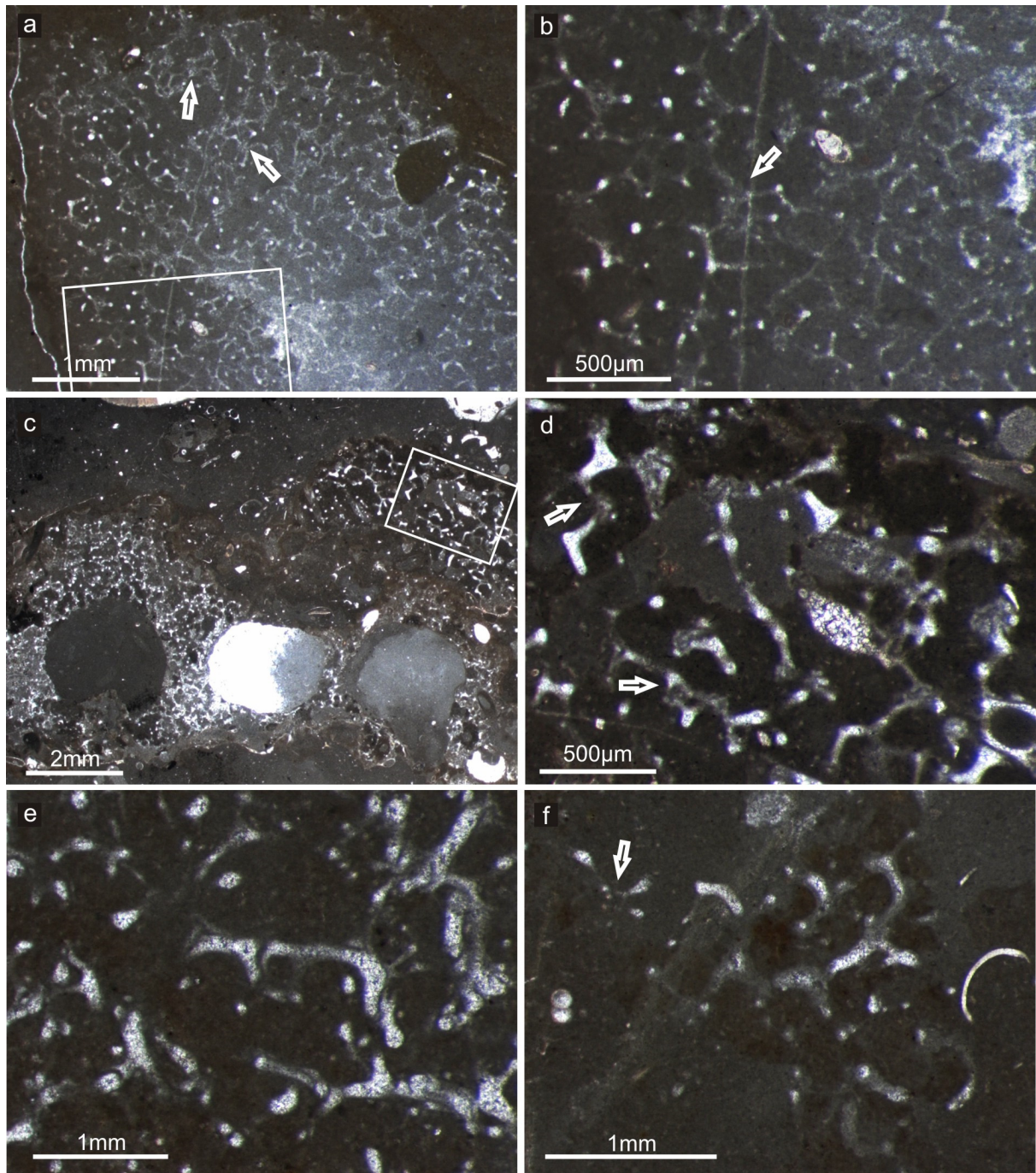


Fig. 5.3 Lithistid sponges from the Middle Eocene, Botaña. Areas in rectangles in **a** and **c** are magnified in **b** and **d**, respectively. Arrows are showing the preserved zygotes. **e** and **f** show a same type of lithistid sponge preserved in different qualities.

II. Lower Cretaceous (Upper Albian); Araya, Spain (Fig. 5.4a–b)

Different from most of the other non-spicular sponges described in this dissertation, this specimen does not show any skeletal elements. In thin section, it consists of a brownish central part surrounded by a belt of meandering structures which are c.a. 80–120 μm in diameter and cemented by brighter calcite crystals (Fig. 5.4a). The central part is composed of allochthonous sediments which are distinctly different from the automicrites surrounding the meandering structures (Fig. 5.4a–b). The preservation of this specimen is comparable with that of a hexactinellid fossil in the same thin section (Fig. 5.4c–d).

The hexactinellid fossil has a central area partly-filled by brownish, geopetal wackestone. This area is surrounded by skeletal frames and obviously represents the spongocoel of this sponge (Fig. 5.4c). This is quite similar to the situation of the non-skeletal sponge. Both fossil organisms seem to have had a bucket- or vase- shaped body, which lay down after death. Lithification of the soft tissue probably happened very early, because the hexactinellid skeletal structure is well preserved. The syndimentary fractures and related micritic geopetal fillings in the hexactinellid fossil indicate that this specimen was already rigid before the deposits were finally stabilized (Fig. 5.4c–d). The same micritic geopetal deposits also partly filled the meandering structures in the non-skeletal fossil, indicating that these structures were originally empty spaces (Fig. 5.4a–b). In contrast, hexactinellid skeletons kept their original shape when buried in similar deposits (Fig. 5.4d).

Based on this comparison, the brownish central part of the non-skeletal specimen is interpreted here as a filled spongocoel, and the meandering structures as branches of the sponge aquiferous system. If this interpretation is correct, this non-spicular specimen may be comparable with *Halisarca*, a modern sponge devoid of any form of skeletons (myxospongid). The meandering voids in the fossil material are indeed similar to the long, tubular and branching choanocyte chambers of this organism (Bergquist and de Cook 2002; Ereskovsky et al. 2011; cf. Fig. 4 of the latter reference).

This type of non-skeletal fossil is very rare in rock samples. The one described here is the single specimen seen so far.

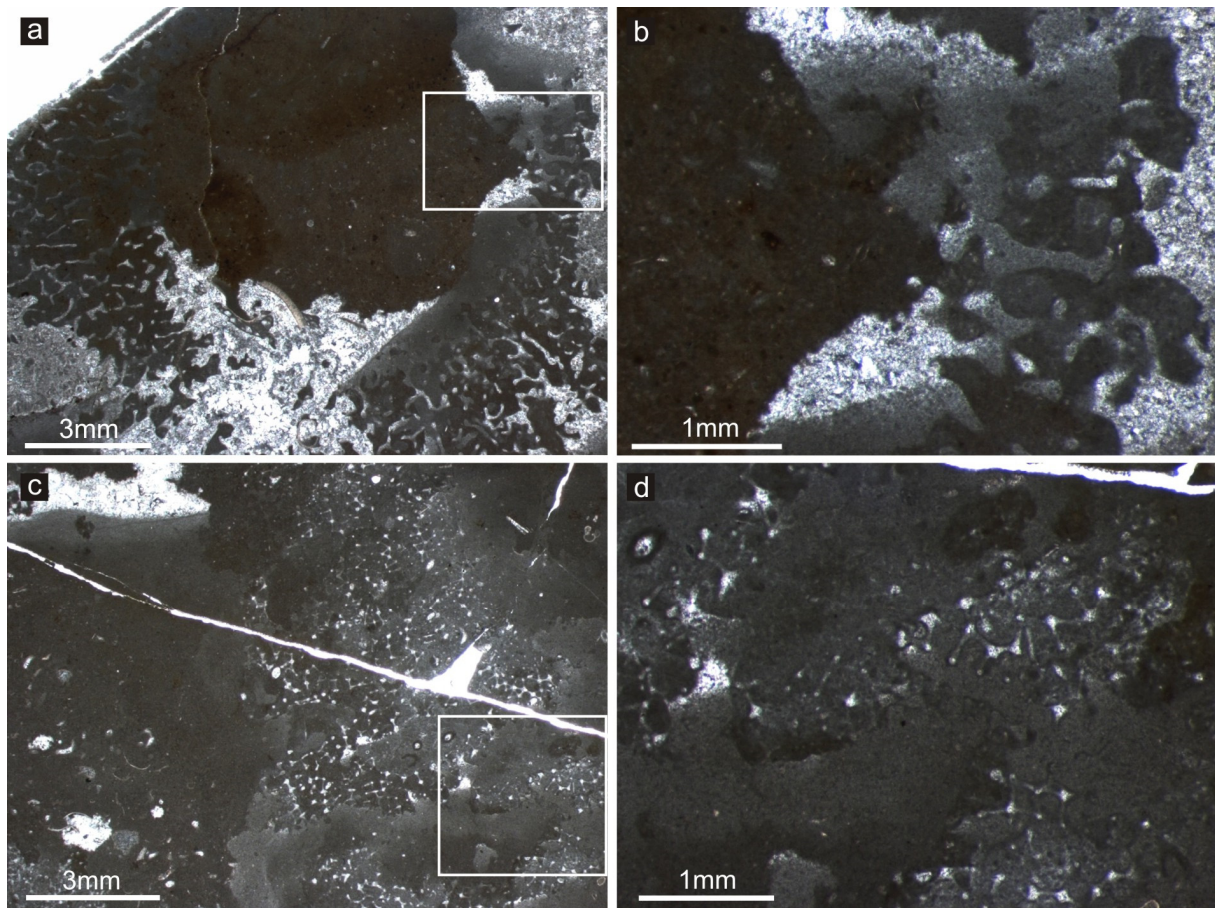


Fig. 5.4 A proposed myxospongid (a–b) and a hexactinellid (c–d) fossil from the Albian of Araya, Spain. Areas in rectangles in a and c are magnified in b and d respectively.

III. Late Jurassic (Lower Kimmeridgian); Langenberg, Germany

From the Jurassic lagoonal patch reefs from the Langenberg hill, probable keratose sponge fossils were illustrated by Reitner (1994, Plate 2, Fig. 6–7; Plate 4, Fig. 5–6, 8), although they were interpreted as endolithic mycelia at that time. These patch reefs were mainly constructed by the oyster *Nanogyra nana*. Various sorts of sponges lived in the cryptic spaces among the reef frames, including a dominant number of the geodiid *Rhaxella sorbyana*, the boring sponge *Aka*, some axinellids and calcareous sponges (Delecat et al. 2001). The proposed keratose sponge fossils show preservation and ecological behavior similar to the other sponges but different from fungi. The existence of fungi was recorded as perforations in the oyster shells (Plate 40, Fig. 8 in Delecat et al. 2001).

These keratose sponges are similar to those described in V (see below) in dwelling in oyster shell facies. However, the abundance of the Jurassic keratose sponges in reefs seems to be much lower than that of their Triassic analogues.

IV. Middle Triassic (Ladinian); Erfurt Formation, Lower Keuper; Kulmbach/Bayreuth, Germany

(see chapter 4)

V. Middle Triassic; Upper Muschelkalk *Placunopsis* reefs; Germany (Fig. 5.5a–d)

In the *Placunopsis* reefs, shells are densely packed and the interspaces are intensively compartmented. These restricted spaces can promote anaerobic decay of the liable soft tissue, benefit the rise of carbonate alkalinity in the microenvironment, and thus provide a better chemical condition for the fossilization of sponges (cf. Delecat 2001). The keratose sponge fossils are generally very well preserved. But some individuals exhibit the coexistence of two preservation qualities: the filaments-bearing micritic clump and structureless peloidal fabric grade into each other (Fig. 5.5b). In addition, the remnants of the older generation can be disturbed by newer generations (e.g. the hollow arrow in Fig. 5.5a).

Biodiversity in these reefs is very low. The non-spicular sponges are nearly the only fossil type beside of the *Placunopsis* shells. Some of the sponge fossils show possible hierarchical differentiation in skeletons (e.g. Fig. 5.5c), while the others do not (e.g. Fig. 5.5a). The thickness of (primary) skeletal filaments varies among individuals. For example, the filaments in Fig. 5.5a are around 60 µm in diameter, while those in Fig. 5.5d are about only 40–45 µm wide. The branching pattern and the manner of soft deformation of the fossil skeletal filaments are comparable with those of modern keratose sponges (e.g. Fig. 5.5h). Aquiferous systems are not well presented in these fossils, whereas the hollow arrows in Fig. 5c–d indicate two possible examples.

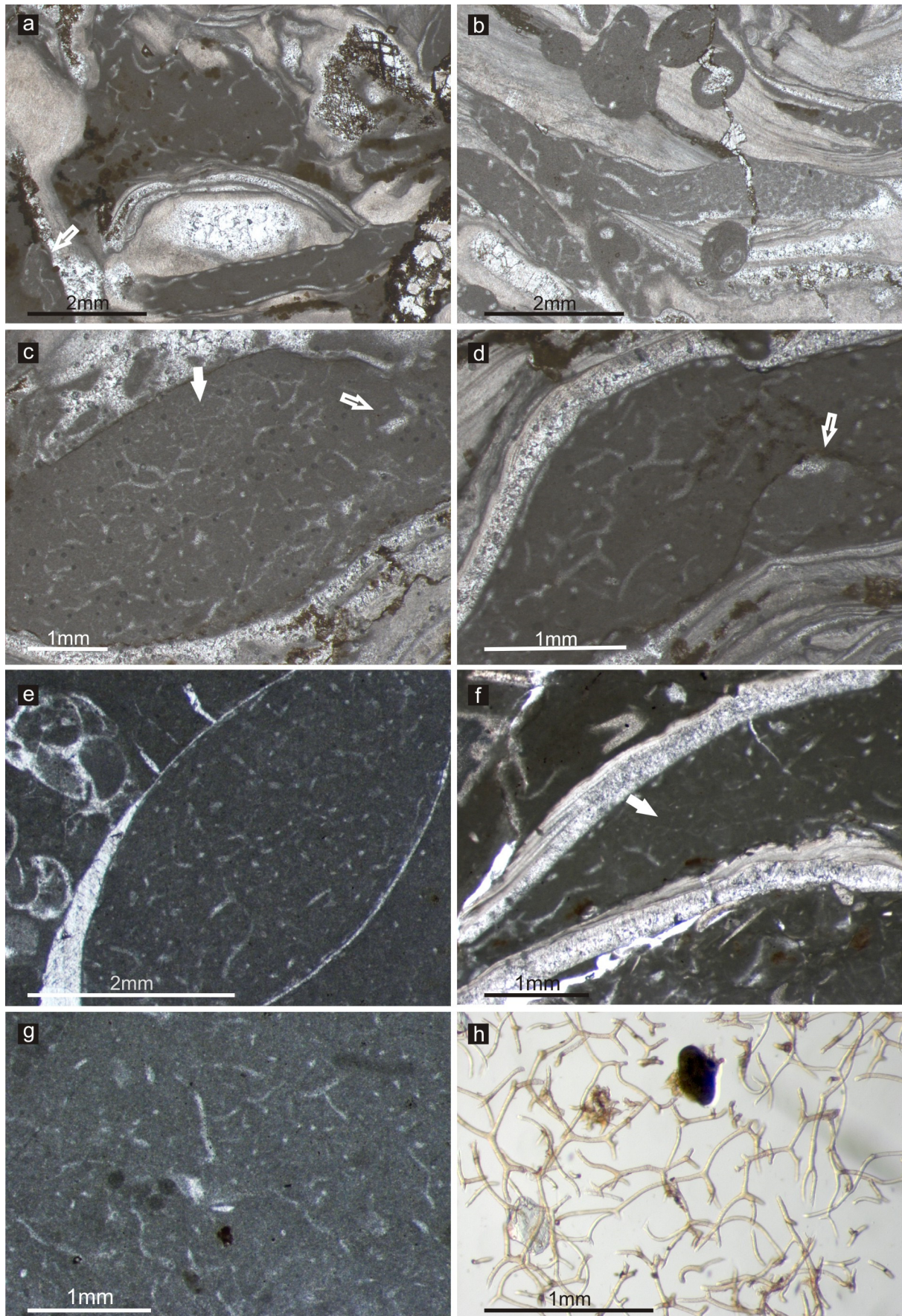


Fig. 5.5 Suggested keratose sponge fossils from the Middle Triassic *Placunopsis* reefs (a–d) and crinoid reef (e–g). h shows the skeleton of a modern dictyoceratid sponge from Lizard Island. Solid arrows indicate probable secondary skeletal fibers; the hollow arrow in a shows a new generation of sponge disturbing the remains of the older generation; hollow arrow in c and d point to possible aquiferous canals.

VI. Middle Triassic; Muschelkalk crinoid reef; SW Germany (Fig. 5.5e–g)

Like III and V, the preservation of these fossils is also related to closed or semi-closed spaces in shell facies. Keratose sponges were well preserved only within relatively complete bivalve shells (Fig. 5.5e). These sponges may have acted as stabilizer of deposited shells (e.g. Fig. 5.5f), but this behavior is not pervasively recorded due to the preservation bias. Some specimens show possible hierarchical differentiation in skeletons (Fig. 5.5f), while the others do not (Fig. 5.5g).

VII. Middle Triassic (Anisian); Middle Muschelkalk *Diplopora* Beds; Libiąż, Poland

(see chapter 3)

VIII. Permian-Triassic boundary; Iran (Fig. 5.6)

Sponges demonstrated in Fig 5.6a–c and e–f are from the lowermost Triassic (personal communication with Dr. Sylvain Richoz, University of Graz). They grew as lenticular clumps between layers of ostracod-containing wackestones. The filaments show clear branching pattern similar to that of some modern keratose sponges (cf. Fig. 5.5h). However, the thickness of each single filament changes rapidly within very small scale (Fig. 5.6b–c). It is unknown whether this is a primary biological feature or a product of special taphonomical processes. This feature also makes it difficult to judge whether the skeletons were hierarchical or not according to the thickness of skeletal filaments. To better understand the architecture of these skeletal networks, a 3-D reconstruction will be necessary. The maximum width of these filaments also varies among individuals, e.g. from about 50–60 μm in the one shown in Fig. 5.6a to about 60–80 μm in the one shown in Fig. 5.6f.

The fossils presented in Fig. 5.6d and g are from the post-extinction Permian (personal communication with Dr. Sylvain Richoz, University of Graz). They stabilized themselves by encrusting on hard substrates and occupying cryptic spaces. Filaments of these fossils are probably hierarchical (Fig. 5.6g). Possible aquiferous canals are preserved with geopetal sediments.

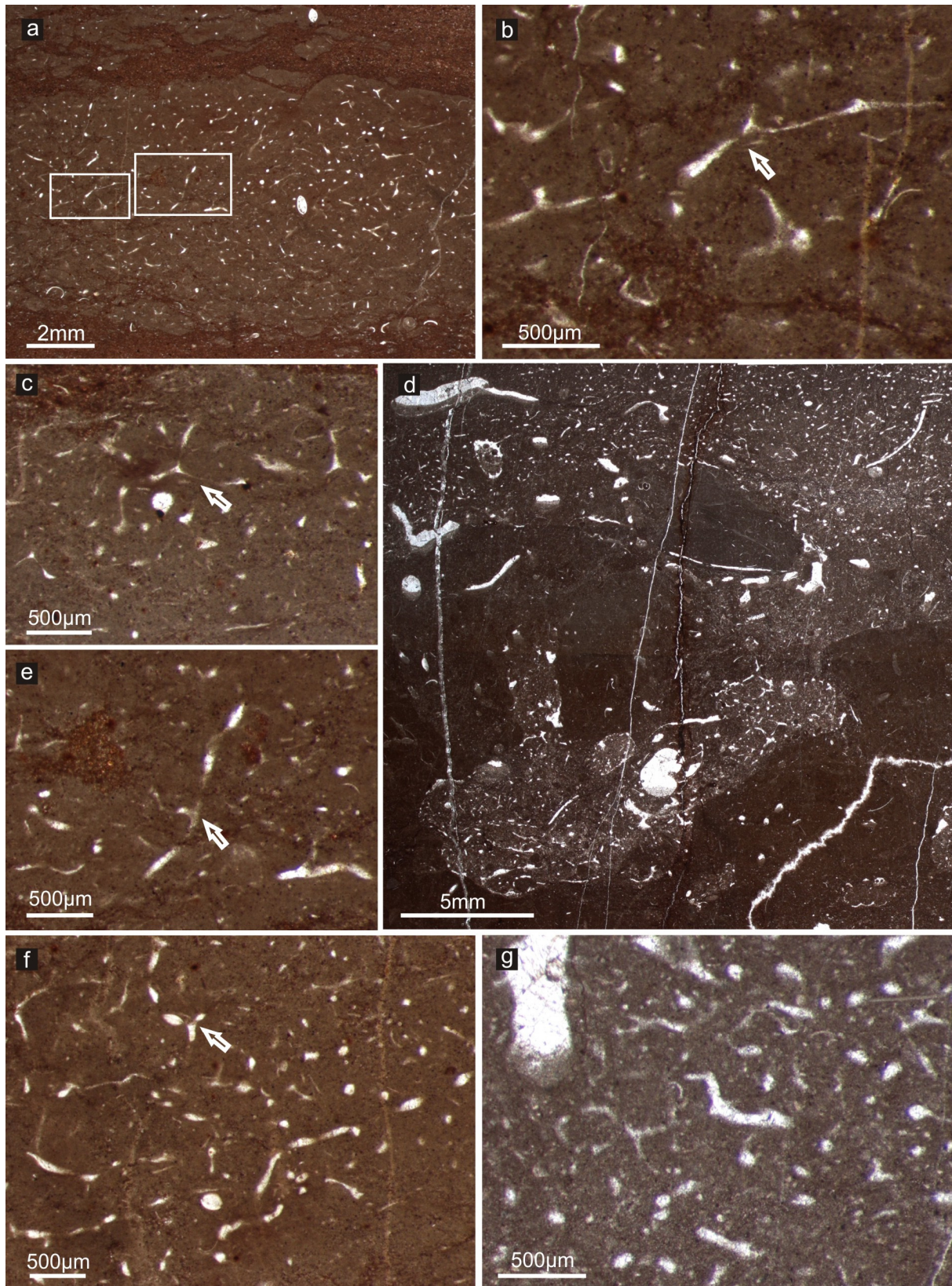


Fig. 5.6 Fossils from the Permian-Triassic boundary, Iran. Areas in the smaller and larger rectangles in **a** are magnified in **b** and **e**, respectively. Arrows point to the trifurcated junctions as well as the rapid change of filament thickness (in **b** and **c**) in the skeletal networks.

IX. Viséan; Clifton Down Limestone; Bristol, UK

(see chapter 4)

X. Late Devonian (Frasnian); Bären Felsen mud mound; Rübeland, Germany (Albrecht 1997; Reitner 2013)

The Bären Felsen mud mound represents the late development stage (terminal cap stage) of a Givetian/Frasnian reef complex (Weller 1991). In this facies, identifiable body fossils are rare except some *Renalcis* and hexactinellids (Reitner 2013).

There are two types of possible non-spicular sponge fossils. The first type is filamentous structures with identical morphology of the proposed keratose sponge fossils. Though these fossils are preserved in the same way as the hexactinellids in the same locality (Fig. 3 and Fig. 11 in Albrecht 1997), they were described as fungal mycelia at that time, following the interpretation of Reitner (1994) (Albrecht 1997, p. 70–71).

The second type is some meandering canals with a width of about 200–300 μm (can reach 400 μm as well) observed in one of the micritic clumps (Fig. 5.7a–b). These canals are not as organized as those described in II, but are also similar to the aquiferous system of modern *Halisarca* (Ereskovsky et al. 2011) and the interpreted water canals in IX. The irregular margins of the canals and their frequent trifurcated junction (not randomly joined or overlapped) reduce the possibility that they are burrows or degassing/dewatering structures. Up to now only one specimen of this type has been observed.

XI. Middle Devonian (Givetian); Membre du Griset, Blacourt Formation; Boulonnais, France

(see chapter 3)

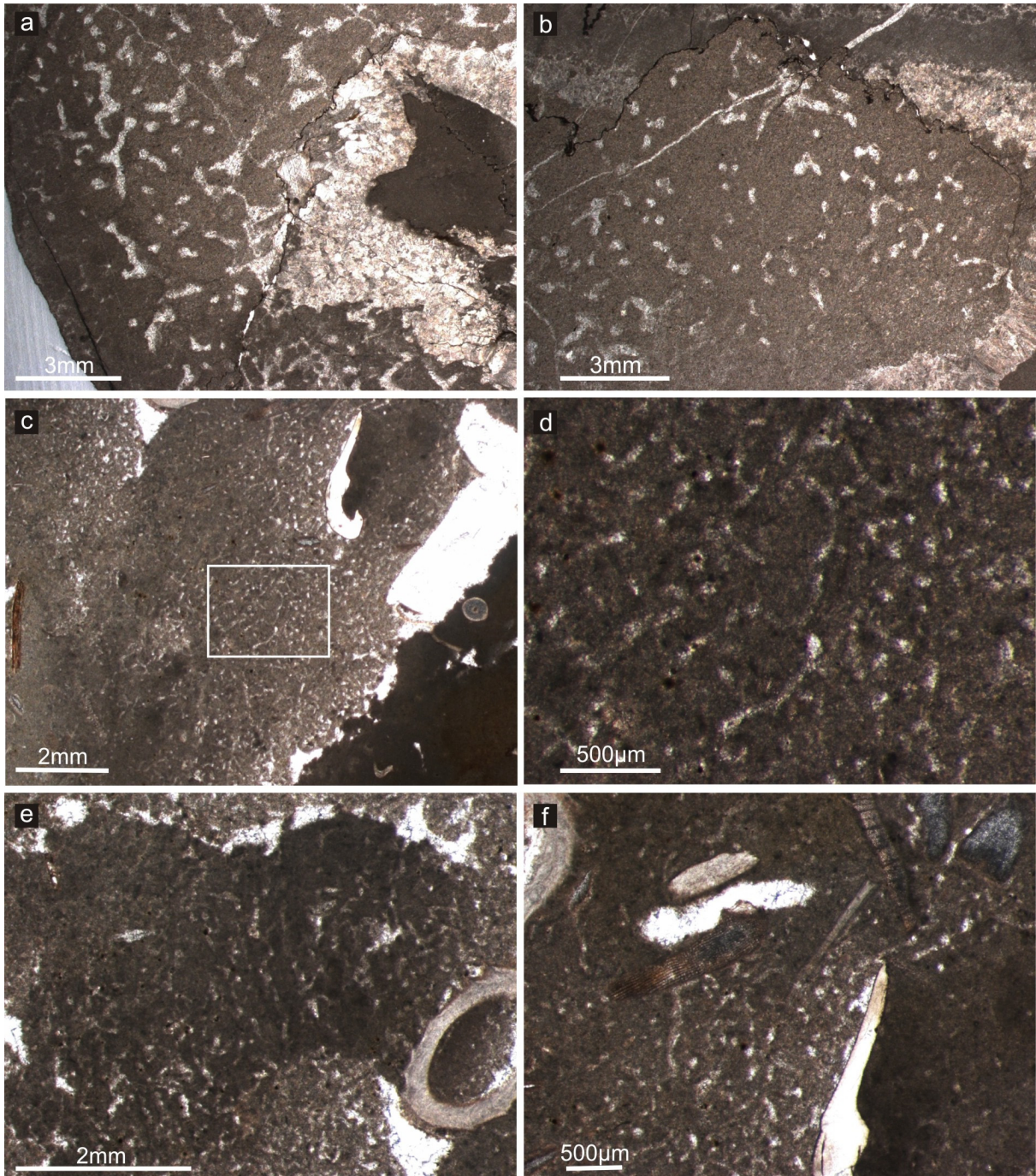


Fig. 5.7 **a–b** a possible myxospongid fossil from the Frasnian of Rübeland, Germany. **c–f** proposed keratose sponge fossils from the Middle Devonian Hollard Mound, Morocco. The area in the rectangle in **c** is magnified in **d**.

XII. Middle Devonian (Efelian–Givetian); Hollard Mound, Morocco (Fig. 5.7c–f)

These fossils are preserved in the mud mounds related to hydrocarbon vents (Peckmann et al. 1999). Filamentous structures related to keratose sponge skeletons occur massively (Fig. 5.7c). The overall outline of these sponges was not clear in thin section, because the preservation gets worse towards the

edge of the fossils and the skeletal networks gradually grade into microsparic or micritic matrix. However, in the massive fossil area, some clumps are darker than the ambient fabrics and the filaments inside of them do not connect to those outside (Fig. 5.7e), possibly representing different individuals. Like the other examples described above, filaments of these fossils also line up the boundary where the sponge body contacts hard substrates (Fig. 5.7e–f). The filaments are non-hierarchical (Fig. 5.7d) and are averagely around 50–60 μm in diameter. Structures related to aquiferous systems are not identified.

XIII. Late Ordovician (Late Katian); Xiazhen Formation; SE China (described in Kwon et al. 2012)

The filamentous networks preserved in dark, pyrite-containing micrites were interpreted as fossils of “siliceous sponges” in the original paper. These sponges contributed to the construction of the shallow marine patch reefs by encrusting on tetradiids, the frame builders. The sponge fossils do not show a distinct outline, but their original volumes can be inferred from the delineation of the filamentous networks or the related peloidal fabrics. Filaments also line up the boundaries between sponge bodies and tetradiids (Fig. 3A in Kwon et al. 2012). The exact size of the filaments was not provided.

XIV. Late Cambrian (Furongian); Chaomidian Formation; Shandong Province, China (described in Lee et al. 2014)

Beside of microstromatolites and calcimicrobes, keratose sponges are one of the major components of the reported maze-like (macerate) bioconstructions which were built in low relief on a storm-dominated, shallow carbonate platform. Similar to XIII, these sponge fossils were originally described as “siliceous sponges”. The skeletal filaments are ~20–60 μm wide. According to the original description and illustration, the skeletal networks are non-hierarchical. Some of these fossils adapt their outline to the surrounding frames (Fig. 6C and Fig. 7A–E in Lee et al. 2014), while the others maintain a certain shape (Fig. 7F in Lee et al. 2014). Sponges of the former shape form an explicit

filamentous ring on the edge of the micritic clump. Probable aquiferous canals are preserved in some of these fossils and are partly or fully filled by micritic sediments (e.g. Fig. 7B, E–F in Lee et al. 2014).

XV. Middle Cambrian (Drumian); Daegi Formation; South Korea (described in Hong et al. 2012)

The fossil structures probably representing keratose sponges were again diagnosed as “siliceous sponges”. These fossils are irregular in shape and grew together with *Epiphyton* in an interlaced pattern. The skeletal filaments are 60–70 μm in diameter, and are worse preserved when the micritic aggregations grade into peloidal fabrics. Because these sponges seem have provided encrusting sites for calcimicrobes, they were interpreted by the authors as the main constructors of the shallow marine buildups. In these buildups, a minor population of possible lithistid sponges and scattered spicules of other siliceous sponges are also preserved.

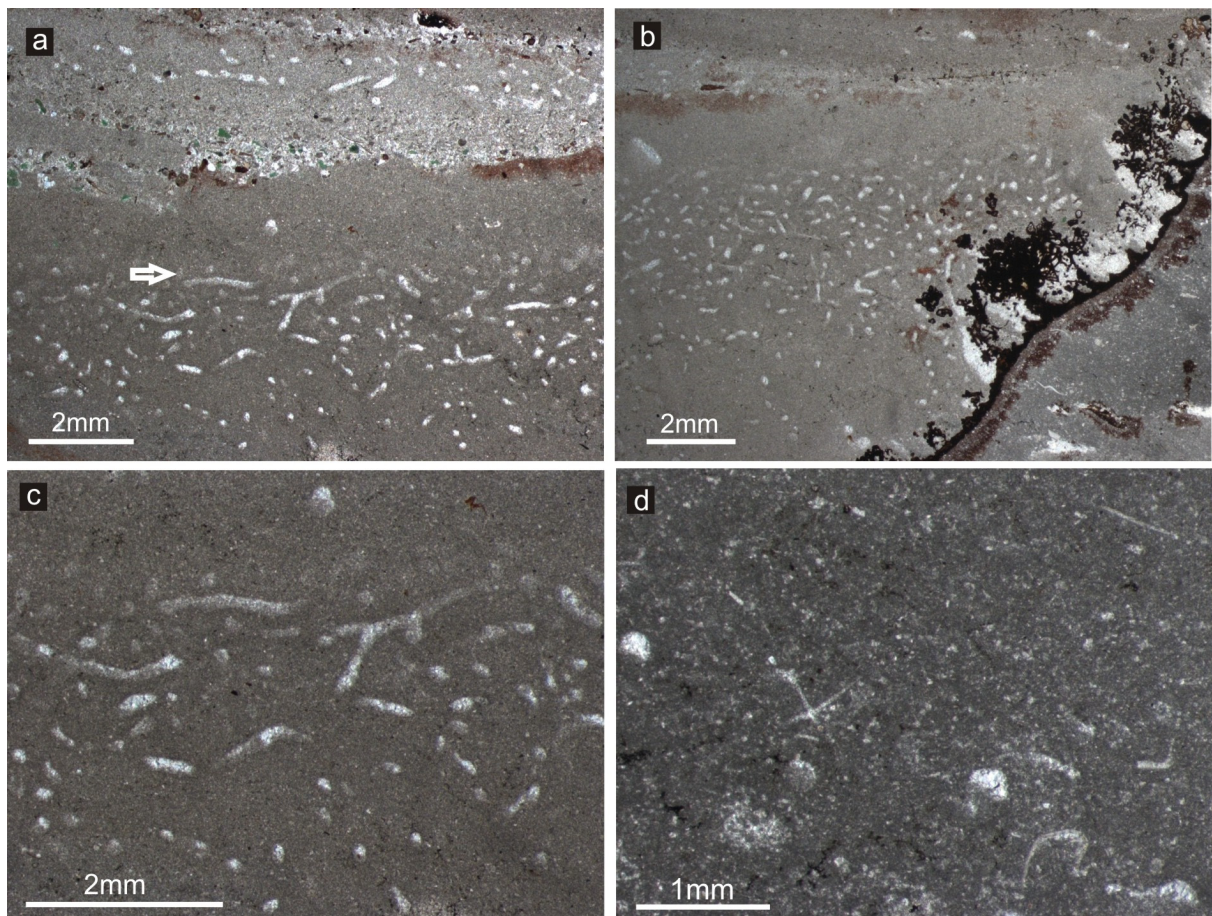


Fig. 5.8 Fossil material from the Cambrian stage 3–4, York Peninsula, Australia. **a–c** a possible myxospongid fossil. **c** is magnified from a part of **a**. **d** skeletal fossils in the bioclastic wackestone where the sponges encrust on. The arrow in **a** indicates the level where almost all the canals become completely filled by sediments.

XVI. Cambrian Stage 5; Burgess Shale; British Columbia, Canada

The family Vauxiidae Walcott, 1920 and its single established genus *Vauxia* Walcott, 1920 were initially ascribed to Hexactinellida, then to lithistid demosponges (Rigby 1980) and were finally settled in order Verongiida Bergquist, 1978 (Rigby 1986). This taxonomic resolution has been recently confirmed by the work of Ehrlich et al. (2013), who found less altered skeletal fibers composed of chitin in this type of fossils from Burgess Shale. Hitherto, more fossils diagnosed as Vauxiidae or *Vauxia* have been reported from various localities and stratigraphic levels, e.g. the Middle Cambrian Kaili Biota of China (Zhao et al. 2011), the Middle Cambrian of Utah (Rigby 1980; Rigby et al. 2010) and the Silurian of Scotland (Botting 2007).

Compared with the other keratose sponge fossils described in this dissertation, *Vauxia* is more organized in morphology. They have a branched or unbranched, conical to cylindrical body which is supported by a double layered skeleton network. The network shows regular polygonal meshes. The diameter of the skeletal fibers varies in the range of 20–50 μm according to different species.

XVII. Early Cambrian (Stage 3–4, Botomian); Parara Limestone; York Peninsula Australia (Fig. 5.8)

This is a single specimen identified by Tucker (1989) as a sponge fossil from the Parara Limestone which was correlated to the Botomian in Siberia (Alexander et al. 2001). The elongated, microspars-cemented voids were regarded as spicules. However, these structures are partly filled by micritic sediments; especially when approaching upward to the erosional surface, their outline is increasingly blurred by the infilled micrites (Fig. 5.8a–c). This is different from the normal preservation of skeletons (see the discussion of II; cf. Fig. 5.6g and Fig. 5.8d). In addition, the width of branches is around 110–140 μm , much larger than that of the skeletal filaments described anywhere else in this dissertation, but close to the size magnitude of aquiferous canals. In addition, the distribution and branching pattern of these structures seem also too well organized to be of bioturbation origin. Therefore, here I temporarily interpret these branching structures in the same way as II and X, as sponge aquiferous canals. To confirm this diagnosis, it is necessary to check more samples and to

reconstruct their architecture in 3-D. These plausible sponges grew by encrusting on the eroded hard surfaces (Fig. 5.8a–b).

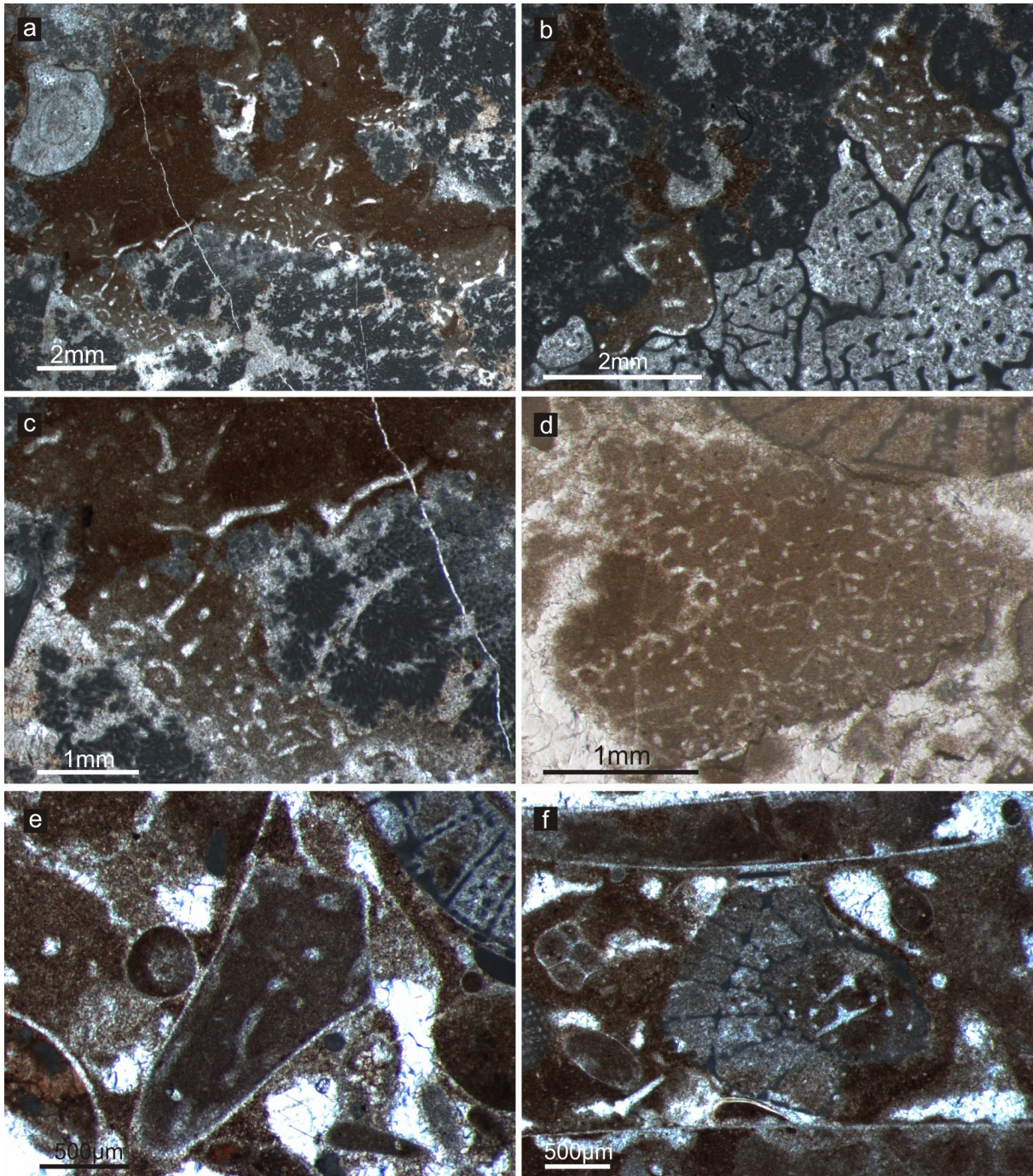


Fig. 5.9 Fossils from the Tommotian, Siberia.

XVIII. Cambrian Stage 2 (Tommotian); Siberia (Fig. 5.9a–c, e)

The suggested keratose sponges are found as cryptic dwellers in the frame constructed by *Epiphyton* and archaeocyaths (Fig. 5.9a–c). In addition, they seem have utilized abandoned shells as living spaces

as well (Fig. 5.9e), although this phenomenon is only observed from few allochthonous clasts. The latter ecological strategy and the mode of preservation are comparable with those of some contemporaneous hexactinellids (Fig. 5.9f). Diameters of the filaments in keratose sponge fossils mostly fall in the range of 60–90 μm . Similar to the behaviour of the other cryptic analogues described above, these Cambrian fossils also show an obvious filamentous ring near to the margin of the micritic body.

It is interesting to see that some archaeocyaths also exhibit skeletal structures looking like anastomosing filamentous networks in thin section (Fig. 5.9b, d). But it is easy to distinguish the suggested keratose sponge fossils from most archaeocyaths by their different preservation: the skeletons of the latter are composed of micrites while the inner spaces are cemented by larger calcite crystals (Fig. 5.9b). However, this criterion becomes questionable on those specimens like the one shown in Fig. 5.9d. Here I adopt a conservative attitude and regard this specimen as a diagenetically altered archaeocyath according to its regular shape.

5.3 Summary

The data demonstrated above support a secular distribution of keratose sponge fossils through the whole Phanerozoic. Myxospongiids may also have been preserved in the fossil record (II, X and XVII), but these records need further confirmation. Carbonate rocks related to rapid micrite precipitation have the potential to preserve the morphological features of sponge organic skeletons and aquiferous systems three-dimensionally, therefore can provide a valuable taphonomical window to peek at the historical abundance and diversity of non-biomineralized sponges.

Most of the listed keratose sponge fossils are found in cryptic spaces of rigid frames. Many of them adapted their body to the shape of the living space and secreted skeletal fibers at the boundary where the body meets the hard substrate. It is also shown that some of these fossils could have a part above the rock surface (e.g. Fig. 5.6d). The second type of life style demonstrated above is to encrust on exposed and consolidated surface (e.g. VII, IX, XVII). This surface can be formed by previously fossilized sponges or lithified sediments. Besides, some fossil keratose sponges developed a certain

body shape (e.g. conical, cylindrical) and grew erectly above the sea floor or in other environments with sufficient space (e.g. II, part of XIV, XVI). However, it is possible that these fossils represent only the overground part of the “cryptic” ones.

These ecological behaviours are comparable with those of modern keratose and myxospongid demosponges. Many of these non-biomineralized sponges need to fix themselves on hard substrates. Also, a rich biodiversity of them is known hosted by marine caves (Manconi et al. 2013). Although I did not find a report emphasizing the endobenthic nature of modern keratose sponges or myxospongids, this life style is known from other demosponges (e.g. Reitner and Keupp 1991).

The skeletal networks in the described fossils are simple in morphology. But they do show some extent of diversity by demonstrating e.g. hierarchical or non-hierarchical architectures, different magnitudes of filament size and various shapes of meshes. It will be another task to classify these fossils and compare them with modern taxa and other fossils (e.g. some archaeocyaths). 3-D reconstructions will be very useful for this purpose. But the related techniques need to be improved and routinized for carbonate materials first.

References

- Ahlbrecht J (1997) Verkalkte Mikrobe-relikte und kryptische Habitate des Rübeldand-Mikrobiaoliths (Elbingeröder Riffkomplex, Harz, Mittel-Oberdevon). Unpublished Diploma thesis, University of Göttingen, Göttingen, 175 pp
- Alexander EM, Jago JB, Rozanov AY, Zhuravlev AY (eds) (2001) The Cambrian biostratigraphy of the Stansbury Basin, South Australia, vol 282. Transactions, Palaeontological Institute. IAPC "Nauka/Interperiodica", Moscow, 344 pp
- Bergquist PR, de Cook SC (2002) Family Halisarcidae Schmidt, 1862. In: Hooper JA, Van Soest RM, (eds) Systema Porifera. Kluwer Academic/Plenum Publishers, New York, Boston, Dordrecht, London, Moscow, pp 1078–1079
- Botting JP (2005) Exceptionally well-preserved Middle Ordovician sponges from the Llandegley Rocks Lagerstätte, Wales. *Palaeontology* 48 (3):577–617
- Botting JP (2007) Algae, receptaculitids and sponges. In: Clarkson ENK, Harper DAT, Anderson L (eds) Silurian Fossils of the Pentland Hills, Scotland. Field Guides to Fossils 11. The Palaeontological Association, London, pp 36–49
- Delecat S, Peckmann J, Reitner J (2001) Non-rigid cryptic sponges in oyster patch reefs (Lower Kimmeridgian, Langenberg/Oker, Germany). *Facies* 45 (1):231–254
- Ehrlich H, Rigby JK, Botting JP, Tsurkan MV, Werner C, Schwillle P, Petrášek Z, Pisera A, Simon P, Sivkov VN, Vyalikh DV, Molodtsov SL, Kurek D, Kammer M, Hunoldt S, Born R, Stawski D, Steinhof A, Bazhenov VV, Geisler T (2013) Discovery of 505-million-year old chitin in the basal demosponge *Vauxia gracilenta*. *Scientific Reports* 3:3497. doi:10.1038/srep03497
- Ereskovsky AV, Lavrov DV, Boury-Esnault N, Vacelet J (2011) Molecular and morphological description of a new species of Halisarca (Demospongiae: Halisarcida) from Mediterranean Sea and a redescription of the type species Halisarca dujardini. *Zootaxa* (2768):5–31
- Hong J, Cho S-H, Choh S-J, Woo J, Lee D-J (2012) Middle Cambrian siliceous sponge-calcimicrobe buildups (Daegi Formation, Korea): Metazoan buildup constituents in the aftermath of the Early Cambrian extinction event. *Sedimentary Geology* 253–254 (0):47–57
- Kwon S-W, Park J, Choh S-J, Lee D-C, Lee D-J (2012) Tetradiid-siliceous sponge patch reefs from the Xiazhen Formation (late Katian), southeast China: A new Late Ordovician reef association. *Sedimentary Geology* 267–268 (0):15–24
- Lee J-H, Chen J-T, Choh S-J, Lee D-J, Han Z-Z, Chough SK (2014) Furongian (Late Cambrian) sponge-microbial maze-like reefs in the North China Platform. *Palaios* 29:27–37
- Luo C, Reitner J (2014) First report of fossil “keratose” demosponges in Phanerozoic carbonates: preservation and 3-D reconstruction. *Naturwissenschaften* 101 (6):467–477
- Manconi R, Cadeddu B, Ledda F, Pronzato R (2013) An overview of the Mediterranean cave-dwelling horny sponges (Porifera, Demospongiae). *ZooKeys* (281):1–68
- Minchin EA (1900) Chapter III. Sponges. In: Lankester ER (ed) A treatise on zoology. Part II. The Porifera and Coelenterata. Adam & Charles Black, London, pp 1–178
- Peckmann J, Walliser O, Riegel W, Reitner J (1999) Signatures of hydrocarbon venting in a Middle Devonian

- Carbonate Mound (Hollard Mound) at the Hamar Laghdad (Antiatlas, Morocco). *Facies* 40 (1):281–296
- Reitner J (1994) Mikrobialith-Porifera Fazies eines Exogyren/Korallen Patchreefs des Oberen Korallenooliths im Steinbruch Langenberg bei Oker (Niedersachsen). *Berliner geowiss Abh* E3:397–417
- Reitner J (2013) Field Trip 3: Middle and Upper Devonian reef carbonates of the central Harz Mountains, Elbingerode Complex. In: Reitner J, Reich M (eds) *Palaeobiology and geobiology of fossil Lagerstätten through earth history. A joint conference of the "Paläotologische Gesellschaft" and "Palaeontological Society of China"*, Göttingen, Germany, September 23–27, 2013. Field guide to excursions. Geowissenschaftliches Museum Göttingen, Göttingen, pp 27–32
- Reitner J, Keupp H (1991) The fossil record of the haplosclerid excavating sponge *Aka* de Laubenfels. In: Reitner J, Keupp H (eds) *Fossil and Recent Sponges*. Springer Berlin Heidelberg, pp 102–120
- Rigby JK (1980) The new Middle Cambrian sponge *Vauxia magna* from the Spence Shale of northern Utah and taxonomic position of the Vauxiidae. *Journal of Paleontology* 50 (1):234–240
- Rigby JK (1986) Sponges of the Burgess Shale (Middle Cambrian), British Columbia. *Palaeontographica Canadiana* 2: 1–105
- Rigby JK, Church SB, Anderson NK (2010) Middle Cambrian sponges from the Drum Mountains and House Range in western Utah. *Journal of Paleontology* 84 (1):66–78
- Rigby JK, Collins D (2004) Sponges of the Middle Cambrian Burgess Shale and Stephen Formations, British Columbia. *ROM Contributions in Science* 1:1–155
- Tucker L (1989) Investigation of the Early Cambrian Parara Limestone–York Peninsula, SA. Department of Mines and Energy, South Australia, Report Book 89 (53):1–36
- Walcott CD (1920) Cambrian geology and paleontology IV, No.6 Middle Cambrian Spongiae. *Smithsonian Miscellaneous Collections* 67 (6):261–364
- Weller H (1991) Facies and development of the Devonian (Givetian/Frasnian) Elbingerode reef complex in the Harz Area (Germany). *Facies* 25 (1):1–49
- Zhao Y, Zhu M, Babcock LE, Peng J (eds) (2011) *The Kaili Biota – Marine organisms from 508 million years ago*. Guizhou Science and Technology Press, Guiyang, 251 pp

- Chapter 6 -

Implication of microstructures of the Precambrian carbonate microbialites

6.1 Introduction

According to the theories introduced in Chapter 1, the Precambrian ancestral animals perhaps possessed a simple body plan and had close ecological relation to microbial mats. The study in Chapter 4 has shown that bioconstructions of some keratose sponges can be similar to microbial buildups in macroscopic morphology. Therefore, it is expected that a careful study of the Precambrian microbialites may yield some new discoveries about early animals. Microbialites are “organosedimentary deposits that have accreted as a result of a benthic microbial community trapping and binding detrital sediment and/or forming the locus of mineral precipitation” (Burne and Moore 1987, p. 241–242; Riding 2011). These microbial-induced deposits can be formed in both siliciclastic and carbonate facies. In the study of carbonate microbialites, a routine has been developed and widely adopted to describe a microbialite in four scales: “megastructure”, “macrostructure”, “mesostructure” and “microstructure” (Grey 1989; Shapiro and Awramik 2000; Shapiro 2000). Definitions of these scales are listed in Table 6.1. The most popular classification of carbonate microbialites, i.e. stromatolites, thrombolites, dendrolites and leiolites, is mainly based on different mesostructures (Riding 2000; Shapiro 2000; Table 6.1). However, to investigate the biological composition of a carbonate buildup, microstructures appear to be more important (details discussed in 6.2–6.3).

My study on microbialite microstructures is just in beginning, but a few interesting structures have already been observed from Neoproterozoic microbialites. They are described and preliminarily discussed in 6.4 and 6.5. Before that, two sections (6.2–6.3) are dedicated to a brief review of our current understanding on Precambrian carbonate microbialites, especially their microstructures.

Table 6.1 The four scales used in microbialite description, according to Grey (1989), Shapiro and Awramik (2000) and Shapiro (2000).

Term	Definition	Examples
Megastructure	Large scale features of the microbialite bed, kilometric to metric scale	Biostrome, bioherm
Macrostructure	Shape of the microbialite bodies, in dimensions of tens of centimeters to meters	Columns, domes, stratiform, etc.
Mesostructure	Internal structure of the microbialites which are visible to naked eyes	Laminated (stromatolites), clotted (thrombolites), dendritic (dendrolites), structureless (leiolite)
Microstructure	Microscopic fabrics	Cements, crystal forms, microbial constituents

6.2 Dendrolites, Leiolites and Thrombolites

Dendrolites are typically formed by calcimicrobes and occurred massively in the Cambrian, the Early Ordovician and the Late Devonian (Riding 2000). Only few plausible occurrences of them are known from the Precambrian, such as the one identified from the Mesoproterozoic Wumishan Formation (Shi et al. 2008) and the “dendriform” microbialites from the Early Neoproterozoic Little Dal Group (e.g. Aitken 1989; Turner et al, 1993).

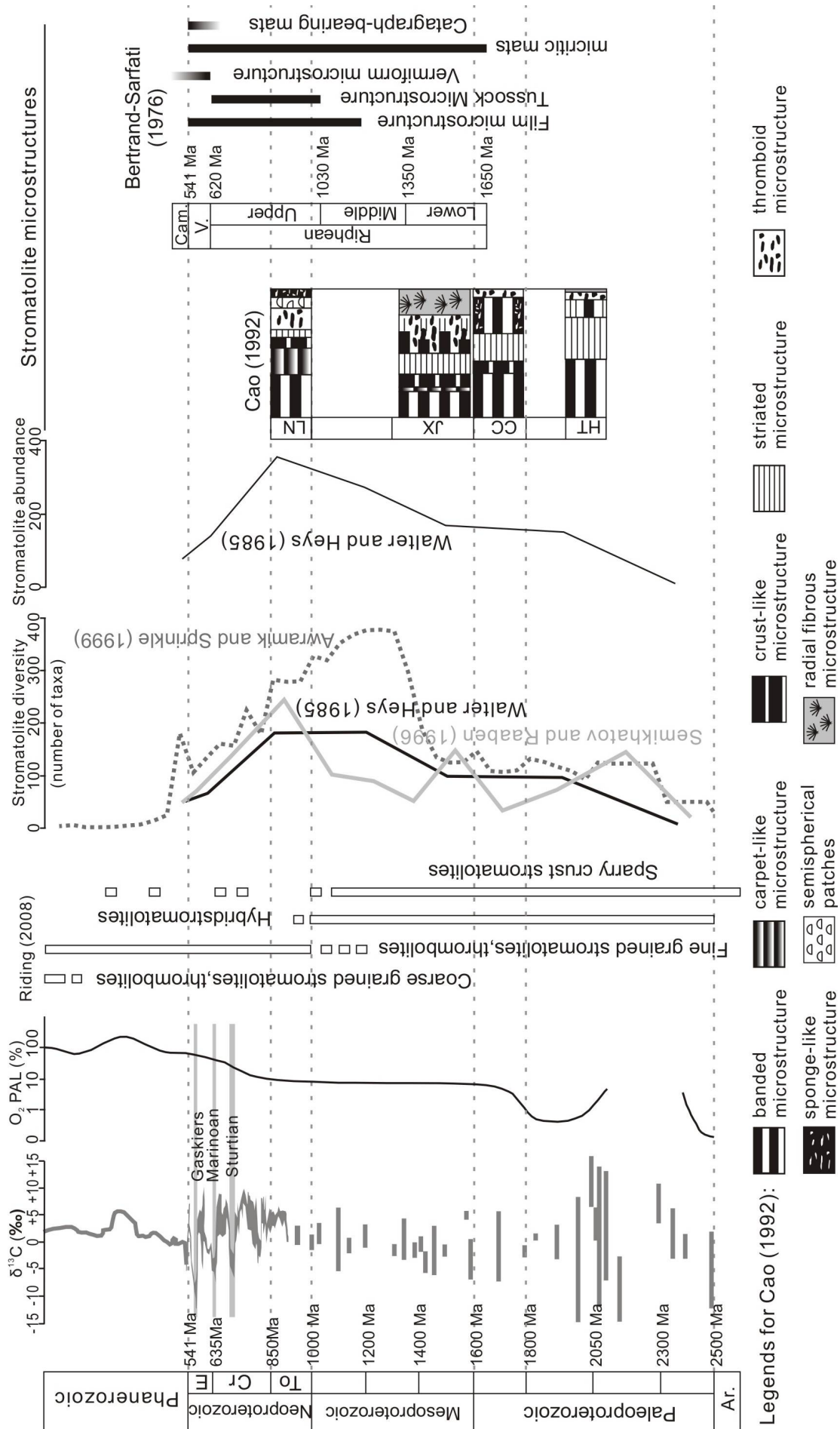
Leiolite was defined as “microbial deposit with structureless macrofabric” (Braga et al. 1995, p. 347). Since this term was introduced parallel to stromatolites and thrombolites because the corresponding microbialites “appear structureless in hand-specimen” (Braga et al. 1995, p. 348), the word “macrofabric” in the original definition should have an equal meaning to “mesostructure”. Leiolites seem to be less common than the other types of carbonate microbialites in geological record, but this can be because the samples were preferentially labeled in other ways, such as “mud mounds” or “stromatolites” based on weak laminations (discussed in Riding 2000; Chen and Lee 2014).

Thrombolites are “cryptalgal structures related to stromatolites, but lacking lamination and characterized by a macroscopic clotted fabric” (Aitken 1967, p. 1164). The expression “macroscopic clotted fabric” was ambiguously applied to both macro- and mesostructures in the beginning, but was later constrained to describe mesostructures only (“mesoclots”, Kennard and James 1986; Shapiro

2000). In the geological history, thrombolites did not become abundant until the Neoproterozoic (e.g. reviewed in Shapiro 2004; Tang et al. 2013). The known earlier occurrences are from the Paleoproterozoic Rocknest Formation, Canada (1.9 Ga, Kah and Grotzinger 1992) and the Mesoproterozoic Wumishan Formation, North China (1.5–1.45 Ga, Tang et al. 2013). Compared with the Neoproterozoic thrombolites, e.g. those from the Little Dal Group, Mackenzie Mountains (Aitken and Narbonne 1989; Turner et al. 1993; Turner et al. 2000) (1080–780 Ma, Batten et al. 2004), the Beck Spring Dolomite, southern California (1080–750 Ma, Harwood and Sumner 2011), the Deep Spring Formation, Nevada (end Proterozoic, Oliver and Rawland 2002) and the Nama Group, Namibia (550–543 Ma, Grotzinger et al. 2000, 2005), the Paleo- and Mesoproterozoic clots seem to contain a larger proportion of crystal crusts surrounding minor organic-rich micrites.

This distribution of thrombolites in geological record is considered by many researchers as a response to historical global environmental changes. However, formation of the clotted mesostructure can be attributed not only to fossilization of microbial communities (e.g. Kennard and James 1986) or biological activities (e.g. perturbation of foraminifera, Bernhard et al. 2013), but also to the sea-level controlled changes of mat consortia (e.g. Feldmann and McKenzie 1998) or only the variation of sedimentation rates (Castro-Contreras et al. 2013). These various opinions on thrombolite formation are probably rooted in different understandings on the nature of “clots”. As listed in Shapiro (2000) and Riding (2011), the clotted mesostructures in thrombolites can be calcimicrobe aggregations, clots with peloidal fabrics, diffused patches of trapped sands or secondarily enhanced clots, etc. In this situation, to study these microbialites on the microstructure level may help to sort out different types of thrombolites according to their provenances and then provide a better basis to discuss the geological history of each of them.

Fig. 6.1 Distribution of microbialites in the Precambrian. The International stratigraphic scheme, carbon isotope and evaluated historical oxygen level are after the references cited in Fig. 1.3. In the column of “stromatolite diversity”, each line and its correspondent reference are marked with the same colour. Stratigraphic correlation of the data from Cao (1992) is based on Du et al. (2010), Gao et al. (2011) and Xiao et al. (2014). The correlation of the Siberia stratigraphic scheme is based on Khudoley et al. (2007). Abbreviations: CC, Changcheng System; HT, Hutuo Group; JX, Jixian System; LN, Liaonan System; V, Vendian. →



6.3 Stromatolites—current understanding on the diversity and secular changes of their microstructures

Stromatolite is probably the most abundant and intensively-studied type of Precambrian carbonate microbialite. The term “Stromatolith” was first coined by Kalkowsky (1908), emphasizing the laminated and biogenic nature of these rocks. Thereafter, many modifications were proposed for the definition (reviewed in Rinding 2011). Now the most commonly adopted version is “laminated benthic microbial deposits” (Riding 1991) (e.g. Rinding 2011; Chen et al. 2014). However, conventionally, stromatolites are expected to be a structure which can be differentiated from those flat, 2-D extending microbial laminates. In this regard, the morphological definition from Semikhatov et al. (1979) has its advantage, it says: “stromatolites are laminated, lithified, sedimentary growth structures that accrete away from a point or limited surface of attachment”. This definition was also preferred by some researchers (e.g. Grotzinger and Knoll 1999). The stromatolites discussed in this chapter are regarded as the intersection of the two definitions, although because of the scope of this dissertation, detailed arguments cannot be provided for the biological origin of each of them.

Stromatolites were first recorded in Archean cherts (e.g. Walter 1980). Carbonate stromatolites greatly developed and diversified from the Mesoproterozoic to the Early Neoproterozoic, and then declined in both abundance and diversity during the Middle to Late Neoproterozoic (Fig. 6.1 and references therein). This “evolutionary pattern”, i.e. diversification and decline, was concluded with two uncertain factors: the quality of the taxonomic work and the reliability of the chronological data (cf. Walter and Heys 1985; Awramik and Sprinkle; Cao and Yuan 2006). Stromatolite “taxonomy” is purely based on morphological characters. This is linked with a debate: what sense can we make out of the secular changes of stromatolite morphology? It is still uncertain, to which extent the biological or environmental factors have affected the morphology of ancient stromatolites.

Among stromatologists, there are two major schools of thought on this issue. One school believes that the macroscopic structures of stromatolites are more closely related to physical environment and the microscopic structures are more determined by biological factors (e.g. Semikhatov 1976; Semikhatov and Raaben 2000). While the other school argues that all the morphological variations of stromatolites

are ultimately determined by environments (e.g. Grotzinger and Knoll 1999). Based on the recent discoveries that sponges can construct buildups similar to stromatolites (Chapter 4), the opinion of the former academic school is preferred here.

However, to study stromatolite microstructure is difficult, because diagenesis can alter the micro- and even mesostructures of microbialites and produce various derivative morphological structures from a single precursor (Knoll and Semikhatov 1998; Turner et al. 2000). A careful investigation on relatively well preserved samples should be possible to extract useful biological information, but this work seems still in its infancy. Even a set of consistent morphological classification and descriptive terminology has not yet been established for stromatolite microstructures. Authors defined their own usage of terms about microstructures by attaching relevant figure plates in their monographs, (e.g. Walter 1972; Raaben et al. 2001; Cao and Yuan 2006). Polysemy and tautonymy are therefore considerably common. Grey (1989) has made a collection of the most popular terms without giving any discussion and comparison. In this list, the large dataset published in Russian was still not included.

In this situation, a few veteran workers have figured out several secular evolutionary patterns of stromatolite microstructures based on their own knowledge, experience, and research focuses (Fig. 6.1). Riding (2008) concluded that the dominance of sparry and hybrid fabrics in Archean and Mesoproterozoic stromatolites was replaced by fine-grained fabrics in the Neoproterozoic, probably because of the decreasing carbonate concentration in sea water.

Bertrand-Sarfati (1976) classified microstructures into “simple microstructures” and “complex microstructures” and suggested that some of them distributed in restricted geological time intervals (Fig. 6.1). For example, the “vermiform microstructures” were found only in Vendian and Cambrian stromatolites, and “catagraphs” were thought dominant in some Vendian forms. However, the usage of these two terms was not consistent in different works. “Vermiform microstructure” was defined as a structure “in which narrow, sinuous, pale-coloured areas (usually of sparry carbonate) are surrounded by darker, usually fine grained areas (usually carbonate)” (brackets are original, Walter 1972, p. 14). It was initially applied to the microstructures in *Madiganites mawsoni*, which are compared to the

skeletal networks of keratose demosponges in this dissertation (4.5.1; chapter 5). Nonetheless, the other authors used this term to describe the probable degassing structures in *Acaciella angepena* (Preiss 1972, p. 73) or the gypsum pseudomorphs in *Baikalia baikalica* (Cao and Yuan 2006, p. 264). In addition, Walter (1972, p. 160) mentioned that “vermiform microstructures” are similar to “*Girvanella* but lack the microgranular boundaries of that form”, indicating that this microstructure may also be easily confused with filamentous structures of cyanobacterial or algal origin.

Similarly confusing definition and usage also happened to the term “catagraph”. This is a type of “microphytolite” (cf. Swett and Knoll 1985) introduced by Russian scientists and used for stratigraphic correlations. But the size, shape and origin of “catagraphs” were described quite differently in previous literature (e.g. see the definitions or descriptions in Trompette 1982; Knoll 1985; Kuznetsov and Suchy 1992). According to Bertrand-Sarfati (1976, p. 256–258), catagraphs are “quite regular spheroids with a dark envelope and clear calcite infilling”, which can occur periodically in microbial mats or in the sediments between the stromatolite columns. Although some kind of oncoids, cortoids or fragments of *Renalcis*-type calcimicrobes fit this description, Bertrand-Sarfati (1976) compared “catagraphs” to calcified cells in modern microbial mats. Knoll et al. (1993) also figured out that the catagraph “species” *Vesicularites concretus* may contain calcified coccoid microbes.

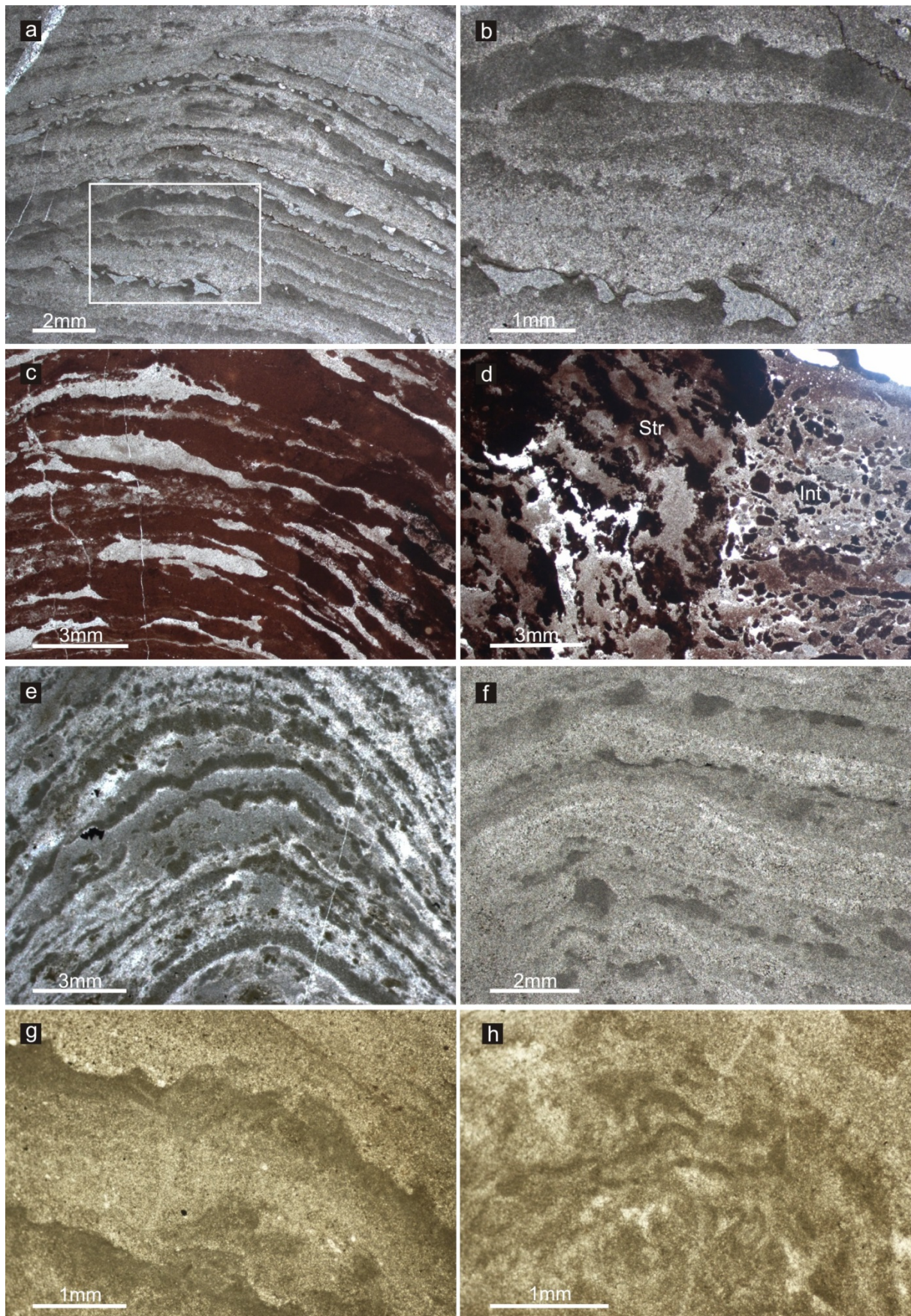
Another effort of studying Precambrian stromatolite microstructures was made by Cao (1992). He checked 235 pieces of Precambrian stromatolite thin sections in his collection, found 161 of them preserved “primary” structures, and then investigated the diversity and abundance of the microstructures in these better preserved samples (Fig. 6.1). However, in this study he adopted his own classification of microstructures (based on Tianjin Institute of Geology and Mineral Resources et al. 1979) and diagenesis was not comprehensively discussed. Although he emphasized the preliminary nature of this work, it was still suggested that the results indicate an increase of stromatolite microstructure diversity from the Paleoproterozoic to the Neoproterozoic and a decline of stromatolites after the Neoproterozoic glaciations.

Besides, stromatolite stratigraphers suggested that some stromatolite “taxa” are restricted to certain geological intervals (e.g. Preiss 1976), and it was estimated that up to 80–85% of stromatolite form-

species are established mainly based on microstructures (Semikhatov and Raaben 2000). However, the detailed information of these stromatolites is very difficult to access, because many of them were originally published in old Russian journals.

On this ground of immature precedent studies, I can only discuss a small part of the Precambrian microbialite microstructures based on the fossil materials accessible for me and interesting enough in the scope of this PhD study. In 6.4–6.5, a few Mesoproterozoic to Middle Neoproterozoic (Cryogenian) carbonate microbialites will be described. All the samples are from the collection of Prof. Dr. Joachim Reitner and are now deposited in the Department of Geobiology, Center of Geosciences of the University of Göttingen. The thin sections were investigated using a Zeiss SteREO Discovery.V8 microscope and photographed using the AxioCam MRc 5-megapixel camera combined with this microscope.

Fig. 6.2 **a–d** Stromatolites from the Jinshanzhai Formation, northern Anhui, China; **e–f** Stromatolites from the top of the Tieling Formation, Tianjin, China; **g–h** Stromatolites from the Juliqiao Formation, northern Anhui, China. **a–d** and **g–h** are of Tonian age (Xiao et al. 2014); **e–f** are of Middle Mesoproterozoic age (Gao et al. 2011). Abbreviations in **d**: Str, stromatolite; Int, inter-column sediments. →



6.4 Microstructures of Mesoproterozoic and Tonian stromatolites

The observed Mesoproterozoic and Tonian stromatolites are generally characterized by simple micritic to microsparic laminations. According to the terminology of Walter (1972, p. 12–14), part of the samples from the Jinshanzhai Formation (Fig. 6.2a–b) and the Jiuliqiao Formation (Fig. 6.2g) bare “streaky microstructure” (both formations are of Tonian age, Xiao et al. 2014), the other Jinshanzhai samples exhibit “banded microstructure” (e.g. Fig. 6.2c), while the Mesoproterozoic samples from the top of the Tieling Formation (c.a. 1400 Ma, Gao et al. 2011) show a mixture of “striated microstructure”, “banded microstructure” and “streaky microstructure” (Fig. 6.2e–f).

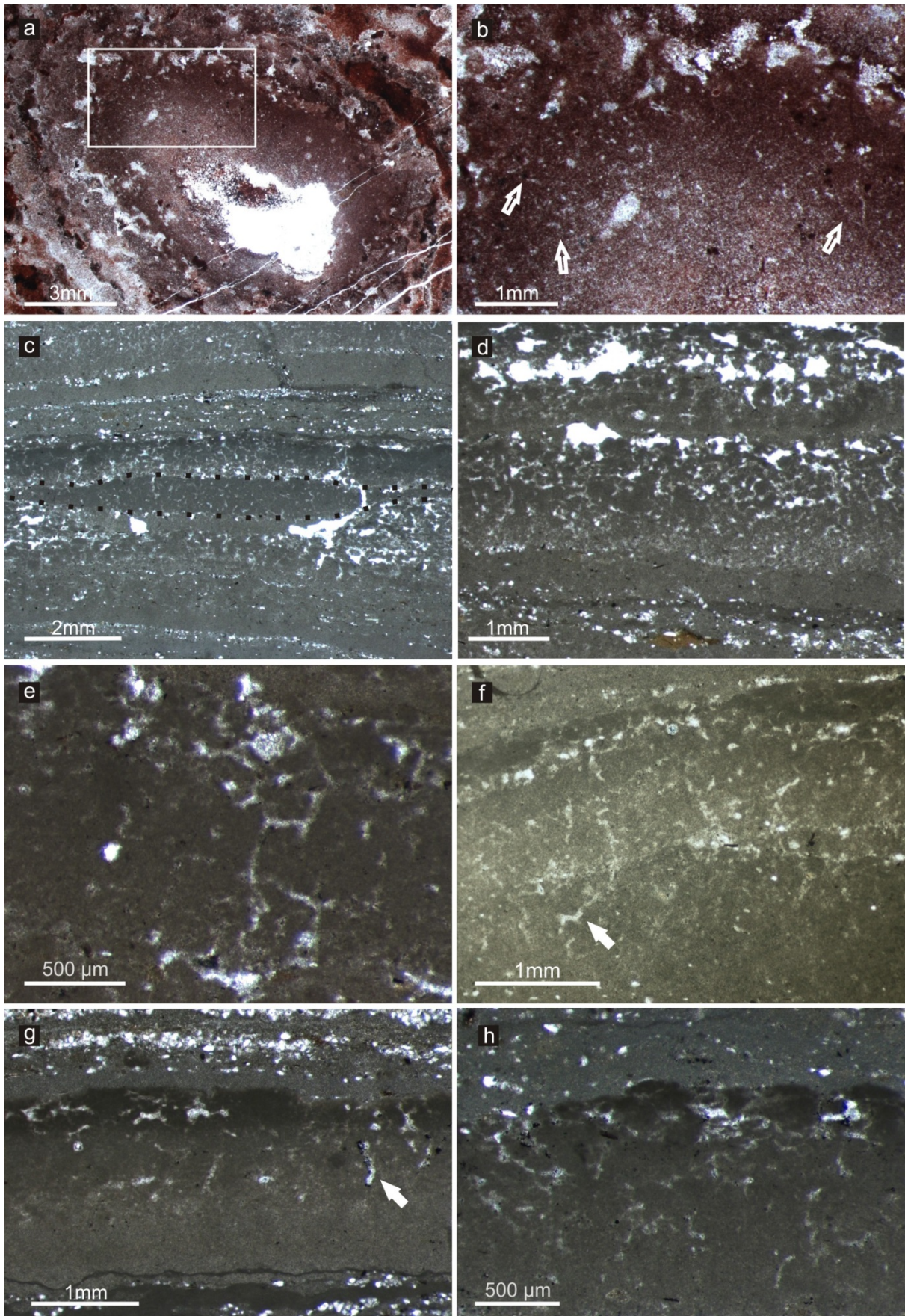
However, from a genetic point of view, the streaky microstructure (Fig. 6.2a–b, g), in which the micrites at the top of the lamination grade vertically into microspars at the bottom, is obviously a product of discrepant neomorphism. This can also be inferred from the obscured outline of the probable microbial mat remains in Fig. 6.2h. The banded microstructure (Fig. 6.2c), which is characterized by continuous laminae with abrupt boundaries, is probably formed due to post-lithification erosion on the micritic laminations. This erosion is very prominent on the margin of some stromatolite columns (Fig. 6.2d). The striated microstructure (Fig. 6.2e–f), in which laminae are composed of chains of lenses, is probably also a phase overprinted by diagenesis. Although these diagenetic phenomena are comparable to those observed and preliminarily analyzed in the stromatolite-like Carboniferous bioconstructions built by keratose sponges (4.4.2), the exact diagenetic mechanisms of these Precambrian stromatolites still deserve further exploration. A lot of questions can be raised. For example, in streaky microstructure, why were the surface layers of the microbial mats preserved differently from the lower part? In some of the Jinshanzhai samples (Fig. 6.2a–b), there are some microspar-cemented irregular clumps embedded beneath the surface of the micritic layers. Do these clumps represent previous voids in microbial mats? If yes, what is the function and origin of these voids? Beside of these laminated structures, some filaments are poorly preserved in some Jinshanzhai samples (Fig. 6.3a–b); these probably are remnants of filamentous cyanobacteria. How did they live and why were they still preserved in the strongly eroded and recrystallized carbonates? Do they indicate a type of microbial consortia different from the precursors of the structureless micritic laminae in the same sample?

Despite of these unresolved questions, these observed fossils fit the image of Mesoproterozoic to Early Neoproterozoic carbonate microbialites depicted by previous publications. That is, fine grained carbonate stromatolites became abundant (Riding 2008), but the identifiable fossils in them are mainly filamentous elements related to cyanobacteria (cf. Grotzinger and Knoll 1999), although coccoid forms can be preserved additionally in the silicified part of these stromatolites (e.g. Knoll et al. 2013).

However, beside of the structures shown above, some of the Early Neoproterozoic stromatolites have started to develop more complex features. The filamentous structures in the stromatolites (Vidal 1972) from the Visingsö Group of the Vättern Lake, Sweden (Upper Riphean, Vidal and Moczydlowska 1995; Samuelsson and Strauss 1999) are probably of other origin than to be cyanobacteria remains. These filaments form networks in some micritic layers or lenticular clumps (Fig. 6.3c, e), while cyanobacteria are not known to construct real networks. Most of these filaments have a consistent thickness of 30–40 μm and some of them show very regular margins (e.g. arrows in Fig. 6.3f–g). In worse preservation, the filaments-baring micritic fabric grade into peloidal fabrics (Fig. 6.3d). These features make them resemble the sponge skeletal networks described in earlier chapters. Nonetheless, in many situations, the Early Neoproterozoic filaments show a tendency of orienting vertically and connecting to irregular voids near to the surface of the micritic layer (Fig. 6f–h). They do not seem to have the function of support like sponge skeletons. Rather, they are more probable to be fluid-conducting canals within thick microbial mats. However, at least to my knowledge, canals with such grade of regularity and organization are not known from other microbial mats. Perhaps, they were produced by a complex microbial consortium with developed organization.

In spite of these filamentous structures, other observed unusual structures in Early Neoproterozoic stromatolites will be discussed in 6.5 as comparisons with the Cryogenian analogues.

Fig. 6.3 a–b Tonian stromatolites from the Jinshanzhai Formation, northern Anhui, China. **b** is magnified from the area in the rectangle in **a**. **c–h** Early Neoproterozoic (probably also Tonian) stromatolites from the Visingsö Group, Vättern Lake, Sweden. Hollow arrows: probable cyanobacterial filaments; Solid arrows: the smooth margin of the filamentous structures. →



6.5 Microbialites in Sturtian cap carbonates

6.5.1 Peloidal grainstone

“Peloid” is a descriptive term and can designate 30–100 μm sized, structureless carbonate grains formed by different mechanisms (cf. Flügel 2010). The peloids discussed in this section are regarded as *in situ* formed ones, because they occur in precipitated (instead of trapped or bound) microbial deposits, and do not show any allochthonous sedimentary structures.

Peloidal grainstone consisting of *in situ* formed peloids is not an innovation of Neoproterozoic carbonate microbialites; at least one example has been illustrated from the Mesoproterozoic Kyutingda Formation, Siberia (Knoll and Semikhatov 1998; Grotzinger and Knoll 1999). However, abundant occurrences of this fabric are known from Phanerozoic rocks (e.g. Riding and Tomás 2006; Spadafora et al. 2010; Matyszkiewicz et al. 2012). Especially interesting is that this peloidal fabric appears also frequently in fossilized sponges (e.g. Reitner 1993; Reitner et al. 1995b; Warnke and Meischner 1995) and mud mounds (e.g. Weller 1995; Rodríguez-Martínez et al. 2010).

In the Neoproterozoic, this fabric was found to occur massively in the cap carbonates after the Sturtian and Marinoan glaciations. In Namibia, these two glaciations are recorded by the Chuos and Chaub diamictites, respectively. Regularly round, almost isometric peloids are found in the Rasthof Formation, which directly overlies the Chuos diamictite (Hofmann 2002). These peloids are embedded in microsparic or sparic cements, distributing discretely or forming clusters (Fig. 6.4a–b). A previous measurement showed that carbonaceous components are still preserved in these globular peloids (Pruss et al. 2010). The lack of other allochthonous grains, the regular shape and distinct margin of the peloids and the carbonaceous remains together indicate that these structures are probably *in situ* permineralized microbes. In contrast, the peloidal fabrics in the shallow marine carbonates from the Namibian Keilberg Member (directly overlying the dunes equivalent to Chaub diamictite) (Fig. 6.4c–d) and the Noonday Dolomite in Death Valley (also post-Marinoan cap carbonate, Corsetti and Grotzinger 2005) show diffuse margins.

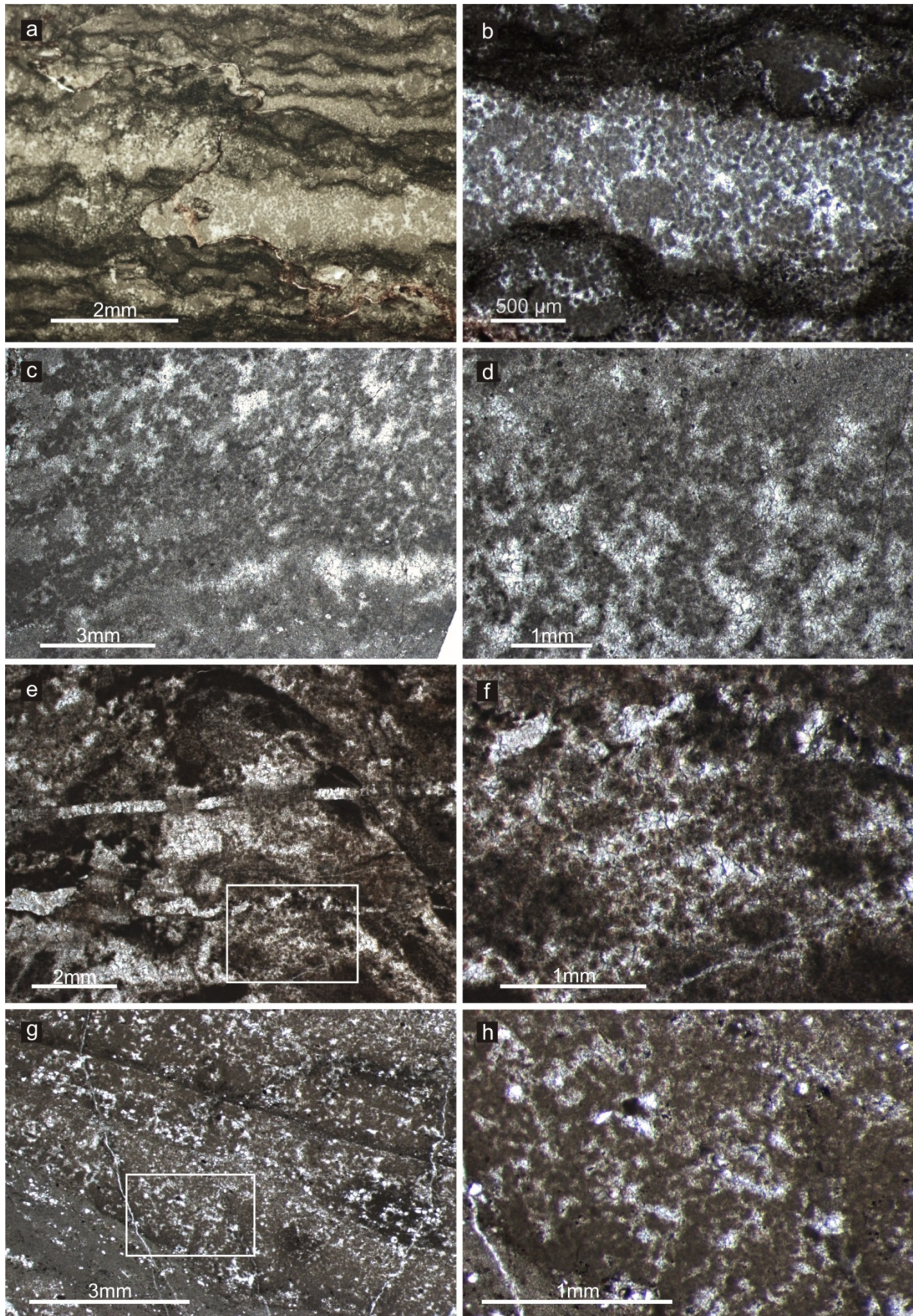
Diffuse margins are also a character of many Phanerozoic peloids. From modern marine cavities, the

in situ formation of two types of peloids has been investigated in detail. One type of peloids was observed in clumpy mucus substances, showing a core composed of micrites plus acidic organic matters and a rim of dentate Mg calcites. The other type was found in decaying sponge tissue and was devoid of the Mg calcite rims. Both types of peloids were suggested to be formed as a consequence of microbial degradation of organic matter (e.g. Reitner 1993; Reitner et al. 1995a). This process can create both initial crystal nucleation sites and sufficient alkalinity for carbonate minerals to grow. The peloids formed in this way have diffuse margins. However, diffuse margins can also indicate slower or incomplete calcification, i.e. deeper decomposition, of coccoidal microbes in early diagenesis (e.g. Adachi et al. 2004).

A comparable analogue to the Rasthof peloids is observed from a Riphean stromatolite from the Baikal Lake (Fig. 6.4e–f). Although detailed stratigraphic information of this specimen is lacking, it is very likely to be of Late Riphean age (Early to Middle Neoproterozoic) according to the peloidal fabric and the “chambered grains” which will be discussed in 6.5.2. These structures make this specimen distinctly different from older stromatolites (6.4). The Early Neoproterozoic stromatolites from the Visingsö Group, Sweden also exhibit peloidal grainstone fabrics in some parts, but these peloids appear to be more irregular (Fig. 6.4g–h). The microbial mats in the Sweden stromatolites are relatively thin and were strongly influenced by the deposition of quartz detritus. *In situ* peloid formation in these very shallow, strongly perturbed microbial mats indicates very high carbonate supersaturation in the water body at that time.

The investigation on *in situ* formed peloids is still far from its close. It still waits to answer why these structures were less common in earlier carbonate record.

Fig. 6.4 Peloidal grainstone from Neoproterozoic microbialites. **a–b** Cryogenian microbialites from the Rasthof Formation, Namibia; **c–d** Post-Marinoan Keilberg Member, Namibia; **e–f** (probably Late) Riphean stromatolite, Siberia; **g–h** stromatolites from the Visingsö Group, Sweden. Areas in rectangles in **e** and **a** are magnified in **f** and **h** respectively. →



6.5.2 Chambered structures

Recently, chambered structures were reported from Cryogenian interglacial carbonates from various localities in Namibia and Australia (Wallace et al. 2014). These structures are millimeter- to centimeter-scaled chambers separated by distinct micritic walls. The walls have smooth margins and are of consistent thickness (20–100 μm). They occur in relatively deep water and in protected spaces, such as cavities, Neptune dikes and inter-space of stromatolite columns. Basically because of the regularity of the walls, these structures were differentiated by the authors from many abiogenic and biogenic chambered structures. The analogues which survived the authors' criticisms include the enigmatic chambered structures *Bacinella* and *Lithocodium* in Late Jurassic to Early Cretaceous reefs, the Archean to Paleoproterozoic fenestrate microbialites and chambered reef-dwelling sponges (e.g. Sphinctozoa). Although the authors admitted that the sponge interpretation was hampered by the lack of pores—the basic structures allowing sponges to live a filter feeding life—in the Cryogenian fossils, they still argued that these chambers might represent a type of proto-sponge which lived on osmotrophy without active water circulation. The Archean and Proterozoic fenestrate microbialites were not preferred as the interpretation of these Cryogenian chambers because this "would require that fenestrate microbialites reappear and become widespread over 1 billion years later" (Wallace et al. 2014, p. 119).

However, according to the observation on our samples, the walls of the Cryogenian chambered structures seem to fit the microbial interpretation better. As described in Wallace et al. (2014, p.113–114), "where the walls are thin, they are generally homogeneous", "when the walls are thicker, they often display a laminated microstructure". In one of our samples, the laminations in the thicker walls seem able to be softly or flexibly peeled off (Fig. 6.5a, c). The wall itself is also not as smooth as expected. Likely due to soft deformation, the marginal laminae form small knolls (Fig. 6.5c). Furthermore, some thinner, single layered "walls" can show very irregular and intensive folds, indicating that they were soft before being lithified. In fact, this type of soft deformation was used by Sumner (1997, 2000) to argue that the "walls" in the Archean fenestrate microbialites originated from microbial mats. These structural characters are different from those of the skeletons of sphinctozoan sponges, which were compared by Wallace et al. (2014) with the chambered structures.

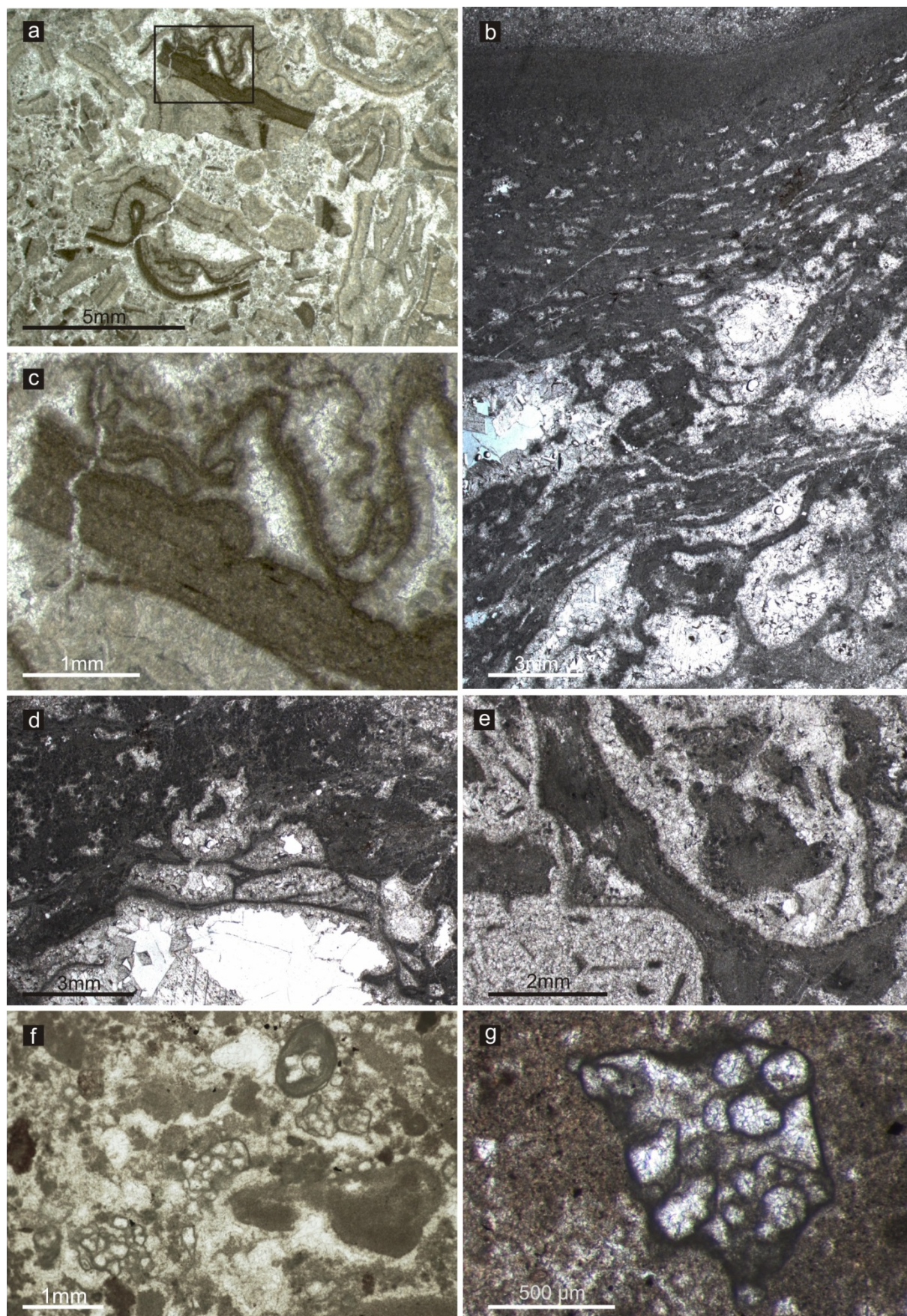


Fig. 6.5 Chambered structures and chambered grains from: the Cryogenian Rasthof Formation, Namibia (**a**, **c**); the Cryogenian Gruis Formation, Namibia (**b**, **d–e**); the (probably Late) Riphean stromatolite, Siberia (**f–g**). The area in the rectangle in **a** is magnified in **c**.

The Archean fenestrate microbialites are different from the Cryogenian chambered structures by showing “walls” of only 1–10 μm thick, much thinner than the Cryogenian analogues (Sumner 1997, 2000). For this reason, the Archean microbial constructors were expected to be as small as a few microns. If so, the thicker Cryogenian “walls” may reflect the participation of larger eukaryotic cells. The second difference is that the Archean microbialites are predominantly composed of lithified thin microbial films and cemented voids (e.g. Hofmann and Masson 1994; Sumner 1997, 2000), while the Cryogenian chambered structures can be closely interweaved with micritic matrix which probably represents thick microbial mats. Compared with examples illustrated by Wallace et al. (2014, e.g. Fig. 7C), our samples from the Gruis Formation, Namibia are more explicitly showing this feature (Fig. 6.5b, d). The Gruis Formation is the rock unit immediately overlying the Rasthof Formation and laterally correlative with the Gauss Formation where part of the samples published in Wallace et al. (2014) was collected (Hofmann 2002). The “walls” in the Gruis samples were not so well preserved as the published ones, but they show the feature of facing to the voids on one side and closely attaching on microbial mat on the other side (e.g. Fig. 6.5e). To some extent, this does resemble the choanoderm of sponges, which locates on the interface between fluid and the symbiont-rich mesohyl and controls the material exchange between them.

Although current evidences do not support a direct correlation between these chambered structures and sponges, these fossils may still well represent a complex eukaryotes-prokaryotes consortium. The occurrences of similar chambered structures in the Archean–Paleoproterozoic, Middle Neoproterozoic and Jurassic–Cretaceous ages can simply be biological responses to the same environmental factor(s) or ecological opportunity, although what the factor(s) exactly is(are) has hitherto been figured out for none of the three occurrences. Convergent evolution is not a rare phenomenon even in more developed life forms.

These chambered structures are probably not unprecedented in the Neoproterozoic. Similar structures were described as “cellular crusts” from the Little Dal Group (Turner et al. 1993). This rock unit was considered as pre-glaciation deposits (Narbonne and Aitken 1995). The fossils were observed crusting on thin micritic laminae, forming parallel but discontinuous layers (compare Fig. 4 in Turner et al.

1993 and Fig. 11D in Wallace et al. 2014). Chambers in these crusts are 30–250 μm in dimension, outlined by micritic walls. They were suggested by the authors as the calcified thallus of metaphytes. Other fossils which may be related to the Namibian and Australian chambered structures are some allochthonous grains in the Riphean stromatolite from Baikal Lake, which show chambered inner structures (Fig. 6.5f–g). The grains vary in size, shape and the number of constituent chambers, but show consistent single-layered walls of around 20 μm thick. The walls are composed of micrites and the chambers are cemented by microspars. Similar grains were also described as a type of “microphytolite” from the Late Riphean Draken Formation, Svalbard (Swett and Knoll 1985). But the chambers in these fossils seem to be partly or completely filled by micrites.

6.6 Conclusion

Microstructures of carbonate microbialites can provide important information about the biology of ancient microbial mats. However, the previous understandings on microbialite microstructures were confused by complex diagenetic overprints and ambiguously defined terminologies. The work to disassemble diagenetic overprints from recorded biological information is still in its beginning. The large dataset accumulated in the previous researches should be valuable for further work if it becomes more readily accessible.

The widely accepted overall developmental trend of Precambrian carbonate microbialites is that the predominance of inorganically precipitated sparry fabric being overtaken by microbially induced, fine grained carbonate precipitation. The literature and fossils seen so far do not contradict this pattern. Compared with the Neoproterozoic examples, the observed Mesoproterozoic carbonate stromatolites either are dominated by structureless micritic or microsparic layers, or show only simple filamentous structures of probable cyanobacterial origin. Also congruent with the previously proposed picture is that stromatolites seem to have decreased after the Neoproterozoic glaciations. According to the mentioned Precambrian microbialites in 6.4 and 6.5 (rock specimens plus literature), well laminated structures became less common in the Neoproterozoic examples (e.g. the stromatolites from Svalbard and Baikal Lake, as well as the microbialites from the Little Dal group). The Cryogenian ones are all

non-stromatolite microbialites except the Noonday Dolomite.

Complex and enigmatic microstructures commenced to be present in the Neoproterozoic. Preliminarily described here are four examples: 1) the organized “fluid canals” in the Early Neoproterozoic Visingsö Group; 2) the very regular peloids (probably lithified microbes) in the Cryogenian Rasthof Formation, Namibia and the (probably Late) Riphean stromatolite, as well as the less regular peloidal fabrics in the post-Marinoan microbialites and the Visingsö stromatolites; 3) chambered structures from the Cryogenian Rasthof and Gruis Formations, Namibia, which probably have an analogue in the older pre-glaciation Little Dal Group; 4) the chambered grains in the Late Riphean stromatolites. All these preserved fossil structures are showing a higher degree of complexity than the simple aggregates of coccoid and filamentous microbe fossils known from older microbialites. This is congruent with the background of eukaryote evolution at that time (1.2).

Reconstructing the “fluid canals” and the chambered structures in 3-D may be the next work in the future. To investigate their spatial organization in the ancient microbial mats will help to understand their function. For the chambered structures and the related grains, it requires further work to figure out whether they are biologically associated with each other and whether they are related to primitive animals. Detailed analyses on the structures and possible diagenetic history of the “walls” may help to obtain useful information.

References

- Adachi N, Ezaki Y, Liu J (2004) The fabrics and origins of peloids immediately after the end-Permian extinction, Guizhou Province, South China. *Sedimentary Geology* 164(1–2):161–178
- Aitken JD (1967) Classification and environmental significance of cryptalgal limestones and dolomites, with illustrations from the Cambrian and Ordovician of southwestern Alberta. *Journal of Sedimentary Petrology* 37 (4):1163–1178
- Aitken JD (1989) Giant "algal" reefs, Middle/Upper Proterozoic Little Dal Group (>770,<1200 Ma), Mackenzie Mountains, N.W.T., Canada. In: Geldsetzer HHJ, James NP, Tebbutt GE (eds) *Reefs, Canada and adjacent areas*. Canadian Society of Petroleum Geologists Memoir, vol 13. pp 13–23
- Aitken JD, Narbonne GM (1989) Two occurrences of Precambrian thrombolites from the Mackenzie Mountains, northwestern Canada. *Palaos* 4 (4):384–388
- Awramik SM, Sprinkle J (1999) Proterozoic stromatolites: The first marine evolutionary biota. *Historical Biology* 13 (4):241–253
- Batten KL, Narbonne GM, James NP (2004) Paleoenvironments and growth of early Neoproterozoic calcimicrobial reefs: platformal Little Dal Group, northwestern Canada. *Precambrian Research* 133 (3–4):249–269
- Bernhard JM, Edgcomb VP, Visscher PT, McIntyre-Wressnig A, Summons RE, Boussein ML, Louis L, Jeglinski M (2013) Insights into foraminiferal influences on microfabrics of microbialites at Highborne Cay, Bahamas. *Proceedings of the National Academy of Sciences* 110 (24):9830–9834
- Bertrand-Sarfati J (1976) An attempt to classify Late Precambrian stromatolite microstructures. In: Walter MR (ed) *Developments in Sedimentology*, vol 20. Elsevier, pp 251–259
- Braga JC, Martin JM, Riding R (1995) Controls on microbial dome fabric development along a carbonate-siliciclastic shelf-basin transect, Miocene, SE Spain. *Palaos* 10 (4):347–361
- Burne RV, Moore LS (1987) Microbialites; organosedimentary deposits of benthic microbial communities. *Palaos* 2 (3):241–254
- Cao R (1992) A preliminary study on microstructure of the Precambrian stromatolites. In: Lan S (ed) *Stromatolites and related mineral resources in the Late Precambrian*. Northwest University Press, Xi'an, pp 1–7
- Cao R-J, Yuan X-L (2006) *Stromatolites*. Press of University of Science and Technology of China, Hefei, China, 383 pp
- Castro-Contreras SI, Gingras MK, Pecoits E, Aubet NR, Petrash, D, Castro-Contreras SM, Dick G, Planavsky N, Konhauser KO (2014) Textural and geochemical features of freshwater microbialites from Laguna Bacalar, Quintana Roo, Mexico. *Palaos* 29 (5):192–209
- Chen J-T, Lee J-H (2014) Current progress on the geological record of microbialites and microbial carbonates. *Acta Geologica Sinica (English Edition)* 88 (1):260–275
- Corsetti FA, Grotzinger JP (2005) Origin and Significance of Tube Structures in Neoproterozoic Post-glacial Cap Carbonates: Example from Noonday Dolomite, Death Valley, United States. *Palaos* 20 (4):348–362
- Du L, Yang C, Guo J, Wang W, Ren L, Wan Y, Geng Y (2010) The age of the base of the paleoproterozoic Hutuo Group in the Wutai Mountains area, North China Craton: SHRIMP zircon U-Pb dating of basaltic

- andesite. *Chinese Science Bulletin* 55 (17):1782–1789
- Feldmann M, McKenzie JA (1998) Stromatolite-thrombolite associations in a modern environment, Lee Stocking Island, Bahamas. *Palaios* 13 (2):201–212
- Flügel E (2010) Microfacies Data: Matrix and Grains. In: *Microfacies of Carbonate Rocks*. Springer Berlin Heidelberg, pp 73–176
- Gao L, Liu P, Yin C, Zhang C, Ding X, Liu Y, Song B (2011) Detrital Zircon Dating of Meso- and Neoproterozoic Rocks in North China and Its Implications. *Acta Geologica Sinica - English Edition* 85 (2):271–282
- Grey K (1989) Handbook for the study of stromatolites and associated structures. In: Kennard JM, Burne R (eds) *Stromatolite Newsletter* 14. The Bureau of Mineral Resources, Geology and Geophysics, Canberra, Australia, pp 82–171
- Grotzinger J, Adams EW, Schröder S (2005) Microbial–metazoan reefs of the terminal Proterozoic Nama Group (c. 550–543 Ma), Namibia. *Geological Magazine* 142 (05):499–517
- Grotzinger JP, Knoll AH (1999) Stromatolites In Precambrian carbonates: Evolutionary mileposts or environmental dipsticks? *Annual Review of Earth and Planetary Sciences* 27 (1):313–358
- Grotzinger JP, Watters WA, Knoll AH (2000) Calcified metazoans in thrombolite-stromatolite reefs of the terminal Proterozoic Nama Group, Namibia. *Paleobiology* 26 (3):334–359
- Harwood CL, Sumner DY (2011) Microbialites of the Neoproterozoic Beck Spring Dolomite, Southern California. *Sedimentology* 58 (6):1648–1673
- Hofmann HJ, Masson M (1994) Archean stromatolites from Abitibi greenstone belt, Quebec, Canada. *Geological Society of America Bulletin* 106 (3):424–429
- Hoffman PF (2002) Carbonates bounding glacial deposits: Evidence for Snowball Earth episodes and greenhouse aftermaths in the Neoproterozoic Otavi Group of northern Namibia. *Excursion Guide*, 16th International Sedimentological Conference. Auckland Park, South Africa. 39 p
- Kah LC, Grotzinger JP (1992) Early Proterozoic (1.9 Ga) thrombolites of the Rocknest Formation, Northwest Territories. *Palaios* 7:305–315
- Kalkowsky E (1908) Oolith und Stromatolith in norddeutschen Buntsandstein. *Zeitschrift der Deutschen Gesellschaft für Geowissenschaften* 60:68–25
- Kennard JM, James NP (1986) Thrombolites and stromatolites: Two distinct types of microbial structures. *Palaios* 1 (5):492–503
- Khudoley AK, Kropachev AP, Tkachenko VI, Rublev AG, Sergeev SA, Matukov DI, Lyahnitskaya OY (2007) Mesoproterozoic to Neoproterozoic evolution of the Siberian Craton and adjacent microcontinents: An overview with constraints for a Laurentian connection. In: Link PK, Lewis RS (eds) *Proterozoic Geology of Western North America and Siberia*. SEPM Special Publication, vol 86. SEPM (Society of Sedimentary Geology), pp 209–226
- Knoll AH (1985) The distribution and evolution of microbial life in the Late Proterozoic Era. *Annual Reviews in Microbiology* 39 (1):391–417
- Knoll AH, Fairchild IJ, Swett K (1993) Calcified microbes in Neoproterozoic carbonates; implications for our understanding of the Proterozoic/Cambrian transition. *Palaios* 8 (6):512–525

- Knoll AH, Semikhatov MA (1998) The genesis and time distribution of two distinctive Proterozoic stromatolite microstructures. *Palaios* 13 (5):408–422
- Knoll AH, Wörndle S, Kah LC (2013) Covariance of microfossil assemblages and microbialite textures across an Upper Mesoproterozoic carbonate platform. *Palaios* 28 (7):453–470
- Kuznetsov VG, Suchy V (1992) Vendian-Cambrian tidal and sabkha facies of the Siberian Platform. *Facies* 27 (1):285–293
- Lee J-H, Chen J-T, Choh S-J, Lee D-J, Han Z-Z, Chough SK (2014) Furongian (Late Cambrian) sponge–microbial maze-like reefs in the North China Platform. *Palaios* 29:27–37
- Matyszkiewicz J, Kochman A, Duś A (2012) Influence of local sedimentary conditions on development of microbialites in the Oxfordian carbonate buildups from the southern part of the Kraków–Częstochowa Upland (South Poland). *Sedimentary Geology* 263–264 (0):109–132
- Narbonne GM, Aitken JD (1995) Neoproterozoic of the Mackenzie Mountains, northwestern Canada. *Precambrian Research* 73 (1–4):101–121
- Oliver LK, Rowland SM (2002) Microbialite reefs at the close of the Proterozoic Eon: the middle member Deep Spring Formation at Mt. Dunfee, Nevada. In: Corsetti FA (ed) *Proterozoic-Cambrian of the Great Basin and Beyond*. Pacific Section, vol 93. SEPM (Society for Sedimentary Geology), Fullerton, California, pp 97–122
- Preiss WV (1972) The systematics of South Australian Precambrian and Cambrian stromatolites. Part 1. *Transactions of the Royal Society of South Australia* 96 (Part 2):67–100
- Preiss WV (1976) International correlations. In: Walter MR (ed) *Stromatolites. Developments in Sedimentology*, vol 20. Elsevier, Amsterdam, Oxford, New York, pp 359–370
- Pruss SB, Bosak T, Macdonald FA, McLane M, Hoffman PF (2010) Microbial facies in a Sturtian cap carbonate, the Rasthof Formation, Otavi Group, northern Namibia. *Precambrian Research* 181 (1–4):187–198
- Raaben ME, Sinha AK, Sharma M (2001) *Precambrian stromatolites of India and Russia*. Birbal Sahni Institute of Palaeobotany, Lucknow, 125 pp
- Reitner J (1993) Modern cryptic microbialite/metazoan facies from Lizard Island (Great Barrier Reef, Australia) formation and concepts. *Facies* 29 (1):3–39
- Reitner J, Gautret P, Marin F, Neuweiler F (1995a) Automicrites in a modern marine microbialite: Formation model via organic matrices (Lizard Island, Great Barrier Reef, Australia). *Bulletin de l'Institut océanographique, Monaco* 14(2): 237–303
- Reitner J, Neuweiler F, Gautret P (1995b) Modern and fossil automicrites: Implications for mud mound genesis. *Facies* 32:4–17
- Tianjin Institute of Geology and Mineral Resources, Nanjing Institute of Geology and Palaeontology, The Inner Mongolia Autonomous Region Bureau of Geology and Mineral Resources Exploration (1979) *Researches on the Sinian stromatolites in Jixian*. Geological Publishing House, Beijing 94 pp
- Riding R (1991) Classification of microbial carbonates. In: Riding R (ed) *Calcareous Algae and Stromatolites*. Springer Berlin Heidelberg, pp 21–51
- Riding R (2000) Microbial carbonates: the geological record of calcified bacterial–algal mats and biofilms. *Sedimentology* 47:179–214

- Riding R (2008) Abiogenic, microbial and hybrid authigenic carbonate crusts: components of Precambrian stromatolites. *Geologia Croatica* 61 (2–3):73–103
- Riding R (2011) Microbialites, stromatolites, and thrombolites. In: Reitner J, Thiel V (eds) *Encyclopedia of Geobiology*. Springer, Dordrecht, pp 635–654
- Riding R, Tomás S (2006) Stromatolite reef crusts, Early Cretaceous, Spain: bacterial origin of in situ-precipitated peloid microspar? *Sedimentology* 53 (1):23–34
- Rodríguez-Martínez M, Reitner J, Mas R (2010) Micro-framework reconstruction from peloidal-dominated mud mounds (Viséan, SW Spain). *Facies* 56 (1):139–156
- Samuelsson J, Strauss H (1999) Stable carbon and oxygen isotope geochemistry of the upper Visingsö Group (Early Neoproterozoic), southern Sweden. *Geological Magazine* 136 (01):63–73
- Semikhatov MA (1976) Experience in stromatolite studies in the USSR. In: Walter MR (ed) *Stromatolites: developments in sedimentology*, 20. Elsevier, Amsterdam, pp 337–358
- Semikhatov MA, Gebelein CD, Cloud P, Awramik SM, Benmore WC (1979) Stromatolite morphogenesis—progress and problems. *Canadian Journal of Earth Sciences* 16 (5):992–1015
- Semikhatov MA, Raaben ME (1996) Dynamics of the global diversity of Proterozoic stromatolites. Article II: Africa, Australia, North America, and general synthesis. *Stratigraphy and Geological Correlation* 4:24–50
- Semikhatov MA, Raaben ME (2000) Proterozoic stromatolite taxonomy and biostratigraphy. In: Riding R, Awramik SM (eds) *Microbial Sediments*. Springer-Verlag, Heidelberg, pp 295–306
- Shapiro RS (2000) A comment on the systematic confusion of thrombolites. *Palaio* 15:166–169
- Shapiro RS (2004) Neoproterozoic–Cambrian microbialite record. In: Lipps JH, Waggoner BM (eds) *Neoproterozoic–Cambrian biological revolutions*, vol 10. The paleontological society papers. pp 5–15
- Shapiro RS, Awramik SM (2000) Microbialite morphostratigraphy as a tool for correlating Late Cambrian–Early Ordovician sequences. *The Journal of Geology* 108:171–180
- Shi X, Zhang C, Jiang G, Liu J, Wang Y, Liu D (2008) Microbial mats in the Mesoproterozoic carbonates of the North China Platform and their potential for hydrocarbon generation. *Journal of China University of Geosciences* 19 (5):549–566
- Spadafora A, Perri E, McKenzie JA, Vasconcelos C (2010) Microbial biomineralization processes forming modern Ca:Mg carbonate stromatolites. *Sedimentology* 57 (1):27–40
- Sumner DY (1997) Late Archean calcite-microbe interactions: Two morphologically distinct microbial communities that affected calcite nucleation differently. *Palaio* 12 (4):302–318
- Sumner DY (2000) Microbial vs environmental influences on the morphology of Late Archean fenestrate microbialites. In: Riding R, Awramik S (eds) *Microbial Sediments*. Springer Berlin Heidelberg, pp 307–314
- Swett K, Knoll AH (1985) Stromatolitic bioherms and microphytolites from the late proterozoic Draken Conglomerate Formation, Spitsbergen. *Precambrian Research* 28 (3–4):327–347
- Tang D, Shi X, Jiang G (2013) Mesoproterozoic biogenic thrombolites from the North China platform. *International Journal of Earth Sciences* 102 (2):401–413

- Trompette R (1982) Upper Proterozoic (1800–570 Ma) stratigraphy: A survey of lithostratigraphic, paleontological, radiochronological and magnetic correlations. *Precambrian Research* 18 (1–2):27–52
- Turner EC, James NP, Narbonne GM (2000) Taphonomic control on microstructure in Early Neoproterozoic reefal stromatolites and thrombolites. *Palaaios* 15 (2):87–111
- Turner EC, Narbonne GM, James NP (1993) Neoproterozoic reef microstructures from the Little Dal Group, northwestern Canada. *Geology* 21 (3):259–262
- Vidal G (1972) Algal stromatolites from the Late Precambrian of Sweden. *Lethaia* 5 (4):353–367
- Vidal G, Moczydłowska M (1995) The Neoproterozoic of Baltica—stratigraphy, palaeobiology and general geological evolution. *Precambrian Research* 73 (1–4):197–216
- Wallace MW, Hood AvS, Woon EMS, Hoffmann K-H, Reed CP (2014) Enigmatic chambered structures in Cryogenian reefs: The oldest sponge-grade organisms? *Precambrian Research* 255, Part 1 (0):109–123
- Walter MR (1972) Stromatolites and the biostratigraphy of the Australian Precambrian and Cambrian. *Special Papers in Palaeontology*, vol 11. The palaeontological association, London, 256 pp
- Walter MR, Buick R, Dunlop JSR (1980) Stromatolites 3,400–3,500 Myr old from the North Pole area, Western Australia. *Nature* 284 (5755):443–445
- Walter MR, Heys GR (1985) Links between the rise of the metazoa and the decline of stromatolites. *Precambrian Research* 29 (1–3):149–174
- Warnke K, Meischner D (1995) Origin and depositional environment of Lower Carboniferous mud mounds of Northwestern Ireland. *Facies* 32:36–42
- Weller H (1995) The Devonian mud mound of Rübeland in the Harz Mountains/Germany. *Facies* 32:43–49
- Xiao S, Shen B, Tang Q, Kaufman AJ, Yuan X, Li J, Qian M (2014) Biostratigraphic and chemostratigraphic constraints on the age of early Neoproterozoic carbonate successions in North China. *Precambrian Research* 246 (0):208–225

- Chapter 7 -

Summary

This PhD study was aimed to explore how to identify the earliest animals in the fossil record. The first encountered question was: how was the earliest animal like?

Modern biological studies have revealed that some unicellular eukaryotic relatives of animals have complex life cycles in which temporary multicellularity is achieved. Based on this fact, some biologists inferred that the metazoan lineage derived from the prolongation and further development of the multicellular stage of a unicellular eukaryotic ancestor (Mikhailov et al. 2009). According to the observed differences between animals and their complex unicellular relatives, the first animal was depicted as “a multicellular bacterivore with an epithelial layer composed, at least in part of unflagellated collar cells...its developing embryos underwent some form of gastrulation or other type of invagination, it was capable of cell differentiation...via specialized stem cells, and it could trigger its constituent cells to undergo apoptosis” (Richter and King 2013, p. 516). In addition to these images, it is also reasonable to expect that the earliest animals had intensive interaction and association with microbes, because they rose from a world dominated by microbes and microbes are known playing important roles in the reproduction, development and metabolism of modern animals (McFall-Ngai et al. 2013).

Based on molecular phylogenetic studies, sponges are widely accepted as the most basic animals known so far. Compared with the features of ctenophores, the other candidate of “the most basic animal”, the poriferan body plan, life cycle, life style and intensive symbiosis with prokaryotes match

the depictions of ancestral animals better (or *vice versa*, people were enlightened by sponges). Adult sponges are sessile filter feeders with developed aquiferous systems. Their bodies are basically composed of a dermal layer, which consists of various dermal types such as exopinacoderm, endopinacoderm and choanoderm, and a bacteria-rich mesohyl (Boury-Esnault and Rützler 1997). Major physiological activities are accomplished in the mesohyl under the cooperation between sponge cells and microbial symbionts (Taylor et al. 2007). It's just like what Reitner and Wörheide (2002, p. 53) once hypothesized: "sponges are highly developed biofilms with a close relationship to choanoflagellate eukaryotic cells" (see also the model in Abb. 1, Reitner 1998).

All these concepts indicate that 1) sponges are probably the most suitable model which can be used to study the common ancestor of animals and 2) in spite of readily recognizable animal fossils, special attention should also be paid to the fossilized microbial bioconstructions. Therefore, the doctoral work was further focused on two questions:

- 1) How could the earliest sponges be preserved in the fossil record?
- 2) Can we find structures comparable to sponge fossils in the Precambrian microbialites?

The earliest sponges were probably not capable of biomineralization (Wood 2011). Partly because most previous paleontological studies of sponges focused on the remains of their mineral skeletons, the earliest reliable fossil record of sponges acknowledged so far is some spicules from the Early Cambrian allochthonous deposits (e.g. Reitner et al. 2012; Antcliffe et al. 2014). This record is around 250 Ma delayed than the time of sponge origin predicted by molecular clocks and indicated by the Precambrian fossil record of other animals. In this study, the non-spicular demosponges (Keratosa +

Myxospongida, *sensu* Minchin 1900), which diverged from their spicular relatives at the early evolutionary stage of demosponges (e.g. Wörheide et al. 2012), were taken as a model for studying the ancestral non-biomineralized sponges.

One keratose fossil taxon, the family Vauxiidae Walcott, 1920, has already been described from the Middle Cambrian Burgess Shale before. But the preservation of sponge soft tissue in siliciclastic facies requires special taphonomical windows, which do not distribute pervasively in the geological record. In contrast, carbonate taphonomical windows are more popular. Phanerozoic fossils and modern observations both show that spicular sponges can be nearly completely preserved *in situ* if micritic precipitation was rapidly generated in the decaying soft tissue. The resulted micritic or peloidal matrix moulds spicules or skeletal frameworks before the silica being replaced by carbonate microspar. In addition, a large proportion of Precambrian microbialites are carbonates. For these reasons, biogenic and organogenic carbonates seem to be better materials for looking for fossils of non-biomineralized sponges and the Precambrian basic animals.

In this study, keratose sponge fossils were identified from carbonate facies for the first time from Anisian microbialites and Middle Devonian bioherms. They were preserved in the same way as the other spicular sponges, only that their skeletons are anastomosing filamentous networks instead of spicules. The architecture of the skeletal networks was further confirmed by a 3-D reconstruction. On this basis, more fossils of this type were recognized in carbonate rocks through the whole Phanerozoic, from the Tommotian to the Middle Eocene.

Some criteria were established during this study to distinguish the proposed keratose sponge fossils from other filamentous fossils such as cyanobacteria and fungi:

- 1) All fossils are preserved as microspar-cemented filamentous networks embedded in

aggregations of homogeneous automicrites, or peloidal fabrics in worse preservation.

2) The filaments branch and connect to each other, forming an anastomosing network which fills up the micritic aggregation with a more or less consistent density but never extend beyond the aggregation. In many cases, the filaments can form a clear ring-like structure parallel and near to the margin of the micritic clump.

3) The filaments are not associated with spicules, sheaths, spores or sporocarps, which may lead to other interpretations.

These criteria appeared to be helpful to identify keratose sponge fossils in the Phanerozoic carbonates. But for the other non-biomineralized demosponges, i.e. the non-skeletal myxospongiids, criteria have not been established, because up to now only few plausible examples of them have been observed. The investigated Phanerozoic keratose sponge fossils show a certain level of diversity by exhibiting hierarchical or non-hierarchical skeletons, different filament sizes and various ecological behaviours. Detailed taxonomic work is to be made in the future.

Besides, an interesting ecological behavior of Phanerozoic keratose sponges was discovered in this study. These sponges built stromatolite-like bioconstructions with the participation of microbes. The studied examples are the Visean “organ-pipe stromatolites” and the stromatolite crusts of the Ladinian *Placunopsis* bioherms. The accretion of these stromatolite-like buildups involves rapid lithification of sponge carcasses, alternated periods of sediment deposition and removing, and encrustation of the new sponge generations. This discovery mirrors the work of Lee et al. (2014), which reported that some Cambrian keratose sponges (diagnosed as “siliceous sponges” in the original paper) constructed thrombolite-like bioherms with calcimicrobes.

These new discoveries about Phanerozoic keratose sponges may benefit our search for ancestral animals in the Precambrian carbonate microbialites.

Corresponding to the second question “can we find structures comparable to sponge fossils in the Precambrian microbialites”, a preliminary investigation on the microstructures of Precambrian microbialites comprises the second part of this doctoral work. As shown above, the macro- and mesostructures of microbialites can be mimicked by sponge buildups. The microstructures of bioconstructions thus become critical for identifying the constructors and studying their biological activities. However, because of the complex diagenetic overprints and the previous chaotic usage of descriptive terminologies, the study of microbialite microstructures is still in its beginning.

During this study, it was observed that compared with the Mesoproterozoic carbonate stromatolites, which show only structureless micritic or microsparic layers or simple filamentous structures, the Neoproterozoic microbialites seem have recorded the start of some unprecedentedly complex or organized microstructures. These include: 1) the organized “fluid canals” in the Early Neoproterozoic Visingsö Group; 2) the very regular peloids (probably lithified microbes) in the Cryogenian Rasthof Formation, Namibia and the (probably Late) Riphean stromatolite, as well as the less regular peloidal fabrics in the post-Marinoan microbialites and the Late Riphean Visingsö stromatolites; 3) chambered structures from the Cryogenian Rasthof and Gruis Formations, Namibia, which probably have an analogue in the older pre-glaciation Little Dal Group; 4) the chambered grains in the Late Riphean stromatolites.

The regular fluid conducting canals and the chambered structures indicate upheaved level of organization in the Early Neoproterozoic microbial mats, while the chambered grains probably

represent a unique life form which may be related to the chambered structures. *In situ* formed peloidal fabrics are rarely known in microbialites older than the Neoproterozoic, but are common in the Phanerozoic microbialites and sponge fossils. It is still unknown what made them massively occur in the Neoproterozoic, especially after the Cryogenian glaciations. In the current stage, it is still too early to draw any conclusion whether these complex microstructures are related to early metazoans or not. But these innovations are congruent with the background of eukaryote evolution. Further investigation with more detailed lithological observation, geochemical analysis and 3-D reconstruction will hopefully improve the current understanding.

In brief, this doctoral work has revealed that non-spicular keratose demosponges have a higher preservation potential and abundance than previously evaluated in fossil record, especially in carbonate facies. The other type of non-spicular demosponge, the myxospongids which are devoid of any skeletons, was probably also fossilized in carbonates, but less common. In addition, keratose sponges were found able to construct microbialite-like bioconstructions together with microbes. All these findings imply that the Precambrian non-biomineralized ancestral sponges should have the potential to be recorded in carbonate microbialites. Although the preliminary study on Precambrian microbialites did not find any structure which is immediately comparable with the Phanerozoic sponge fossils, it showed that a few complex and enigmatic microbialite microstructures did start to appear in the Early to Middle Neoproterozoic (Tonian to Cryogenian). To determine whether these structures are related to the advent of animals requires further research.

References

- Antcliff JB, Callow RHT, Brasier MD (2014) Giving the early fossil record of sponges a squeeze. *Biological Reviews* 89:972–1004
- Boury-Esnault N, Rützler K (1997) *Thesaurus of sponge morphology*. Smithsonian Contributions to Zoology Number 596. Washington, D.C., Smithsonian Institution Press, 55 pp
- Lee J-H, Chen J-T, Choh S-J, Lee D-J, Han Z-Z, Chough SK (2014) Furongian (Late Cambrian) sponge–microbial maze-like reefs in the North China Platform. *Palaios* 29:27–37
- McFall-Ngai M, Hadfield MG, Bosch TCG, Carey HV, Domazet-Lošo T, Douglas AE, Dubilier N, Eberl G, Fukami T, Gilbert SF, Hentschel U, King N, Kjelleberg S, Knoll AH, Kremer N, Mazmanian SK, Metcalf JL, Neilson K, Pierce NE, Rawls JF, Reid A, Ruby EG, Rumpho M, Sanders JG, Tautz D, Wernegreen JJ (2013) Animals in a bacterial world, a new imperative for the life sciences. *Proceedings of the National Academy of Sciences* 110 (9):3229–3236
- Mikhailov KV, Konstantinova AV, Nikitin MA, Troshin PV, Rusin LY, Lyubetsky VA, Panchin YV, Mylnikov AP, Moroz LL, Kumar S, Aleoshin VV (2009) The origin of Metazoa: a transition from temporal to spatial cell differentiation. *BioEssays* 31 (7):758–768
- Minchin EA (1900) Chapter III. Sponges. In: Lankester ER (ed) *A treatise on zoology*. Part II. The Porifera and Coelenterata. Adam & Charles Black, London, pp 1–178
- Reitner J (1998) Herr Reitner: Bericht aus seinem Arbeitsgebiet (Vorstellungsbericht). *Jahrbuch der Akademie der Wissenschaften zu Göttingen*: 230–235
- Reitner J, Luo C, Duda JP (2012) Early sponge remains from the Neoproterozoic–Cambrian phosphate deposits of the Fontanarejo Area (Central Spain). *Journal of Guizhou University (Natural Sciences)* 29 (Sup. 1):184–186
- Reitner J, Wörheide G (2002) Non-Lithistid Fossil Demospongiae — Origins of their Palaeobiodiversity and Highlights in History of Preservation. In: Hooper JA, Van Soest RM, Willenz P (eds) *Systema Porifera*. Springer US, pp 52–68
- Richter DJ, King N (2013) The Genomic and Cellular Foundations of Animal Origins. *Annual Review of Genetics* 47 (1):509–537
- Taylor MW, Radax R, Steger D, Wagner M (2007) Sponge-associated microorganisms: Evolution, ecology, and biotechnological potential. *Microbiology and Molecular Biology Reviews* 71(2):295–347
- Walcott CD (1920) Cambrian geology and paleontology IV, No.6 Middle Cambrian Spongiae. *Smithsonian Miscellaneous Collections* 67 (6):261–364
- Wood RA (2011) Paleocology of the earliest skeletal metazoan communities: Implications for early biomineralization. *Earth-Science Reviews* 106 (1–2):184–190
- Wörheide G, Dohrmann M, Erpenbeck D, Larroux C, Maldonado M, Voigt O, Borchellini C, Lavrov DV (2012) Chapter one - Deep phylogeny and evolution of sponges (Phylum Porifera). In: Becerro MA, Uriz MJ, Maldonado M, Xavier T (eds) *Advances in Marine Biology*, Volume 61. Academic Press, pp 1–78

Curriculum vitae

Date of birth: June 22, 1985

Place of birth: Chongqing, P. R. China

2011–Present: Doctoral student in Georg-August University of Göttingen

2008–2011: Master in Geology and Paleontology, Nanjing Institute of Geology and Paleontology, Chinese Academy of Sciences

Thesis: *Neoproterozoic medusoid fossils from Xingmincun Formation, southern Liaodong Peninsula, China*

2004–2008: Bachelor in Geology (Paleontology), Nanjing University, China

Thesis: *Acritarchs from the Doushantuo Formation, Xiaofenghe area, Yichang—and about the extinction event of large acanthomorphic acritarchs* (translated title)

Awards

Tilly Edinger Prize, 2013

Travel Grant from the International Office of Georg-August University of Göttingen, 2013

PhD scholarship (36 months) from Chinese Scholarship Council (CSC), 2011–2014

Published Papers

Luo C., Reitner J (2014) First report of fossil "keratose" demosponges in Phanerozoic carbonates: preservation and 3-D reconstruction. *Naturwissenschaften*, 101(6):467–77

Luo C., Schäfer N, Duda J-P, Li L-X (2014) Preservation of organic matter in sponge fossils: a case study of “round sponge fossils” from the Cambrian Chengjiang Biota with Raman spectroscopy. *Göttingen Contributions to Geosciences*, 77: 29–38

Submitted Papers

Luo C., Reitner J (submitted) “Stromatolites” built by sponges and microbes – a new type of Phanerozoic bioconstruction. *Lethaia*

Contributions to Academic Conferences

- Luo C (2013) Possible “keratose” demosponge fossils in Phanerozoic carbonates. Plaeobiology and Geobiology of Fossil Lagerstätten through Earth History – a Joint conference of the “Paläontologische Gesellschaft” and the “Palaeontological Society of China”. Göttingen. (Oral presentation)
- Luo C, Reitner J (2013) Are there “keratose” demosponges in the Phanerozoic fossil record? 9th World Sponge Conference. Fremantle. (Oral presentation)
- Luo C, Zhu M-Y, Reitner J (2012) Enigmatic Cryogenian medusoid fossil from North China: A unique bauplan with possible metazoan affinity. Centenary Meeting of the Paläontologische Gesellschaft. Berlin. (Oral presentation)
- Reitner J, Luo C, Duda J-P (2012) Early sponge remains from the Neoproterozoic-Cambrian phosphate deposits of the Fontanarejo area (Central Spain). 17th Field Conference of the Cambrian Stage Subdivision Working Group, International Subcommittee on Cambrian Stratigraphy & Celebration of the 30th Anniversary of the Discovery of the Kaili Biota. Guizhou. Journal of Guizhou University (Natural Sciences), 29 (Sup. 1): 184-186. (coauthor of extended abstract)
- Reitner J, Luo C, Zhu M-Y, Lü M, He T-C, Duda J-P, Schäfer N, Hansen B, Blumenberg M (2012) Cap carbonate related microbial biosignatures. Fermor Meeting 2012 - The Neoproterozoic Era: Evolution, Glaciation and Oxygenation. London. (Poster)

Other publications (not directly related to the PhD study)

- Luo C, Zhu M, Reitner J (in review) Jinxian Biota revisited: Taphonomy and body-plan of the Neoproterozoic discoid fossils from southern Liaodong Peninsula, North China. Paläontologische Zeitschrift